Simplifying Accelerated Electromigration Testing of Solder using Wire-based DUTs

by

Sudharsan Azisur Venkatesan

A thesis
presented to the University of Waterloo
in fulfillment of the
thesis requirement for the degree of
Master of Applied Science
in
Mechanical and Mechatronics Engineering

Waterloo, Ontario, Canada, 2021

© Sudharsan Azisur Venkatesan 2021

AUTHOR'S DECLARATION

I hereby declare that I am the sole author of this thesis. This is a true copy of the thesis, including any required final revisions, as accepted by my examiners.

I understand that my thesis may be made electronically available to the public.

Abstract

A novel and accelerated method for the characterization of Electromigration (EM) in a solder material typically used in electronics packaging is proposed in this report. The method includes a novel approach to prepare EM specimens from solder wire by manufacturing a constriction, which added typically a few milliohms to the resistance. The method further includes a fusion-current based procedure to select the stressing current level, as a defined percentage of fusion current (*FCP*) of each specific specimen. The method is validated using EM experiments of constricted wire specimens made from Sn-0.7Cu solder. The experiments were organized in a 2x2 DOE (Design of Experiments) with *FCP* and specimen temperature T_S as the factors. The value of T_S was adjusted using the ambient temperature T_A with a process based on measured values for thermal resistance between specimen and ambient (R_{th} = 280 K/W) and for the temperature coefficient of resistance (*TCR* = 0.004183 1/K at 25 ºC) of the specimen. The DOE levels for T_S were 181.25 ºC and 165.95 ºC and for *FCP* were 75 % and 80 % of the fusion current. *MTTF* (Mean Time to Failure) is calculated using a conventional Weibull, Lognormal and a Censored Lognormal distribution for all four DOE legs and the effects are reported. Censored Lognormal analysis is found to be the best fit for data collected using this method. A 3% change in Fusion Temperature Percentage (*FTP*) is found to have an effect 2.22 time greater than a 5% change in *FCP*. The proposed method is also tested on SAC305 solder and the comparative results are reported. Future steps to study the combined effects of EM and TM are proposed.

Acknowledgements

Greatest gratitude goes to my parents for supporting me through these 2 years. This has been the best of privileges that I have been afforded. I would like to thank Dr. Michael Mayer for accepting me as a research student, and his patience and willingness to teach me throughout this period. I would like to thank Mostafa AbdelAziz for his support and insight with this research. I would like to thank Future Way for funding this research, and Erick Di for getting me started with my study.

I would also like to thank CMC Microsystems for the provision of products and services that facilitated this research, including the service of COMSOL Multiphysics®.

Table of Contents

AUTHOR'S DECLARATION ... ii

Abstract ... iii

Acknowledgements ... iv

List of Figures ... vii

List of Tables ... x

List of Abbreviations ... xi

Chapter 1 Introduction ... 1

1.1 Objectives ... 5

Chapter 2 Literature Review ... 6

2.1 Electromigration Failure Modes ... 6

2.2 Coexisting Material Migration Phenomena ... 7

2.2.1 Thermomigration ... 7

2.2.2 Stress Migration ... 8

2.2.3 Unified Material migration models ... 9

2.3 Black’s Equation ... 10

2.4 Contemporary Statistical Models ... 11

2.4.1 Weibull Distribution ... 11

2.4.2 Lognormal Distribution ... 12

2.4.3 Lognormal Distribution with Right Censoring ... 13

Chapter 3 Experimental Design ... 14

3.1 Fabricating a Constricted Wire Sample for EM Current Stressing ... 14

3.2 Test Vehicle Proposal ... 16

3.3 Specimen Simulation ... 18

3.4 Testing Setup ... 25

Chapter 4 Design of Experiment ... 27

4.1 Fusion current Characterization ... 27

4.2 Thermo-Electric Characterization ... 29

4.3 DOE Cell determination ... 34

Chapter 5 Results ... 38

5.1 Realtime Viewing of EM Failure ... 39

5.2 DOE Data analysis ... 41

5.3 SAC305 vs SnCu Comparison 47
Chapter 6 Discussion 50
6.1 Raw data curves 50
6.2 Effect of Acceleration 50
6.3 DOE Effect Analysis 51
Chapter 7 Conclusion 52
7.1 Conclusions 52
7.2 Recommendations 52
References 54
Appendix A Matlab and Python Code 58
Appendix B COMSOL Simulation Results 81
Appendix C Anode Side Defect Images 84
Appendix D Recommendation for future improvements 86

List of Figures

Figure 1: Example of hillock and void formation in microstructure due to EM (Used with Permission from [1]) 1

Figure 2: Change in interconnect parameters over time, indicating that as current density and AoC decrease at given rates, current density *J* increases (Used with Permission from [1]) 2

Figure 3: Projection of EM-robust solutions over time (Used with Permission from [1]) 3

Figure 4: a) Initial presence of vacancies normally seen in conductor lattice b) Void nucleates when vacancies coalesce under presence of electron flow c) Void growth over time while picking up nearby vacancies d) Void growth eventually leading to fusion (after [17]) 7

Figure 5: Interaction Effects between EM, TM, and SM (Used with Permission from [1]) 9

Figure 6: EM cross-phenomenal feedback loop (Used with Permission from [1]) 11

Figure 7: Design of constriction in wire sample [Dimensions in mm] 14

Figure 8: (a) Tools used for manufacturing DUT specimen, (b) Cutting tool with zoomed section of retention notch 15

Figure 9: Solder sample example average resistance (n = 20) between 2 probes 5 mm from midline, for wire piece (a) in original form, (b) flattened shape, (c) with constriction cut. 16

Figure 10: Test Vehicle PCB Design. Specimen is placed in Area 2. Areas 3 are used to attach the current inducing contact fingers. Areas 1 are used to attach the voltage sensing contact fingers. 17

Figure 11: Custom designed test vehicle with mounted specimen 17

Figure 12: (a) Mesh build of constricted wire specimen under 'Extremely Fine' Setting, (b) Close up of constricted segment, (c) Section view of constriction 18

Figure 13: COMSOL simulation of voltage drop across sample when subject to a lead current of 0.1 A, measured in mV 19

Figure 14: Iso-potential plot of constricted specimen under 5 A current, ambient temperature of 23 °C, measured in V 20

Figure 15: (a) Current density simulation of modified solder wire specimen, under a stress current of 5 A, (b) Zoomed image of micro constriction indicating current crowding at notch, measured to be 1.199 x 10^5 A/cm^2, (c) Current density study of constriction (section view) 22

Figure 16: (a) Temperature profile of fully modified specimen under 5 A, 23 °C, (b) zoomed section of constriction temperature profile 23

Figure 17: Iso-thermal surface plot of fully modified specimen 23

Figure 18: (a) Temperature gradient across specimen at current of 5 A, and ambient temperature 23 °C, (b) Zoomed view of constricted section, peak value measured at 395 K/cm 24
Figure 19: Iso-surface analysis of thermal gradient for fully modified specimen 25
Figure 20: Test setup block diagram 26
Figure 21: Fusion current testing example. The current is varied from 0.1 A in steps of 0.5 A up to 5 A, and then steps of 0.1 A until failure (fusion point at 6.6A). R_0 was 12.546 mΩ 28
Figure 22: Initial resistance vs Fusion current for modified Sn-0.7Cu specimen 28
Figure 23: Sn-0.7Cu Specimens aged at ambient temperature of 23°C, and 80% *FCP* (Yellow), 75% *FCP* (Red), and 70% *FCP* (Blue), indicating a ΔR of 44.8%, 13.38% and 7.12% respectively. 29
Figure 24: Data from three Sn-0.7Cu specimens stressed with various current levels up to 3.5 A and heated to various ambient temperatures from 25 °C to 100 °C 30
Figure 25: (a) Sn-0.7Cu Resistance vs Current plot for ambient temperature ranging from 25°C to 100°C (b)Ambient temperature vs initial resistance R_0 fit used to find *TCR* 31
Figure 26: Sn-0.7Cu Specimen resistance for various power levels and T_A values. Data used to find thermal resistance R_{th} 32
Figure 27: Sn-0.7Cu Specimen temperature fit as a function of stress current *I* and ambient temperature T_A 33
Figure 28: (a) Sn-0.7Cu Specimen aged in room temperature [23°C] at 80% *FCP* [I_{Fuse} = 6.32 A, I_{Stress} = 5.05 A], (b) Zoomed image of aging section highlighted in (a) 35
Figure 29: DOE cell in contour plot of Sn-0.7Cu specimen temperature as a function of current and ambient temperature 36
Figure 30: Flow chart of proposed EM sample preparation and testing process 37
Figure 31: EM test results of voltage across Sn-0.7Cu constricted specimens tested at *FCP* = 80 % (*I* ranging from 4.4 A to 5 A) and T_A = 65 °C 38
Figure 32: Realtime EM inspection setup used for visually recording EM degradation and resistance change while current stressing Sn-0.7Cu 39
Figure 33:(a) Sn-0.7Cu specimen aged at 60% and then 80% *FCP* [I_{Fuse} = 5.99A, T_A = 23 °C]. (b) Voltage Drop of region under 80% *FCP* 40
Figure 34: Real time image of Sn-0.7Cu specimen stressed at 60% and 80% *FCP* over 4.5 h 40
Figure 35: 24 Sn-0.7Cu specimens aged at (a) TL Corner [*FCP* = 75%, T_A = 78 °C] (b) TR Corner [*FCP* = 80%, T_A = 65 °C] (c) BL Corner [*FCP* = 75%, T_A = 65 °C] (d) BR Corner [*FCP* = 80%, T_A = 52 °C]41
Figure 36: Weibull distribution of Sn-0.7Cu T-R data 42

Figure 37: Lognormal distribution of Sn-0.7Cu T-R data 42
Figure 38: Weibull analysis of Sn-0.7Cu *TTF* data collected from (a) TL corner, (b) TR corner, (c) BL corner, (d) BR corner of DOE, with measured points shown in blue, and fit line shown in red 44
Figure 39: Lognormal analysis of Sn-0.7Cu *TTF* data collected from (a) TL corner, (b) TR corner, (c) BL corner, (d) BR corner of DOE, with measured points shown in blue, and fit line shown in red 45
Figure 40: Censored Lognormal analysis of Sn-0.7Cu *TTF* data collected from (a) TL corner, (b) TR corner, (c) BL corner, (d) BR corner of DOE, with measured points and fit line shown in blue, censored points shown in red, and point of censoring shown in black (Left y-axis represents Cumulative Probability and right y-axis represents associated Z-score) 46
Figure 41: Voltage vs time raw data of 24 SAC305 specimen aged at FCP = 80%, T_A = 65 °C 48
Figure 42: Censored Lognormal analysis of SAC305 *TTF* data tested at T_A = 65 °C, FCP = 80%, with measured points and fit line shown in blue, censored points shown in red, and point of censoring shown in black (Left y-axis represents Cumulative Probability and right y-axis represents associated Z-score)...... 48
Figure 43: Example of hillock and whisker defects seen on Anode side of solder wire [FCP = 75%, T_A = 65°C] 51

List of Tables

Table 1: COMSOL Simulation Parameters 19
Table 2: Comparison between simulated and measured resistance 20
Table 3: DOE Testing Conditions........ 36
Table 4: DOE test results - Lognormal and Weibull Analysis of Sn-0.7Cu data 43
Table 5: DOE test results – Censored Lognormal analysis of Sn-0.7Cu data 47
Table 6: Comparison between Sn-0.7Cu and SAC305 tested at TR conditions 49

List of Abbreviations

EM : Electromigration

IC : Integrated Circuits

AoC : Area of Cross-section

IoT : Internet of Things

MTTF : Mean Time to Failure

TM : Thermomigration

SM : Stress migration

PoF: Physics of Failure

DUT : Device under test

DOE : Design of Experiments

CAD : Computer Aided Design

FCP : Fusion Current Percentage

TCR : Temperature Coefficient of Resistance

FTP : Fusion Temperature Percentage

Chapter 1

Introduction

The phenomenon of Electromigration (EM) continues to be researched as a major reliability concern in the field of microelectronics, especially in the modern Integrated Circuit (IC) environment. This phenomenon can be described as the diffusion of mass in a conductor due to momentum transfer between electrons and the positively charged ions of the metallization lines. This leads to two main forms of degradation in the conductor: the formation of hillocks due to atom accumulation on the anode side, and the formation of voids in the cathode side due to vacancy propagation. This is shown in Figure 1.

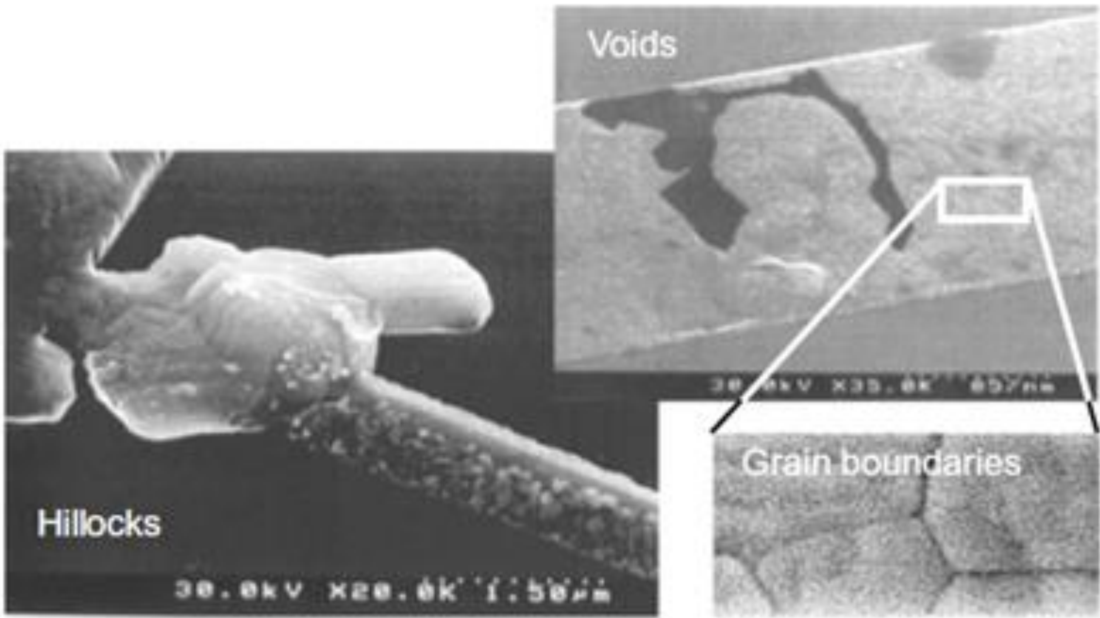

Figure 1: Example of hillock and void formation in microstructure due to EM (Used with Permission from [1])

While the EM phenomenon has been known since the 1860s, identified first by French physicist M. Gerardin [2], it did not become a concern until the recent advent of IC design. This is due to the ever-decreasing Area of Cross-section (AoC) in IC conductors. With the increasing rate of electrification in IoT (Internet of Things) devices and electric vehicles, EM has been identified as one of the leading causes of reliability issues in low-voltage electronics [3-4]. As the IC industry continues to shrink to the 10 nm level and lower, EM has come to be considered a severe problem [1]. While the current levels in IC are reducing

over time, the AoC in conductors reduces a lot faster. This has led to a gradual increase in current densities in IC conductors. This is depicted in Figure 2. The quadrilateral reduction of AoC with diameter occurs along with the linear reduction of surface area of conductors. It is also predicted that as the current densities required to operate gates increases, manufacturable EM-robust solutions are unknown [1]. This is shown in Figure 3. This increases the urgency towards developing a greater understanding of the EM phenomenon.

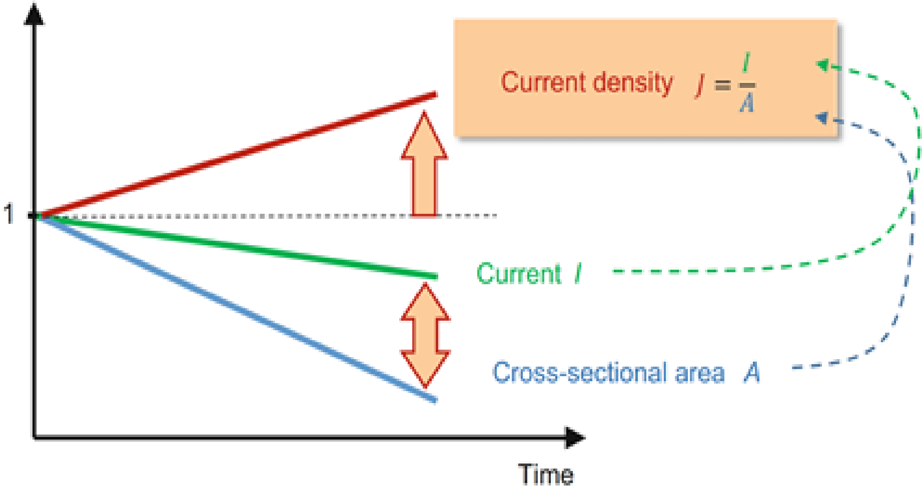

Figure 2: Change in interconnect parameters over time, indicating that as current density and AoC decrease at given rates, current density *J* increases (Used with Permission from [1])

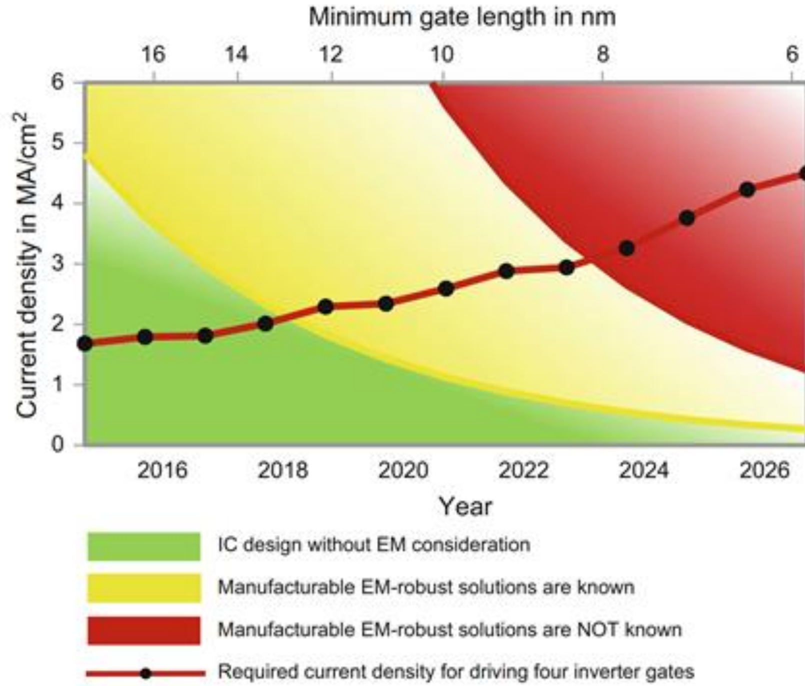

Figure 3: Projection of EM-robust solutions over time (Used with Permission from [1])

The relationship between the AoC of conductors and the mean time to failure (*MTTF*) was first identified by J.R. Black in 1969 [5] and modelled as an Arrhenius equation. It has since been updated and is given in Equation 1.

$$MTTF\ (h) = A.J^{n}.\exp\left(\frac{E_a}{K.T}\right) \tag{1}$$

where E_a is the activation energy of the most dominant failure mode, *A* is a constant related to cross sectional area and interconnect geometry, *n* is a scaling factor, typically between 1 or 2, *K* is Boltzmann's constant, and *T* is temperature in Kelvin.

From this equation, it can be inferred that *MTTF* is a function of current density, temperature, and the activation energy of the most dominant failure mode for the material being tested. Typical current densities for Cu or Al conductors where EM is observed is between 10^6 – 10^7 A/cm^2, while for solder material, it ranges at lower current densities from 10^3 to 10^4 A/cm^2 [1]. While the effort started with studying EM in metallization materials like Cu and Al, recently the concern has shifted to studying the effects of EM

on Pb-free solder materials, due to the significantly lower current density to start failure. The increasing rates of thermocycling in low-voltage electronics also increases the chance of EM failure in solder, with added effects of thermomigration (TM) and stress migration (SM). This makes it crucial to identify the limitations of popular Pb-free solder such as SAC305, SnCu, SnAg etc. In order to facilitate these studies on a global scale, and to obtain comparable data, it is essential to have testing processes and samples that can be replicated reliably and with ease.

While consumer electronics are designed to last for 5-10 years, based on their application, it is not practical to assign equally long test cycles [6]. For this reason, accelerated testing processes are used by varying temperature and/or current. It is crucial for this process to make an initial estimate of failure time in the ideal use case, using a Physics of Failure (PoF) model [7]. This model is then used to select parameters for accelerated tests. The outcome of the accelerated tests is decelerated using the calculated Acceleration Factor A_F. When it comes to testing for EM in solder, there is currently an absence of PoF models which capture all the factors that influence EM failure [8]. This introduces a need for finding a way to identify accelerated testing conditions without the use of PoF models. In addition to this, there exists a need to visually observe EM in metals while it is in progress. When testing solder material, real time visual inspection is difficult to do with contemporary ball-solder test samples. This is because the samples would have to be cross sectioned in order to view under the microscope, which irrevocably changes the geometry of the sample. This change in geometry essentially accelerated the aging, in a manner which can not be decelerated theoretically, as no contemporary model accurately quantifies AoC. Hence, it is desired to have a Device Under Test (DUT) and test vehicle model which can be observed under a microscope, without having to modify the tested geometry.

Current standards, such as JEDEC JEP 154A which describes the procedure for EM testing in solder, expect to yield results in x1000 hours [9]. This is due to their prescription of testing current densities between 3×10^3 to 2×10^4 A/cm^2, leading to current levels of 250 mA to 1.5 A. Accelerating the test beyond or less than this has been found to favor failure mechanisms other than EM, namely Joule heating for higher current density levels. However, it should be noted that these standards have been prepared exclusively for testing ball solder in standard sizes, either as single samples or in a daisy chain configuration. In this study, we aim to overcome the long testing periods by testing solder in its wire form, instead of the conventional ball form, as a means to control the effect of Joule heating. The specimens are also accelerated with increased current and ambient temperature to ensure fusion in approximately 24 h. The recommendation

from Section 5.2 from JEP 154A, to keep the stress temperature at least 25 °C below the melting point of the material is followed for this study.

1.1 Objectives

This study aims to provide tools which can improve the understanding of the EM phenomenon, by approaching it from a first principles basis.

The following objectives are chosen for the scope of this research:

1. Develop an algorithm which can be used to repeatedly determine accelerated testing conditions for solder, so that datasets of comparable results can be achieved over time and scale.
2. Identify the range of acceleration conditions that enable specimen failure within 24 h.
3. Propose a DUT and Test Vehicle which allows for real time observation of EM and can be used to obtain comparable samples from various materials.
4. Improve the understanding of the effect of current and temperature on EM failure, using DOE testing techniques.

Chapter 2

Literature Review

It is expected that solder joints perform reliability over a long period of time, especially in harsh and critical applications such as automotive, aerospace and medical. For this purpose, the effect of EM on solder has been studied in both the chip level and solder level. Over the past 50 years of studies, it has been identified that EM is affected by a multitude of factors. Some of these factors include length of sample, grain size and rotation, alloy type, nature of stress current etc. This makes it a complex phenomenon to accurately model in physics, but the role of each effect has been studied with great detail. The effect of the length of the sample with mean time to failure was explored by Blech, and the "Blech's critical length" was proposed, below which mass diffusion due to EM is counteracted by stress migration [10]. This was further studied by Schafft *et* al. and concluded that for standardized testing, having long testing lines is better for comparative EM testing due to shorter failure time [11]. Grain size and structure is also shown to have a significant effect on EM lifetimes, with larger grain sizes leading to longer lifetimes [12]. Similarly, reduction in triple points junctions have also been shown to increase EM lifetimes [13]. The effect of current nature on EM has also been studied. While most EM experiments happen with DC conditions, AC is also studied for implementation in IC design. It is observed that reversal of current direction, like in AC current, or cessation of applied current, leads to recovery of EM induced damage[14]. In order to increase EM lifetime, pulsed AC or DC current is also used, as EM lifetime is inversely proportional to duty cycle of current [15]. For the scope of this study, only the effects of temperature and current are explored, and other factors that affect EM are not be varied.

2.1 Electromigration Failure Modes

Regardless of the driving force, EM failure is led by two dominant failure mechanisms, void nucleation and void growth. It is observed that when the sample is stressed sufficiently, the vacancies in the lattice structure of the test material coalesce to form a sizable void. This is known as the void-nucleation phase. Following this, the void continues to grow under the presence of stress, known as the void-growth phase. This leads to a decrement in the AoC of the conductor, hence increasing the stress being applied. This further accelerated the growth of the void. This process is represented in Figure 4.

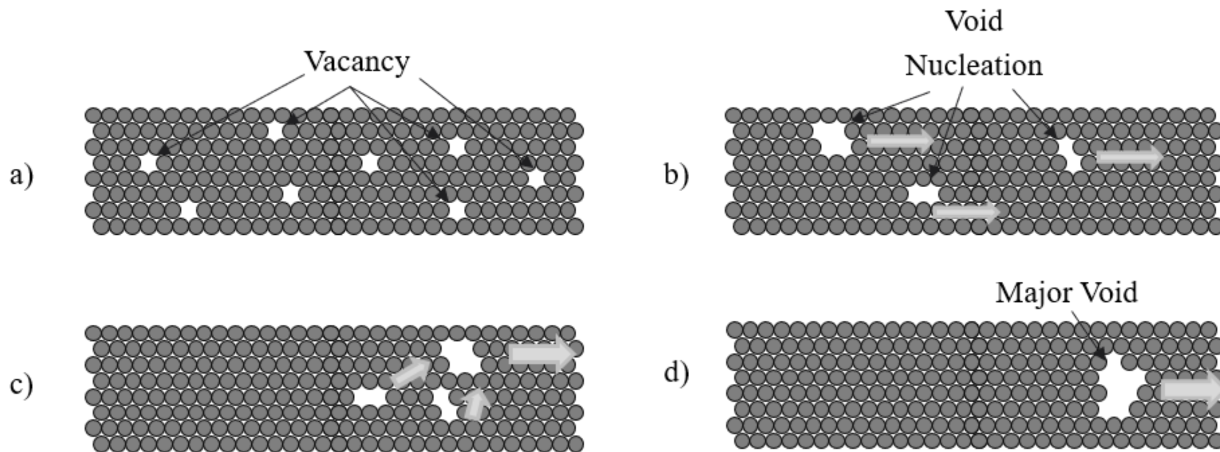

Figure 4: a) Initial presence of vacancies normally seen in conductor lattice b) Void nucleates when vacancies coalesce under presence of electron flow c) Void growth over time while picking up nearby vacancies d) Void growth eventually leading to fusion (after [17])

It is still debated as to which one these stages is the rate limiting process in the general case [16-17]. These processes are explored in greater detail in Li *et* al. [18]. The formation and growth of these voids can be registered electrically as a permanent resistance change, due to the reduction in the AoC. The effect of void formation and growth is captured in Black's model using the current density exponent 'n', which varies from values of 1 to 2. JR Lloyd reports that EM limited by void-nucleation is characterized by $n = 2$, whereas void-growth results in $n = 1$ [19].

2.2 Coexisting Material Migration Phenomena

In addition to EM, other material migration phenomena, being TM and SM, are also known to affect the reliability of conductors. It is often seen that these effects occur at the same time, and it is difficult to isolate the effects of 2 or more of such factors. In this section, the unique characteristics of these phenomena are explored.

2.2.1 Thermomigration

As mentioned previously in Chapter 1, the flow of high current density increases the resistance of the conductor over time. This leads to a phenomenon known as Joule Heating, which introduces a

temperature gradient to the conductor. As the temperature increases, the average speed with which the atoms move also increases. This increases the rate of diffusion from high to low temperature areas where forces due to temperature are lesser, leading to significant mass transfer. This phenomenon is called TM. In addition to Joule heating, uneven ambient temperature either due to localized heating or cooling, can also introduce temperature gradients. While TM has less influence in Cu or Al interconnects due to their high thermal conductivities, it plays a significant role in the degradation of alloys such as solder. It is generally accepted at temperature gradients of around 1000 K/cm is required for TM in solder joints [21]. Soret effect, which is the phenomenon that describes the differential mobility of components of a mixture in the presence of a temperature gradient, also plays a role in alloys. *MTTF* due to TM is given below in Equation 2.

$$MTTF\ (h) = B.\left(-\frac{dT}{dx}\right)^{-2}.\exp\left(\frac{E_a}{K.T}\right) \tag{2}$$

where *B* is a constant, and $\frac{dT}{dx}$ is the thermal gradient.

2.2.2 Stress Migration

Similar to EM and TM, Stress Migration (SM) is the diffusion of atoms stemming from an imbalance of mechanical stresses in the conductor. However, the fundamental difference is that EM and TM are irreversible processes, due to the presence of electron or heat flow. In the case of SM, atoms flow out of regions under compressive stresses, into regions of tensile stress. In modern circuit boards, such stress gradients are often caused due to a mismatch of thermal expansion coefficients between boards, packages, metallization lines etc. Temperature changes between fabrication, usage and storage conditions lead to differential stresses developing in these materials, leading to the formation of stress gradients. Similar to EM, SM also follows a void nucleation followed by a growth process. This subsequently leads to the formation of cracks in the conductor, thereby reducing the tensile stress and achieving equilibrium [22]. *MTTF* due to stress migration is modelled in Equation 3.

$$MTTF\ (h) = G.\left(-\frac{d\sigma}{dx}\right)^{-2}\exp\left(\frac{E_a}{K.T}\right) \tag{3}$$

where *G* is a constant, and $\frac{d\sigma}{dx}$ is the stress gradient.

2.2.3 Unified Material migration models

It is observed that EM, TM and SM have features that are interrelated and may even be self-reinforcing. The dislocation of atoms due to EM induces a mechanical stress gradient, which is the driving force behind SM. However, SM works against EM as the flow of atoms due to SM is from compressive to tensile. This is the opposite direction of EM where material flows from the cathode to the anode, leading to the development of tensile and compressive stresses respectively. Similarly, the decrement in the AoC due to EM, increases the temperature gradient across the weakest section which motivates TM. Unlike SM however, there is less direction dependency on the flow of current during EM. TM is still considered for developing solutions against EM, where a temperature gradient is induced in the direction opposite to the flow of EM so that the two phenomena can counteract each other [23]. The interactive effect of all three mechanisms is depicted in Figure 5.

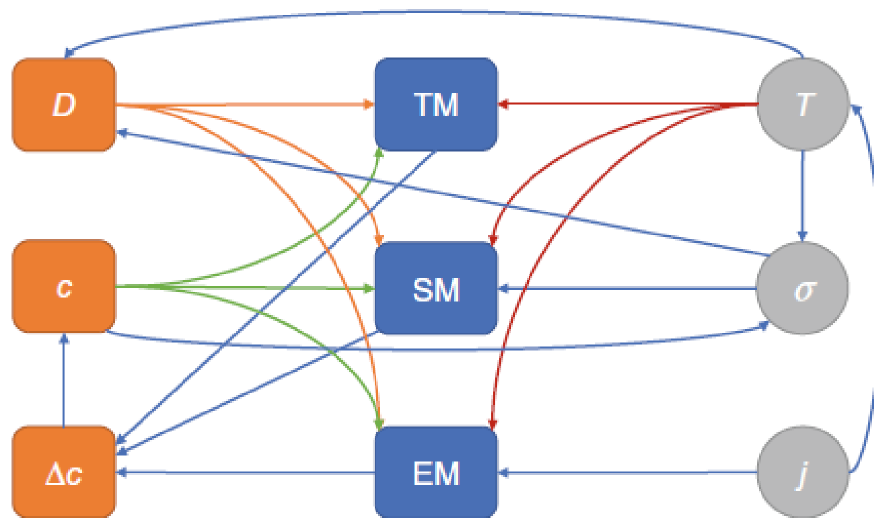

Figure 5: Interaction Effects between EM, TM, and SM (Used with Permission from [1])

It is seen that the current density increases the specimen temperature through Joule heating, which leads to stress and temperature gradient build up, due to mismatch of thermal coefficients. These stresses then affect the diffusion coefficient, which is critical to all 3 processes. This validates the claim that the three phenomena are inextricably connected. For this reason, recent research efforts have been focused on developing unified EM-TM-SM models which attempt to account for the effect of all three phenomena on *MTTF* [24-25].

2.3 Black's Equation

While Black's equation has been the popular model used for studying EM, there are several assumptions it makes about the phenomenon, which are not seen in practice. This rules it out as a possible PoF mechanism. Looking at Eqn. 1, it is seen that Black uses an Arrhenius fit with empirically determined variables to model the *MTTF*. Firstly this is an empirical model that realises its strength, only with a large number of samples tested. Given the number of factors that affect EM rates (eg: grain size and rotation, temperature, current density, alloy shape and type, etc.), this equation is incapable of capturing the individual effects of these factors. This makes it a useful tool in predicting the failure time of any single sample type tested, but it is hard to gain a general understanding of EM across multiple sample types of the sample material. Secondly, the long testing period (in the range of several 1000 hrs) of EM experiments even under accelerated conditions, means that researchers would have to wait for a significant period before obtaining usable data. The empirical nature of this model also means that researchers would have to test a significant number of samples, of the same sample type, at different temperatures and current densities before identifying the values for activation energy E_a, current density exponent n, and cofactor A, making the testing cycle even longer. This leads into the implicit assumptions made by the equation which are not seen in practice. Firstly, being an exponential fit, the model assumes that the sample being tested has a constant and fixed rate of failure. This is seen to be false in Minhua et al. where multiple samples of SnCu and SnAg are tested and shown to have significant differences in rate of failure [20]. This is captured in the data presented in this study as well and are be discussed in later sections. Black's equation also assumes a linear conductor, meaning that it does not account for change in material along a line being tested. For example, call solder, which is the conventionally tool for testing EM characteristics, is sandwiched between two copper metallization lines, and often have Ni as a metallization coating in the contact point. Black's model would consider this sample to be uniform and would take into account the several intermetallic layers. Black's equation also assumes a constant temperature and current density, while it is seen experimentally that the current density increases constantly due to Joule heating and loss of AoC due to EM, which also increases the specimen temperature. This feedback loop is depicted in Figure 6.

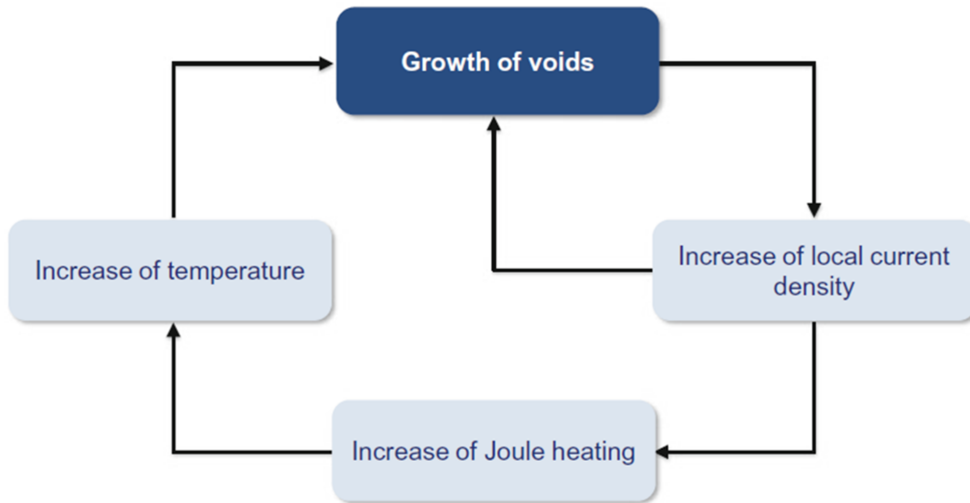

Figure 6: EM cross-phenomenal feedback loop (Used with Permission from [1])

2.4 Contemporary Statistical Models

Due to the difficulties faced when using Black's equation for data fitting in EM, other models which better capture the reliability behavior of mechanical and electrical failures are used, namely Weibull and Lognormal distributions [26]. This is because both models are quite effective in fitting skewed data sets, which tends to be the case with EM. In this section, these models are be explored. A special version of Lognormal distribution geared towards better handling of right-censored data is also discussed.

2.4.1 Weibull Distribution

As mentioned, Black's equation is an exponential distribution which assumes that the degradation rate is constant, which has been found to be inaccurate. For this reason, Weibull distribution is considered, as exponential distributions are a special case of Weibull, where the shape parameter β is 1. The general form of the probability density function for a 2-parameter Weibull distribution is given below in Equation 4 [27].

$$f(t) = \frac{\beta}{\eta}.\left(\frac{t}{\eta}\right)^{\beta-1}.e^{-\left(\frac{t}{\eta}\right)^{\beta}}\ (for\ t > 0) \quad (4)$$

where β is the shape parameter (slope), and η is the scale parameter (characteristic life by which ~63% of samples fail).

The linearized form of this equation is given below and is used for generating the code listed in Appendix A.

$$\ln(-ln\, R(t)) = \beta . \ln(t) - \beta . \ln(\eta) \quad (5)$$

$$R(t) = 1 - F(t) = \exp\left[-\left(\frac{t}{\eta}\right)^{\beta}\right] \quad (6)$$

Using this form, β and η are calculated as the slope and function of the intercept.

2.4.2 Lognormal Distribution

In addition to Weibull, Lognormal distributions are also used for characterizing EM failure. While it is typically used for modelling cycles-to-failure in fatigue or material strengths, it is also observed in time to failure data, when their natural logarithms are normally distributed. One of the advantages of this method is that the *MTTF* can be calculated as the time by which 50% of the samples tested would have failed. The general form of Lognormal Probability Density Function is,

$$f(t) = \frac{1}{t\sigma'\sqrt{2\pi}} \exp\left[-\frac{1}{2}\left(\frac{t' - \mu'}{\sigma'}\right)^2\right] for\ (t > 0) \quad (7)$$

$$t' = \ln(t)$$

The Mean and the Standard Deviation of the function can then be calculated as,

$$MTTF = \exp\left(\mu' + \frac{\sigma'^2}{2}\right) \quad (8)$$

$$St.Dev. = \sqrt{\left(\left(e^{2\mu' + \sigma'^2}\right)\left(e^{\sigma'^2} - 1\right)\right)} \quad (9)$$

The linearized form of the lognormal distribution is generated, and if used to develop the code in Appendix A. This is found to be,

$$\Phi^{-1}(r) = z = \frac{\ln(t) - \mu'}{\sigma'} = \frac{1}{\sigma'}\ln(t) - \frac{\mu'}{\sigma'} \quad (10)$$

The *MTTF* and *St. Dev.* can be calculated using the slope and intercept of the fitting line.

2.4.3 Lognormal Distribution with Right Censoring

It is common for EM experiments to be concluded before all samples fail. This leads to Type II-censoring in the data set, which is also known as 'right-censored' data. If not handled accordingly, this censoring can lead to errors in calculated values such as *MTTF* or η. JEDEC JESD37A describes the procedure to analyze right-censored data using the Persson and Rootzen Method as a Lognormal distribution [28]. For *N* samples tested where *K* samples fail, the process for calculating *MTTF* is,

$$MTTF = \exp\left(MPR + \left[\left[\frac{0.98}{K} + \frac{0.068\,N}{K^2} - \frac{1.15}{N}\right] s_{PR\ unbiased}\right]\right) \quad (11)$$

Here, *MPR* is the biased estimate of the mean of the log failure set, and $S_{PR\ unbiased}$ is the unbiased standard deviation of the censored log failure set. These are calculated as,

$$MPR = [M + \alpha_{PR} \times s_{RML}] \quad (12)$$

$$s_{PR\ unbiased} = \left(\frac{K}{K-1}\right)\left(\frac{1.8\,N+5}{1.8\,N+6}\right) s_{PR\ biased} \quad (13)$$

M is defined as the calculated mean of the censored log failure set. $S_{PR\ biased}$ is the biased standard deviation estimate of the censored lognormal data. This, along with the variables used for *MPR* are calculated as,

$$s_{PR\ biased} = \sqrt{\frac{(K-1)Std.Dev^2}{K} + \alpha_{PR}(\alpha_{PR} - z_0)s_{RML}^2} \quad (14)$$

$$s_{RML} = \frac{1}{2}\left[z_0(C_R - M) + \sqrt{z_0(C_R - M)^2 + 4\left[(C_R - M)^2 + \frac{(K-1)Std.Dev^2}{K}\right]}\right] \quad (15)$$

$$\alpha_{PR} = \frac{N}{K\sqrt{2\pi}} \exp\left(ln\frac{z_0^2}{2}\right) \quad (16)$$

$$C_R = \ln(t_{f-cen}) \quad (17)$$

$T_{f\text{-}cen}$ is the censor time beyond which the unfailed samples may fail. *Std.Dev.* is the standard deviation of the censored log failure set. The code used for automation this calculation is given in Appendix A – A.7.

Chapter 3

Experimental Design

The specimen is prepared by taking a strip of wire solder and modifications are made to introduce a current density hot spot. This helps localize the EM failure to a known fixed point in the sample. It is then mounted on a custom test vehicle, which arrests the sample to be stressed with temperature and current. It also provides contact points for four wire resistance measurement. The test vehicle design also allows for the sample to be visually inspected while aging.

3.1 Fabricating a Constricted Wire Sample for EM Current Stressing

A 40 mm long 0.5 mm diameter Sn-0.7Cu solder [29] wire specimen is modified using pliers to compress the middle section until it reaches a thickness of 0.1 - 0.05 mm. The flattened section is then partially cut using a knife with a retention notch, leaving a constriction, i.e., an uncut width of approximately 0.18 mm. The cut is then flayed open, leaving the constriction as the only path of contact. This opening also prevents molten flux from the wire core to bridge the gap during EM testing. The CAD design for the specimen is shown in Figure 7. The tools used for making the specimens are shown in Figure 8.

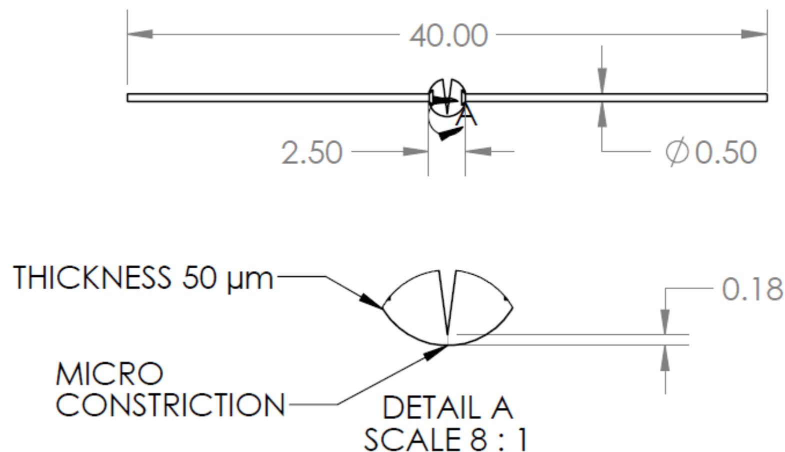

Figure 7: Design of constriction in wire sample [Dimensions in mm]

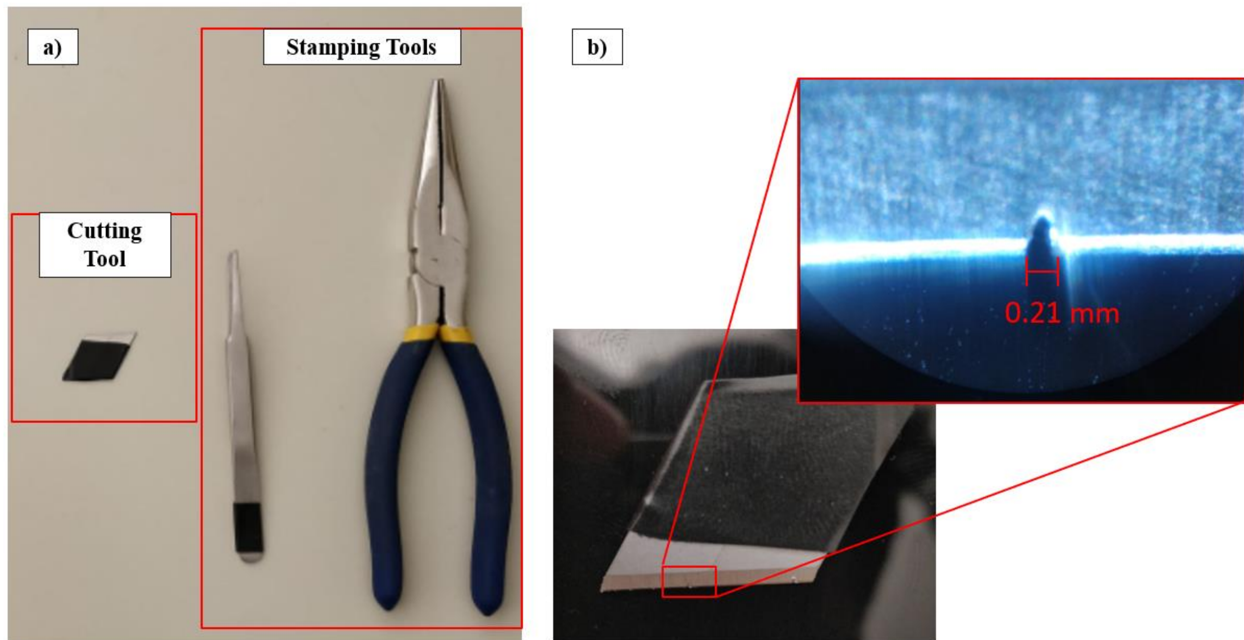

Figure 8: (a) Tools used for manufacturing DUT specimen, (b) Cutting tool with zoomed section of retention notch

The resistance of the sample is measured at each stage of the sample preparation process. For this, a constant current of 0.1 A is guided through the sample via two copper connection probes with contact points 15 mm on either side of the midline. The voltage drop across the middle of the wire is measured via a second set of two connection probes with contact points 5 mm on either side from the midline. Images of an example sample with room temperature resistance results are shown in Figure 9 (a), (b), and (c) for original, compressed, and constricted cases, respectively. The average resistance of the unmodified wire was 4.94 mΩ. The average resistance rose by 37 % to 6.75 mΩ after flattening, and then again by 119 % to 14.76 mΩ by cutting the constriction, leading to the conclusion that more than half of the measured resistance is caused by the constriction.

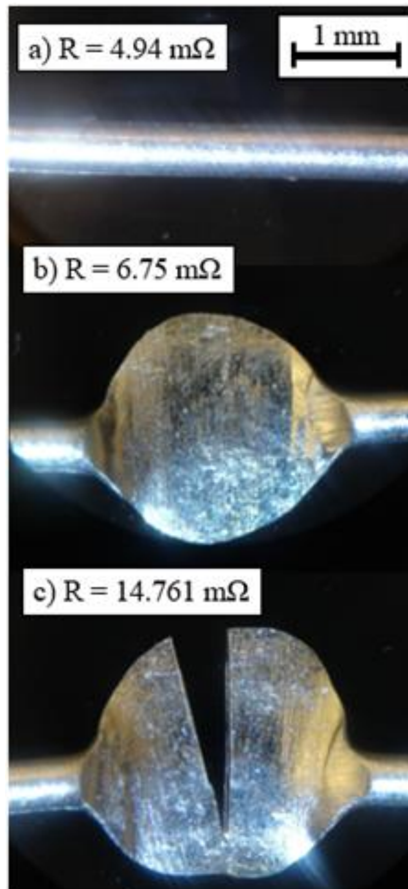

Figure 9: Solder sample example average resistance (n = 20) between 2 probes 5 mm from midline, for wire piece (a) in original form, (b) flattened shape, (c) with constriction cut.

3.2 Test Vehicle Proposal

A PCB test vehicle is proposed for holding and stressing the solder specimens. The PCB layout is shown in Figure 10, and the finished test vehicle is shown in Figure 11.

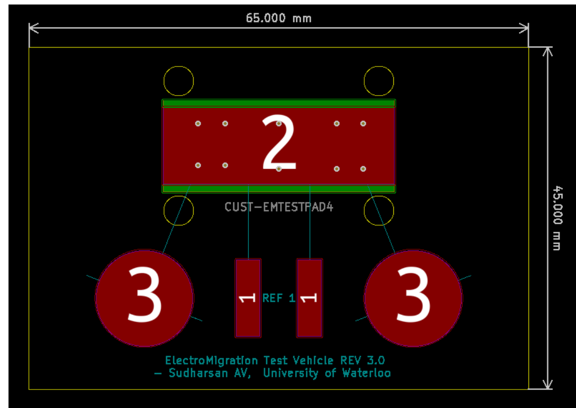

Figure 10: Test Vehicle PCB Design. Specimen is placed in Area 2. Areas 3 are used to attach the current inducing contact fingers. Areas 1 are used to attach the voltage sensing contact fingers.

Copper tabs serve as contact fingers, are soldered onto areas 1 and 3, and are used to hold the specimen in place and to act as current and voltage probes. Insulated wire pieces are then soldered onto the copper tabs and their other ends are screwed in an appropriate connector. This forms a rats-tail which can be used to connect the test vehicle quickly and securely to the setup described in the next subsection. The specimen is attached to the test vehicle by prying open the tabs and fitting the constricted wire underneath. This allows for a 4-wire resistance measurement setup.

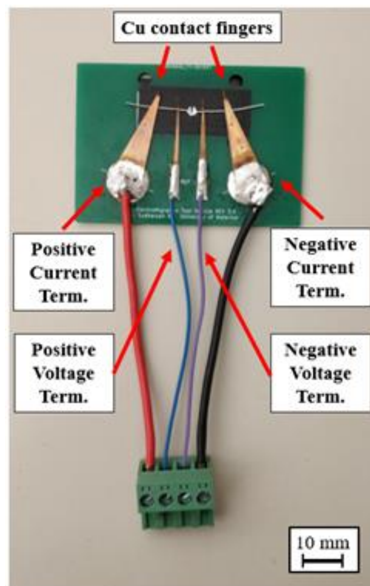

Figure 11: Custom designed test vehicle with mounted specimen

3.3 Specimen Simulation

Models of the specimen at various stages for modification are simulated in COMSOL Multiphysics®, to study the effect of current flowing through the member [28]. As mentioned in Section 3.1, the 3 stages are when the sample is unmodified, when it is stamped, and after the constriction has been applied. Figure 12 shows the mesh build of the fully modified sample, with 'Extremely Fine' mesh setting (423876 elements) being the highest grade. Number of faces, edges and points were 22, 58 and 38, respectively.

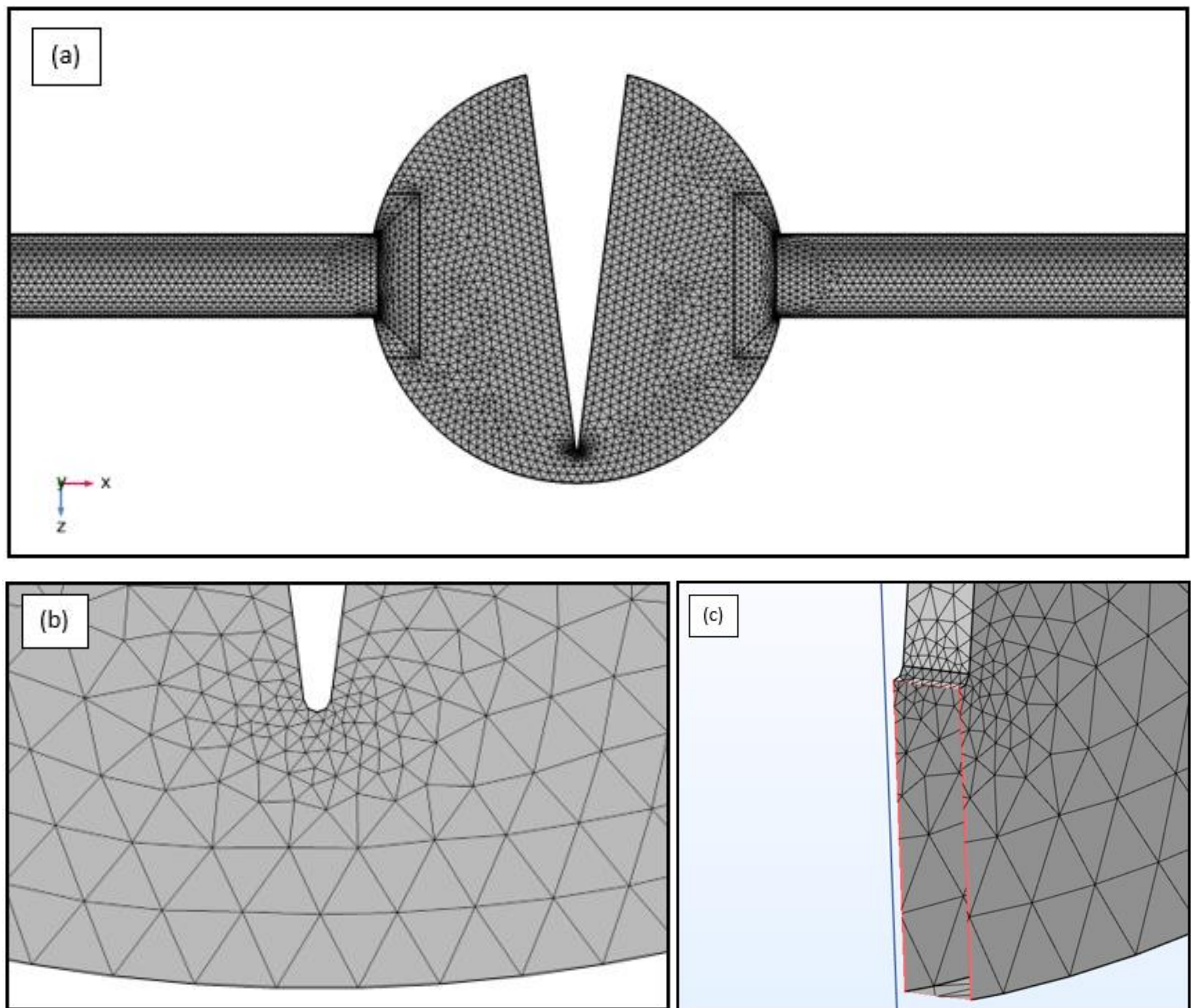

Figure 12: (a) Mesh build of constricted wire specimen under 'Extremely Fine' Setting, (b) Close up of constricted segment, (c) Section view of constriction

The settings used for generating the following results, including material properties of Sn-0.7Cu, are listed in Table 1 [31-32]. The resistance of the specimen is calculated at each stage and is presented in Table 2. An example of the resistance simulation is shown in Figure 13.

Table 1: COMSOL Simulation Parameters

Parameter	Value
Density [kg/m^3]	7300
Heat capacity at constant pressure [J/kg.K]	223
Thermal Conductivity [W/m.K]	53
Electrical Conductivity [MS/m]	7.54
Heat transfer coefficient of air [W/m^2.K]	25
Mesh size	Extremely Fine
Current [A]	5.0 (or 0.1)
Ambient Temperature [K]	296.15

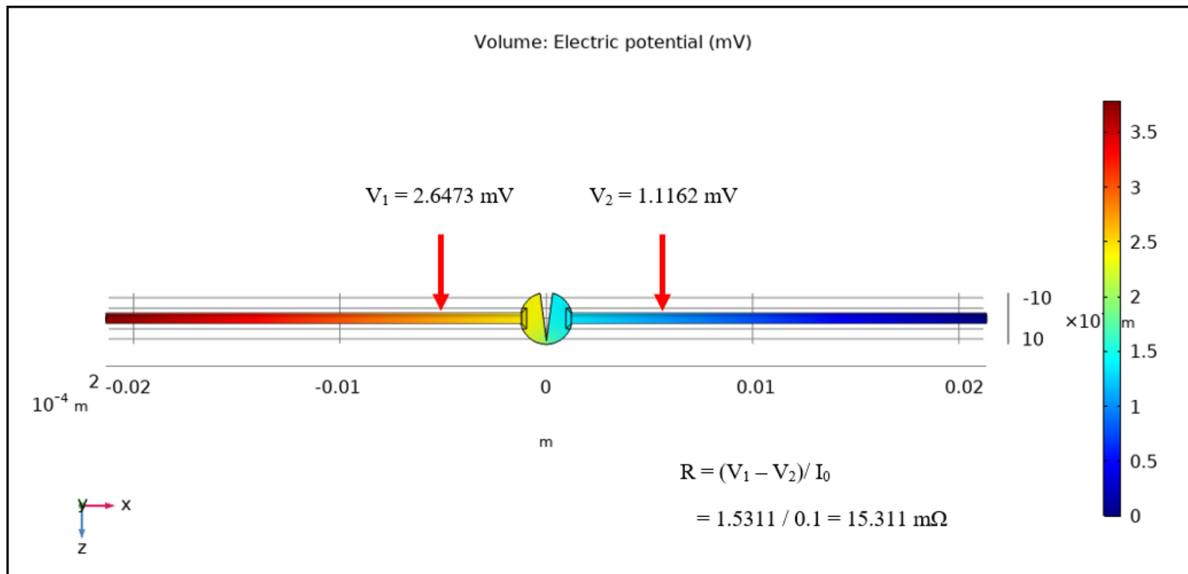

Figure 13: COMSOL simulation of voltage drop across sample when subject to a lead current of 0.1 A, measured in mV

The current flowing through the specimen model is set to be 0.1 A. Similar to the test vehicle design in Section 3.2, the voltage is measured at 5 mm from either side of the midline of the specimen. The difference in the voltage is divided by the load current, being 0.1 A, to calculate the resistance. In the micro constricted specimen shown in Figure 13, the resistance is found to be 15.311 mΩ. The simulation is repeated for the unmodified and stamped specimen, and the data is presented in Table 2. It is seen that the simulated and measured resistance values are comparable. Deviations between the values mainly occur after the sample has been stamped and squeezed, which are done by hand.

Table 2: Comparison between simulated and measured resistance

Parameter	**Simulated Resistance [mΩ]**	**Average Measured Resistance [mΩ] (n = 20)**
Unmodified Wire	4.947	4.94
Stamped Wire	6.945	6.75
Micro Constricted Wire	15.311	14.761
Stress Current [A]	0.1	

An iso-potential plot of the specimen is generated using a 5 A stress current, and ambient temperature of 23 °C. This is shown in Figure 14.

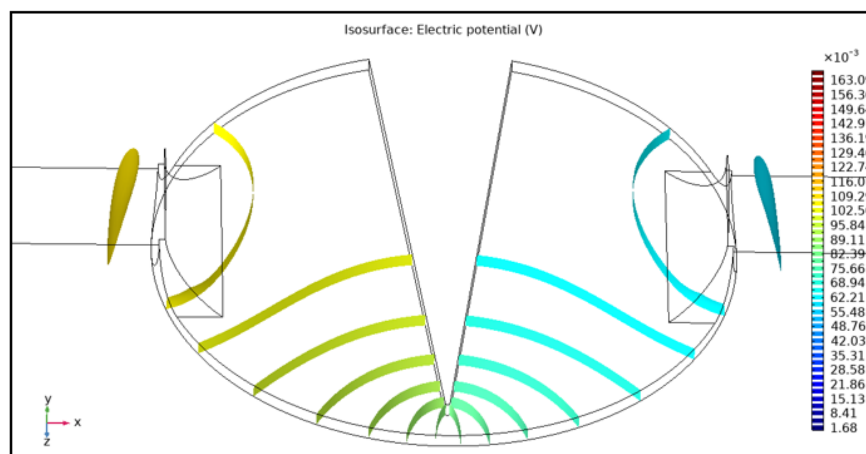

Figure 14: Iso-potential plot of constricted specimen under 5 A current, ambient temperature of 23 °C, measured in V

The COMSOL Joule Heating Multiphysics toolbox is used to study the current density and temperature profiles of the specimen, in stationary condition. The temperature profile is the end result of Joule heating and ambient temperature. This is shown in Figure 15 and Figure 16. Time dependant analysis is not conducted as there are no parameters that vary with time. The current used for these simulations is 5 A, and the ambient temperature of 23°C is set as the boundary condition for the unmodified surfaces of the wire. This approximates the real specimens being tested, as the copper probes act as heat sinks. The rest of the surfaces are modelled to be in free convection in air. The convection heat transfer coefficient is set as 25 $W/m^2.K$ as mentioned in Table 1. The iso-thermal plot of the specimen in shown in Figure 17.

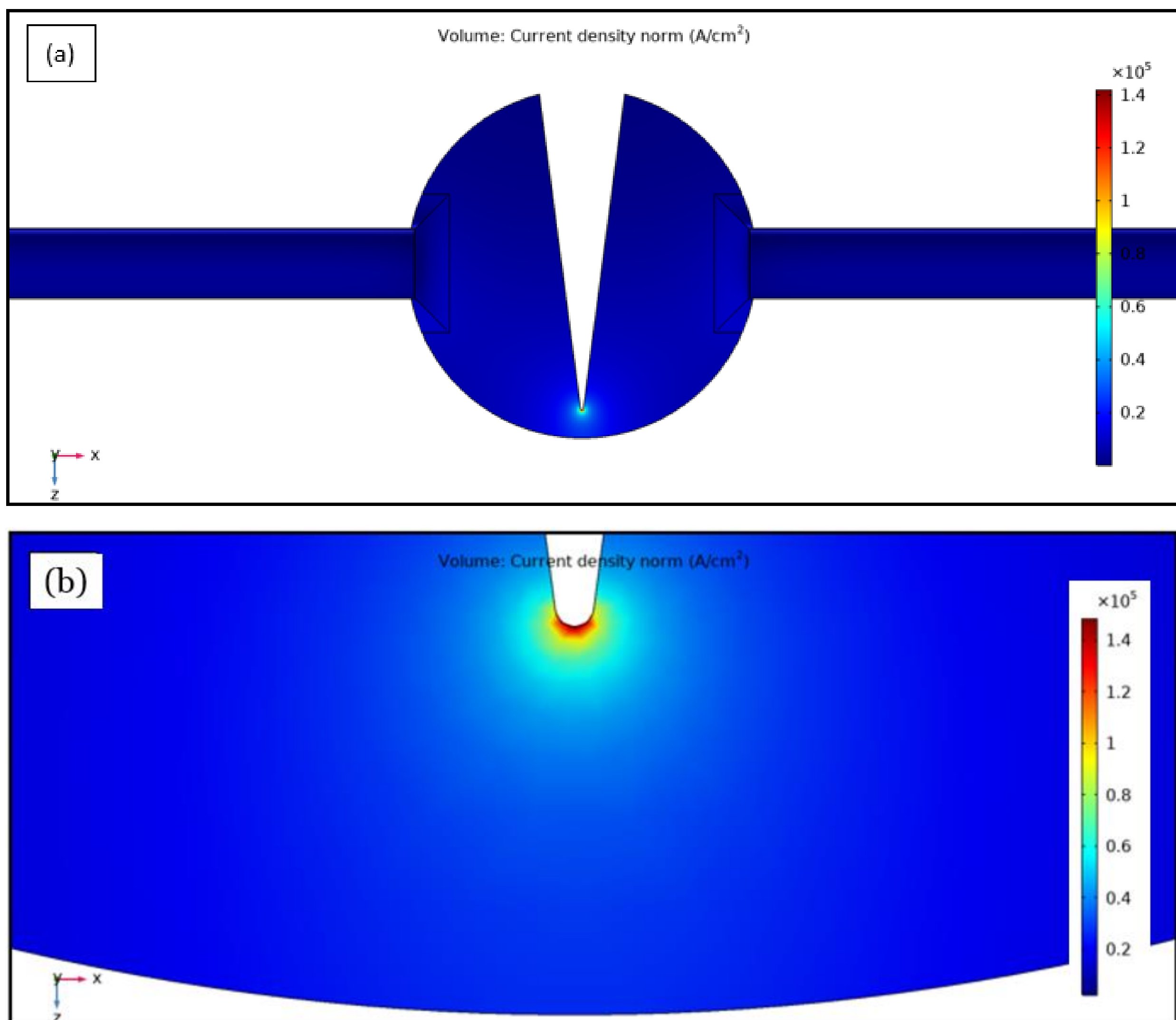

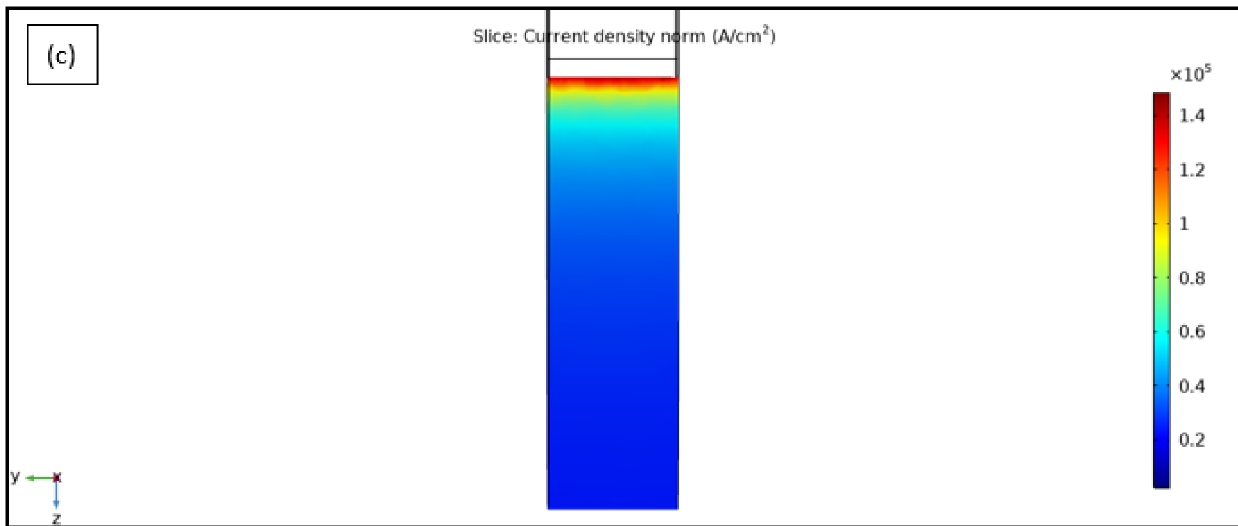

Figure 15: (a) Current density simulation of modified solder wire specimen, under a stress current of 5 A, (b) Zoomed image of micro constriction indicating current crowding at notch, measured to be 1.199 x 10^5 A/cm^2, (c) Current density study of constriction (section view)

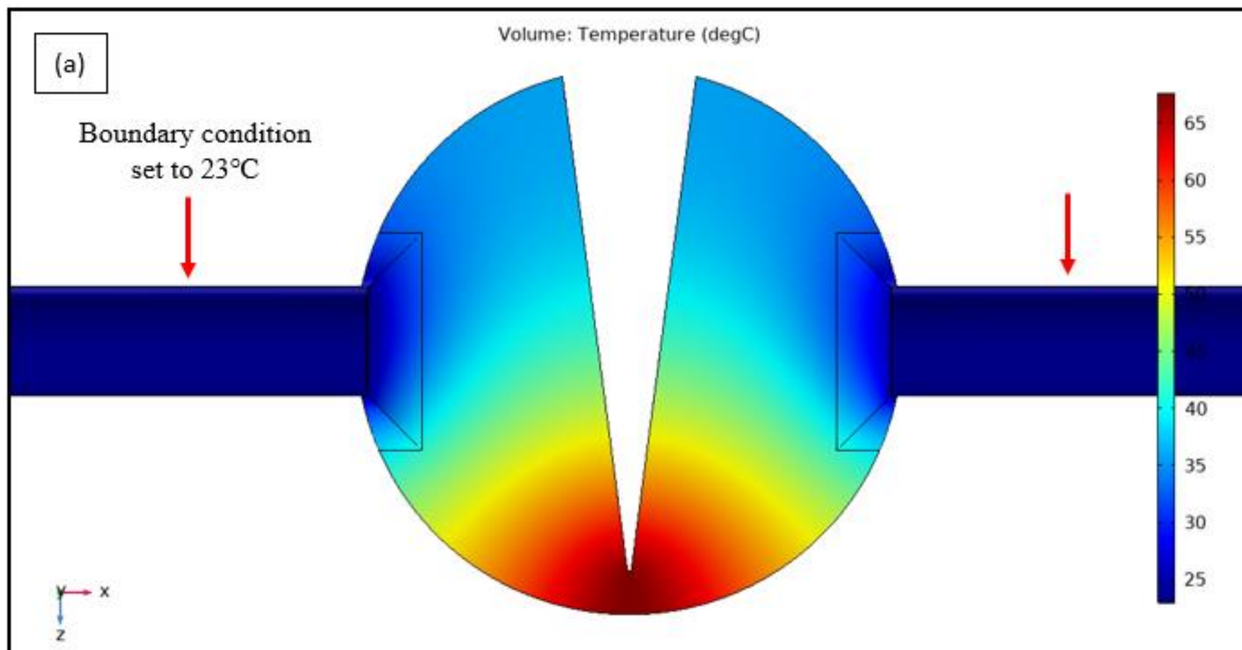

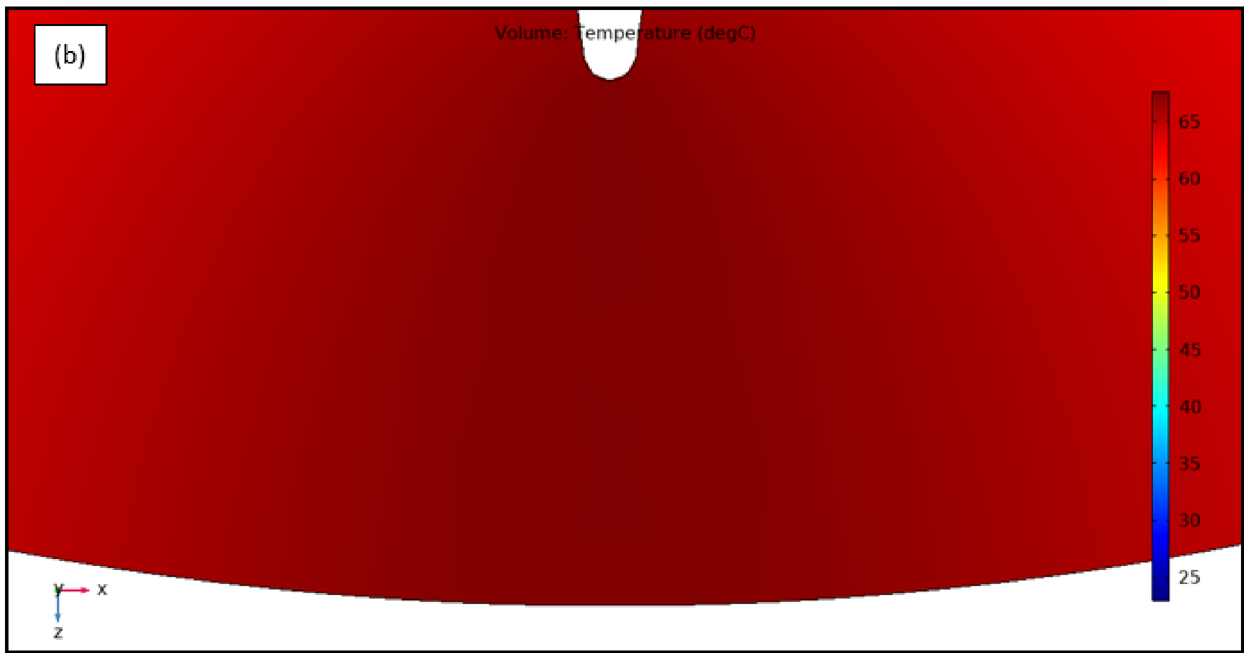

Figure 16: (a) Temperature profile of fully modified specimen under 5 A, 23 °C, (b) zoomed section of constriction temperature profile

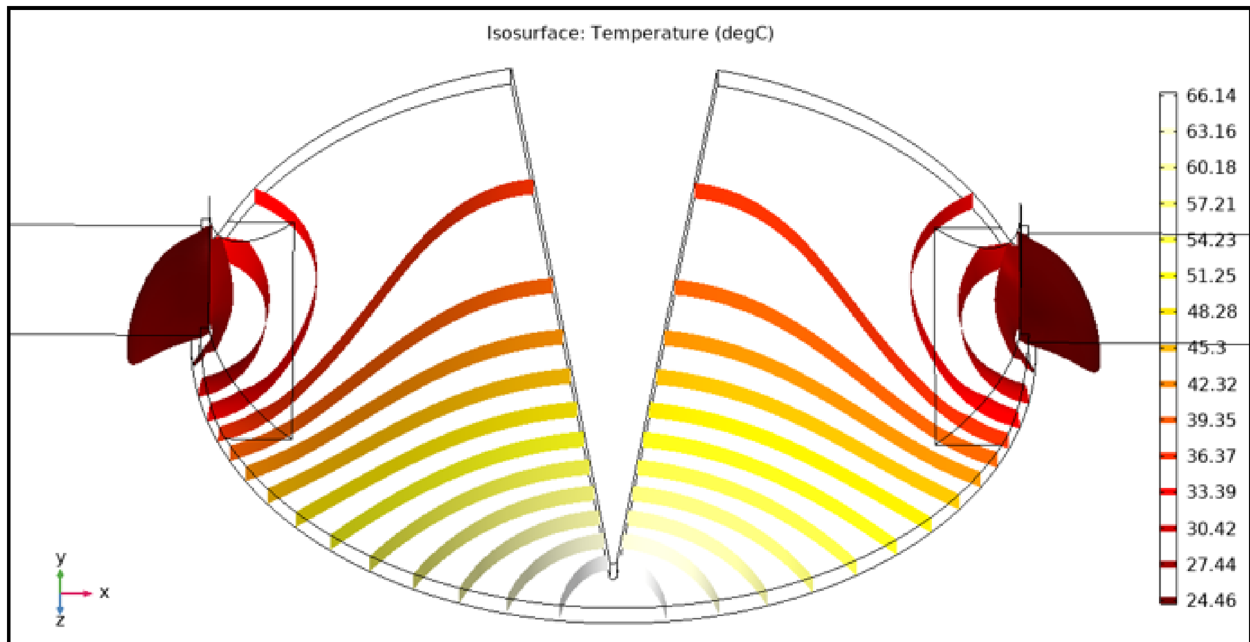

Figure 17: Iso-thermal surface plot of fully modified specimen

Using the temperature and current density data calculated so far, the temperature gradient of the specimen can also be simulated to identify the potential for thermomigration. This is shown in Figure 18. The iso-level plot for the thermal gradient simulation is generated and shown in Figure 19.

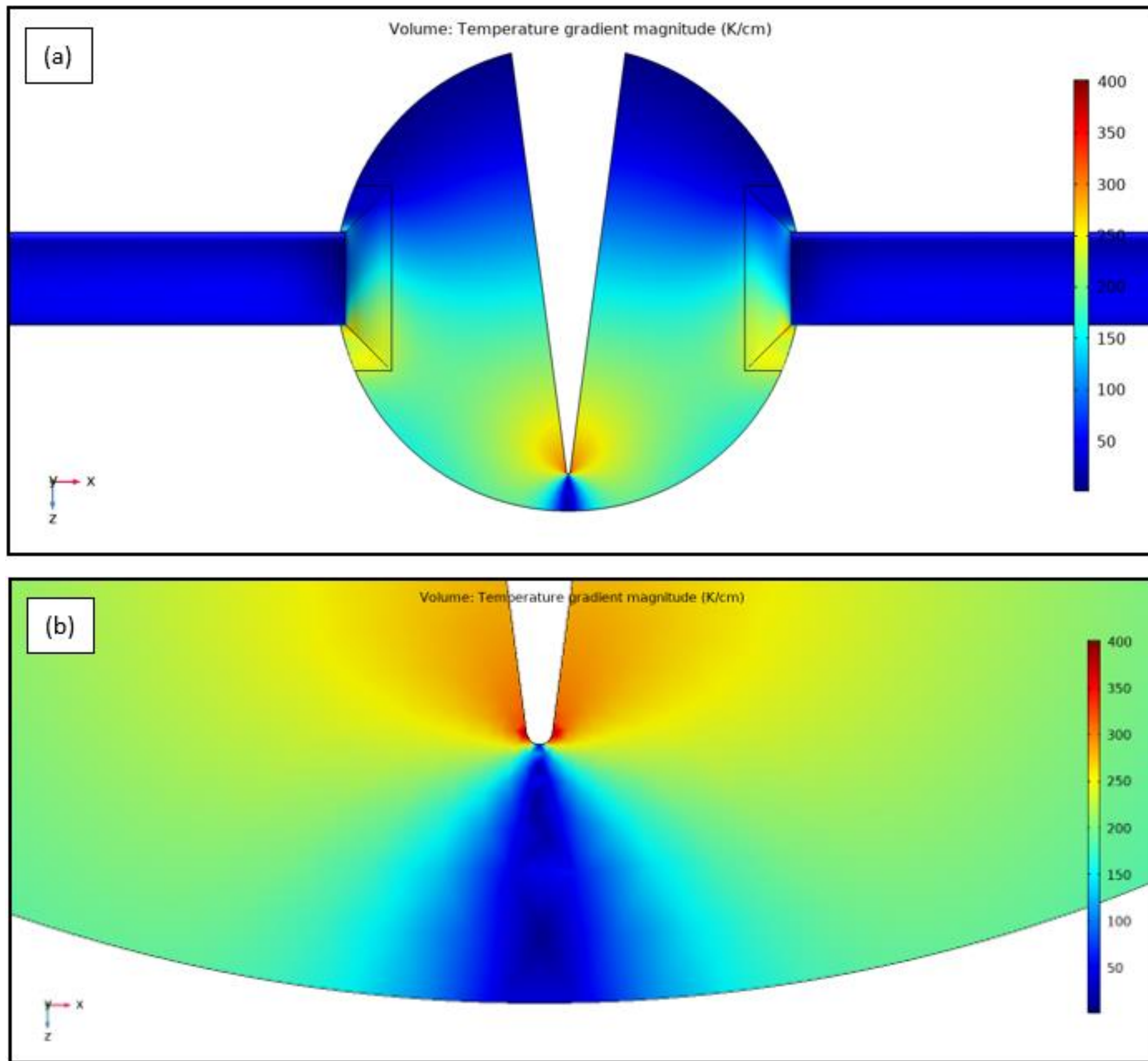

Figure 18: (a) Temperature gradient across specimen at current of 5 A, and ambient temperature 23 °C, (b) Zoomed view of constricted section, peak value measured at 395 K/cm

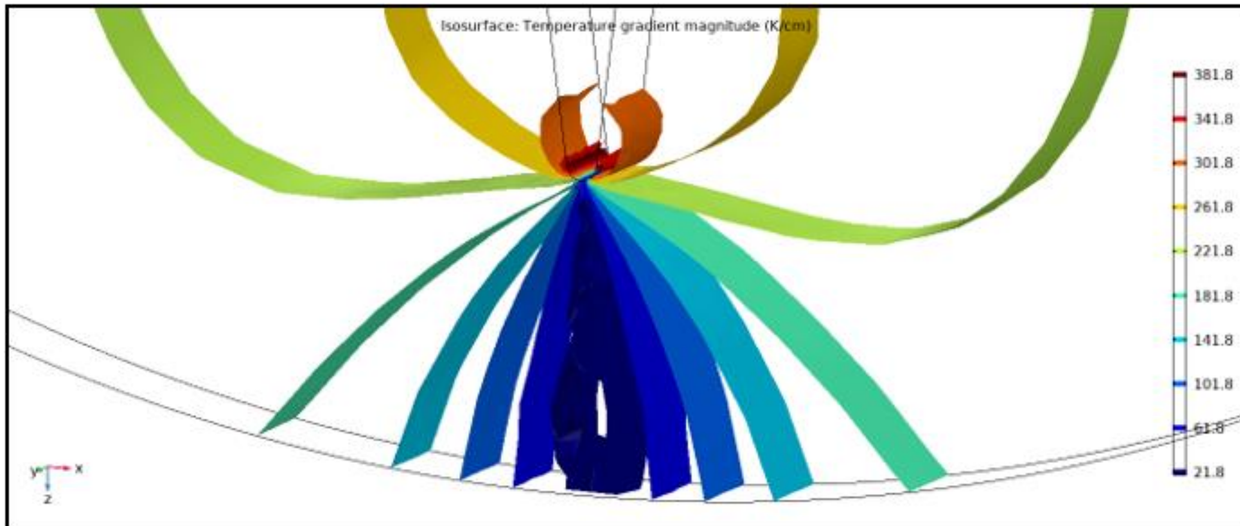

Figure 19: Iso-surface analysis of thermal gradient for fully modified specimen

It is seen that the current density hotspot is localized at the tip of the micro constriction notch from Figure 15. This isolates the region that is most susceptible to EM failure. With a 5 A current, the current density is found to be 1.199 x 10^5 A/cm^2, which is well over the minimum requirement for inducing EM in solder. From Figure 16, it is seen that there is significant Joule heating induced in the specimen due to current flow. The peak temperature is found to be 66.14 °C. The presence of Joule heating and ambient temperature induces a temperature gradient across the sample, with a peak value of 395 K/cm, as seen in Figure 18. However, this is within the 1000 K/cm requirement for TM predicted in Tu *et* al. [21]. Hence, it is expected that the dominant failure mode for this specimen model to be due to EM. It is also observed from Figure 15 and Figure 19 that the locations of peak current density and peak thermal gradient are different. This implies that if required conditions are met, EM and TM failure would originate from different locations. Additional results of the simulation are presented in Appendix B.

3.4 Testing Setup

This section describes the testing system used to age and record the resistance characteristics of solder wire specimens during characterization and EM experiments. A block diagram of the system is shown in Figure 20.

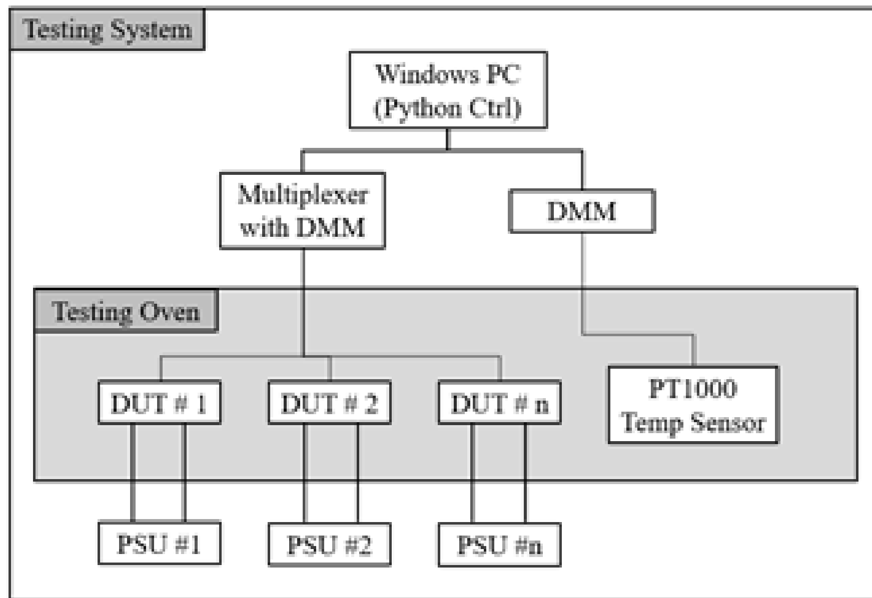

Figure 20: Test setup block diagram

The chamber with temperature control is realized using a testing oven [Binder GmbH - FP 53-UL (E1.1)]. A multiplexer (Keithley 6700) is chosen for voltage measurement so that multiple specimen voltages can be recorded in an experiment. The temperature of the chamber is recorded using a DMM (KeySight 34661A) with a PT100 temperature probe. Specimens are submitted to EM currents with individual power supply units (PSUs). The devices are connected to a PC using either GPIB or USB interfaces. The voltage measurement is automated using a custom-built code in Python 3.9 with the Spyder IDE [33-35]. This is given in Appendix A. The current levels in the PSUs are set manually to provide constant current. The data files recorded are stored in .mat format and are analyzed using MATLAB or GNU Octave [36-37].

Chapter 4
Design of Experiment

A 2-factor DOE is proposed to demonstrate the efficiency of the accelerated method described in Section 1.1, and to study the effect of temperature and current on EM in Sn-0.7Cu solder. The test conditions of the DOE cell are selected as a function of fusion current and thermo-electric characteristics of the solder.

4.1 Fusion current Characterization

The first phase of establishing a testable DOE cell is the fusion current characterization of the solder specimen. To determine the stressing current for an accelerated EM test, a characterization of the fusion current is carried out with 12 solder specimens. Each specimen resistance is first measured using 0.1 A at room temperature to obtain the initial resistance R_0. Then, the current is varied from 0.1 A to 5 A in steps of 0.5 A. Each current level is held for 30 s. The voltage is recorded to measure for continuity. The specimen is then stepped from 5 A until fusion in steps of 0.1 A held at 30 s. The value at which the voltage starts reading the fusion voltage, 8V in this case, indicates the fusion current. This voltage value does not influence the testing and is used only to identify the specimen having fused. An example of this process is shown in Figure 21. Data from the 12 specimens is shown in a plot versus R_0. The linear fit of the data is shown in Figure 22.

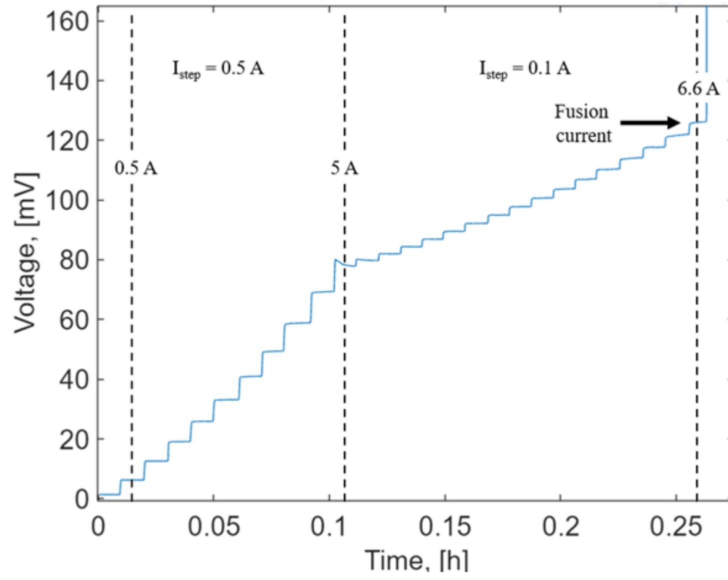

Figure 21: Fusion current testing example. The current is varied from 0.1 A in steps of 0.5 A up to 5 A, and then steps of 0.1 A until failure (fusion point at 6.6A). R_0 was 12.546 mΩ.

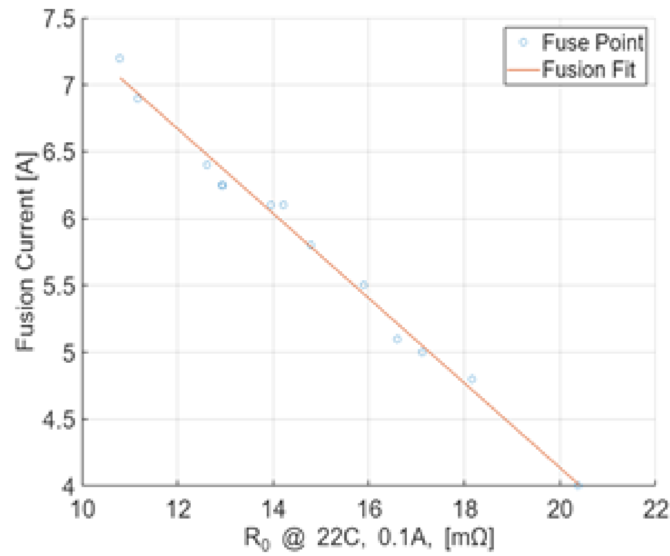

Figure 22: Initial resistance vs Fusion current for modified Sn-0.7Cu specimen

This shows the fitting equation linking fusion current and initial resistance to be,

$$I_{Fuse}[A] = (-0.317) \times R_0\ [m\Omega] + 10.47 \quad (18)$$

The selection of the current for an EM test is carried out for each specific specimen. The current is selected as a percentage of fusion current (*FCP*), e.g., $FCP = 80\ \%$ of the fusion current calculated from the measured R_0 of the specimen using Equation 6. An example of this process is shown in Figure 23 where specimens are tested at 70%, 75% and 80% *FCP* respectively, and at ambient temperature of 23 °C. It is seen that the specimen tested at 80% *FCP* fused first after 11.33 h, followed by 75% *FCP* in 102.61 h, and no fusion was seen in the 70% *FCP*, after 175 h of aging.

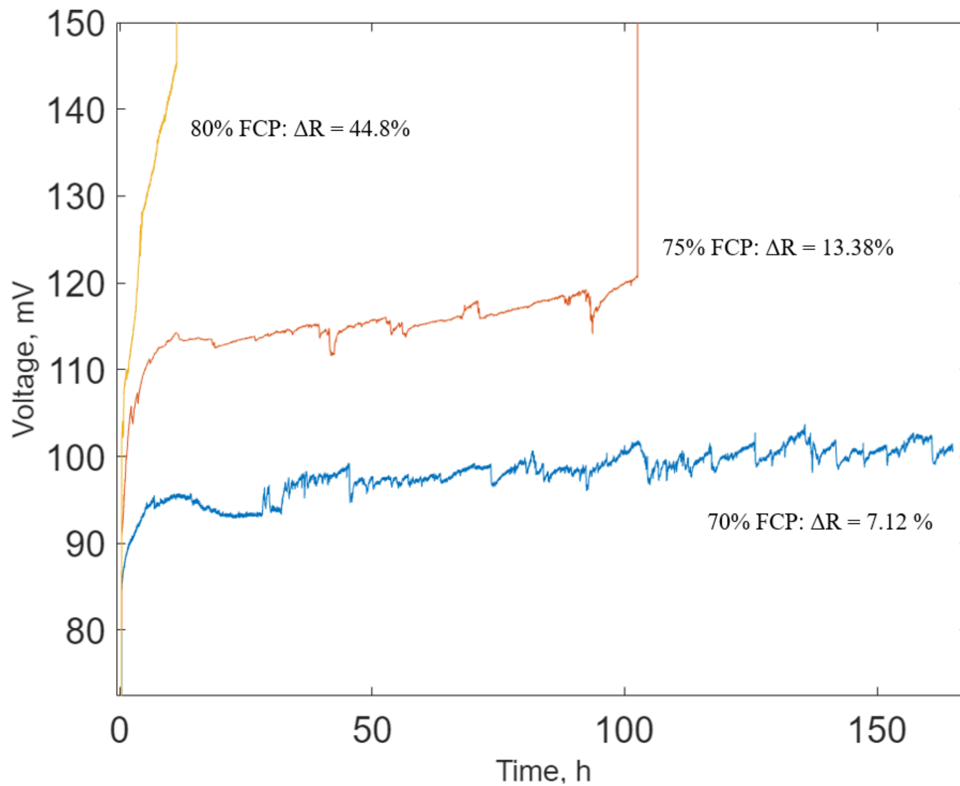

Figure 23: Sn-0.7Cu Specimens aged at ambient temperature of 23°C, and 80% *FCP* (Yellow), 75% *FCP* (Red), and 70% *FCP* (Blue), indicating a ΔR of 44.8%, 13.38% and 7.12% respectively.

4.2 Thermo-Electric Characterization

This phase of the characterization process consists of a thermal and a power characterization and involves applying different stress currents and temperatures and measuring the voltage drop across specimens. The characterization current levels were 0.1 A, then 0.5 A to 3.5 A in steps of 0.5 A. The hold

time was 5 min for each step. The characterization temperature levels (ambient temperature T_A) used were 25 °C, 45 °C, 65 °C, 85 °C and 100 °C, adjusted inside the oven. An example plot of the specimen voltage data is shown in Figure 24.

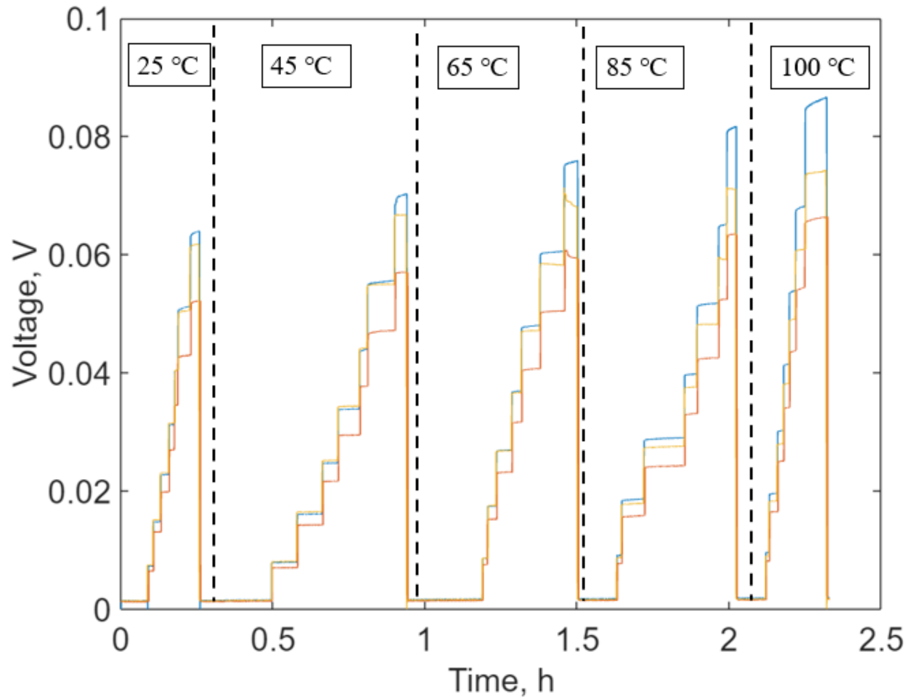

Figure 24: Data from three Sn-0.7Cu specimens stressed with various current levels up to 3.5 A and heated to various ambient temperatures from 25 °C to 100 °C

The dependence of the resistance, $R = V / I$, of a specimen on T_A and I was determined experimentally from the measured voltage, V. The peak resistance value for each current and temperature level is derived from Figure 24, and is plotted. This data was used to calculate the ideal unstressed resistance R_0 as the y-axis intercept value of the R versus I fits. The raw R vs I and the resulting R_0 versus T plot is shown in Figure 25.

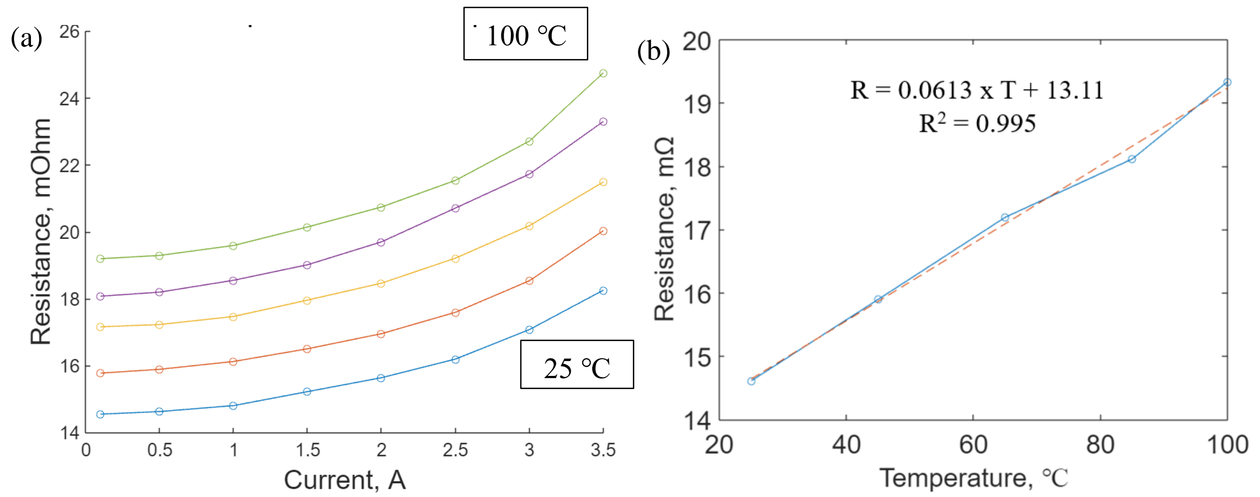

Figure 25: (a) Sn-0.7Cu Resistance vs Current plot for ambient temperature ranging from 25°C to 100°C (b)Ambient temperature vs initial resistance R_0 fit used to find *TCR*

The slope and intercept of this data is calculated to find the Temperature Coefficient of Resistance (*TCR*) of the specimen using,

$$TCR_{25°C} = \left[25°C + \frac{Intercept}{Slope}\right]^{-1} \tag{19}$$

The *TCR* value is found to be 4.183×10^{-3} K^{-1}.

The R-P characteristics of the sample can also be calculated from the raw data, by plotting the relation between the resistance at each current level with the power drawn. This is shown in Figure 26. The slope of these lines can be calculated to identify the thermal resistance (R_{th}) of the sample, at each temperature level. This relation is given as,

$$R_{th,T°C} = Slope_{T\,°C} \times \left(TCR \times R_{0.1\,A,T\,°C}\right)^{-1} \tag{20}$$

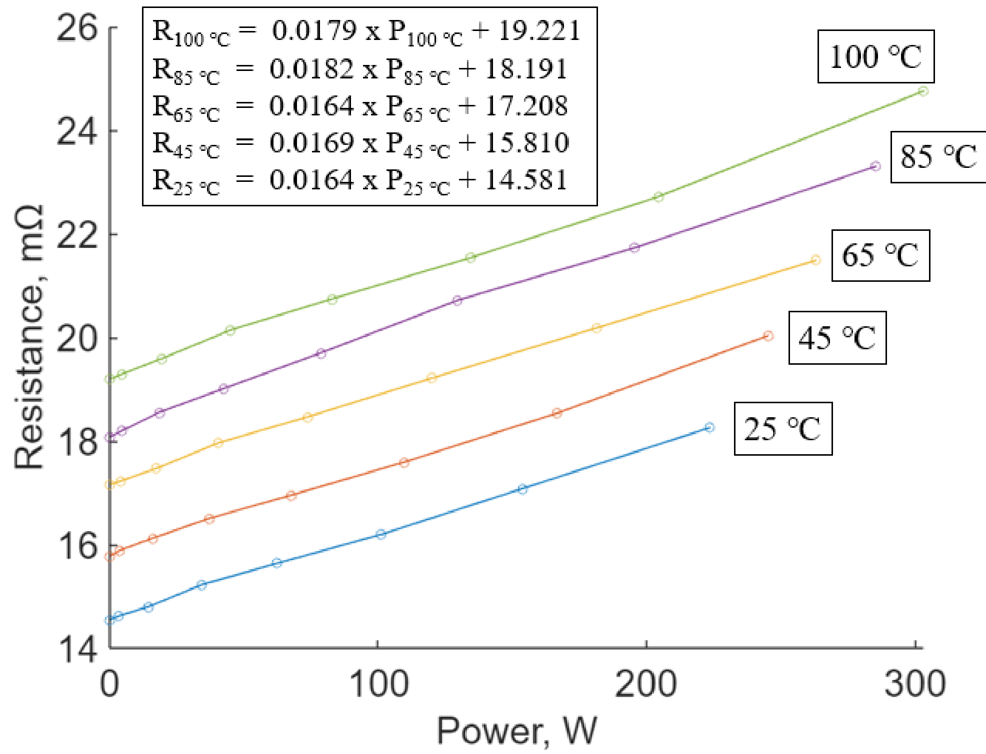

Figure 26: Sn-0.7Cu Specimen resistance for various power levels and T_A values. Data used to find thermal resistance R_{th}

Averaged over the five T_A values, the thermal resistance was found to be R_{th} = 280 ± 7 K/W. The specimen temperature T_S at each current and temperature level is then calculated using the R-P characteristics and the R_{th} values obtained and using,

$$T_S = P_S \times R_{th} + T_A \tag{21}$$

The relationship between the specimen temperature, stress current and ambient temperature is then obtained. This is shown in Figure 27.

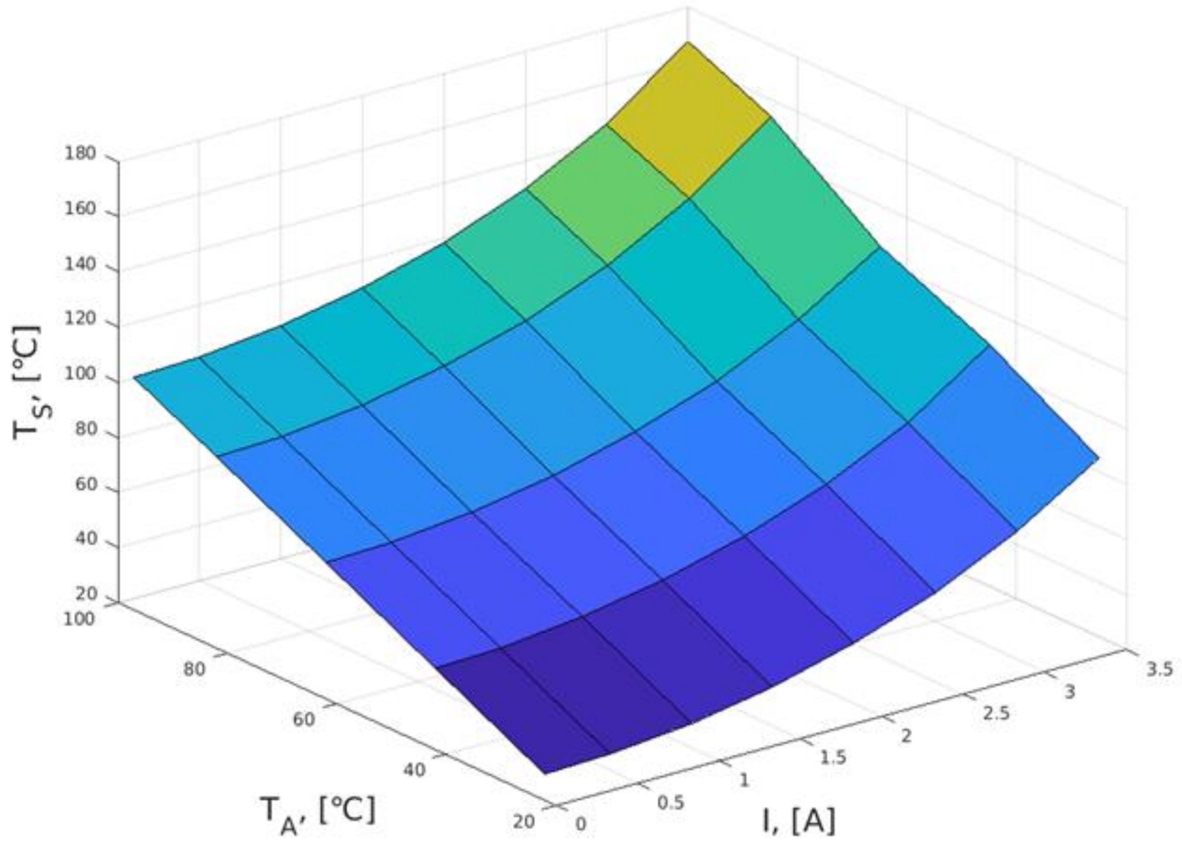

Figure 27: Sn-0.7Cu Specimen temperature fit as a function of stress current I and ambient temperature T_A

The 2D equation that fits specimen temperature to stress current and ambient temperature is obtained using a 3rd party algorithm [38] and is given as,

$$T_S = P_1 x^2 y^2 + P_2 x^1 y^2 + P_3 x^0 y^2 + P_4 x^2 y^1 + P_5 x^1 y^1 + P_6 x^0 y^1 + P_7 x^2 y^0 + P_8 x^1 y^0 + P_9 x^0 y^0 \qquad (22)$$

where x is current in A, y is ambient temperature in °C, and P_1 = 1.476e-4, P_2 = -2.543e-4, P_3 = 9.161e-5, P_4 = -6.871e-3, P_5 = 1.989e-2, P_6 = 0.992, P_7 = 5.913, P_8 = -4.103, P_9 = 1.261

The maximum error of this function, as difference between predicted and measured values, is found to be 0.945 °C. This equation can be inverted to calculate oven temperature as a function of specimen

temperature and current, or vice-versa. The inversion to find T_A for a desired set of T_A and I, is used in the next section and is given below in Equation 12.

$$0 = (P_1 I^2 + P_2 I^1 + P_3) {T_A}^2 + (P_4 I^2 + P_5 I^1 + P_6) T_A + (P_7 I^2 + P_8 I + P_9 - T_S) \quad (23)$$

4.3 DOE Cell determination

2-factor DOE testing is a powerful tool that can yield both qualitative and quantitative data. While it is ideal that the outcome of experiments is quantitative, when the model being tested is as complex as EM tends to be, it might be more practical to obtain accurate qualitative data. This section aims to use the characterization obtained so far to design a 2-factor DOE cell by varying current and specimen temperature. While it may be intuitive to vary the oven temperature, it is seen that there is a discrepancy between the oven and sample temperatures due to Joule Heating. Since Joule heating plays a crucial role in EM, it would be more useful to fix the specimen temperature instead of ambient temperature for DOE testing.

It is expected that the Top-Right (TR) corner of the cell would have the most extreme effect, in this case having the shortest *MTTF*, while the Bottom-Left (BL) corner has the least extreme effect. The other two corners would have a combined effect of the varied parameters. Samples are tested at room temperature and current levels from 75% to 90% of fusion current level, with steps of 5%, to identify a value at which samples fail in 2-3 hours. This is done so that when the test temperature is elevated to higher levels, the sample would fail in approximately 1-2 hrs. This current level was found to be 80%. An example test is shown in Figure 28.

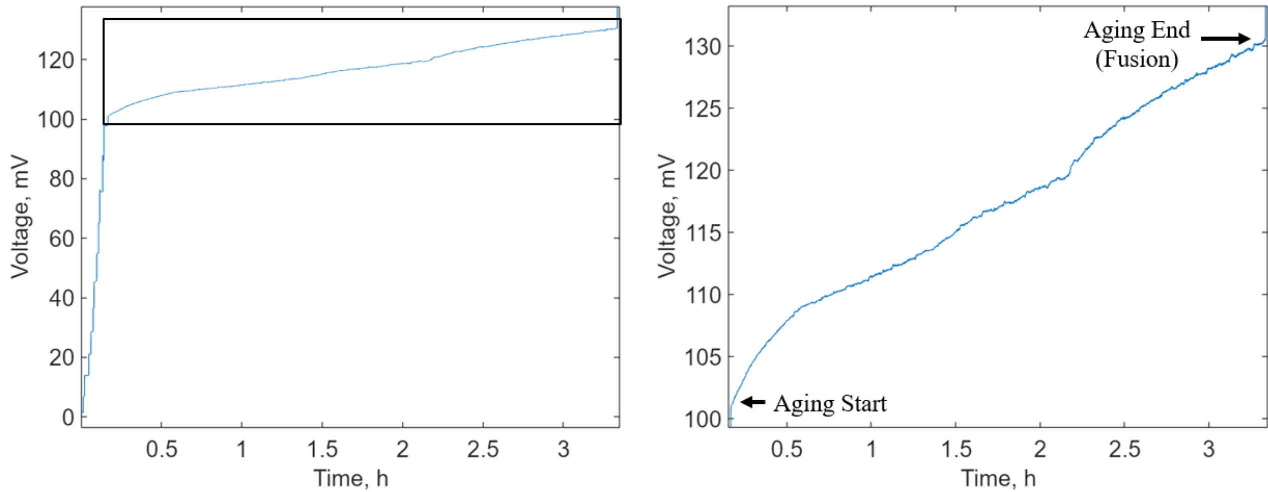

Figure 28: (a) Sn-0.7Cu Specimen aged in room temperature [23°C] at 80% *FCP* [I_{Fuse} = 6.32 A, I_{Stress} = 5.05 A], (b) Zoomed image of aging section highlighted in (a)

This sets the current level for the TR corner at 80% of fusion current, as well as the Bottom Right (BR) corner. The oven temperature is chosen to be 65 °C, approximately 50% of the temperature range of the characterization test. This is done in order to maximize the range of temperatures available for the rest of the DOE cell. Using the thermo-electric characterization, the specimen temperature at this level is found to be 181.25 °C, using Equation 12. This is be retained for the Top Left (TL) corner as well. The temperature for the BL corner is retained at 65 °C, and the current is experimentally chosen to be 75%, so that a majority of samples would fail within 24 hours. The specimen temperature at this level is found to be 165.95 °C. The TL corner is tested at 75% as well. With the specimen temperature and current level known for the BR corner, the ambient temperature is found to be 52 °C using Equation 12. Similar to *FCP*, the two specimen temperature levels can be presented as a percentage of fusion temperature. The Fusion Temperature Percentage (*FTP*) was found to be approximately 91% and 88% for the upper and lower levels respectively. Using the specimen temperature and current levels, the corresponding oven temperature is calculated. The testing condition data is summarized in Table 3, where *FCP* is varied by 5%, and *FTP* is varied by 3%. The DOE cell is presented in an ambient temperature vs current contour plot in Figure 29.

Table 3: DOE Testing Conditions

DOE Corner	FCP (%)	T_S (°C)	T_A (°C)
Top Right	80	181.25	65
Top Left	75	181.25	78
Bottom Right	80	165.95	52
Bottom Left	75	165.95	65

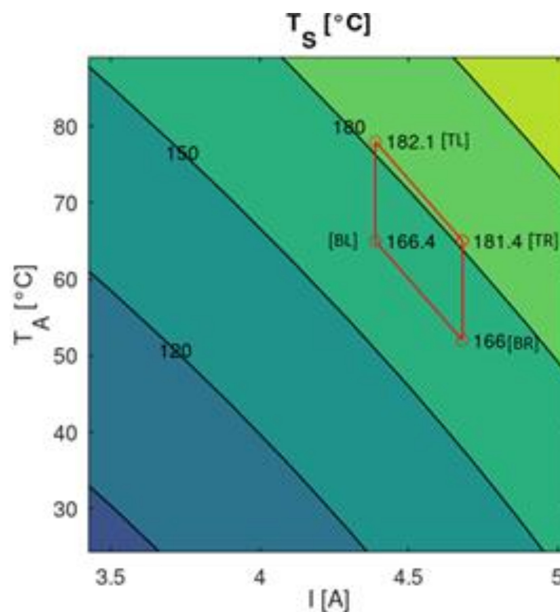

Figure 29: DOE cell in contour plot of Sn-0.7Cu specimen temperature as a function of current and ambient temperature

Having established the accelerated test conditions, samples are now tested at each corner of the DOE and failure data is collected. After failure, the samples are physically examined under a microscope for evidence of EM, which is indicated by voids at the constriction region and the presence of hillocks or whiskers on the anode (positive) side. The process flow for making and testing the samples, and reviewing the evidence is shown in Figure 30.

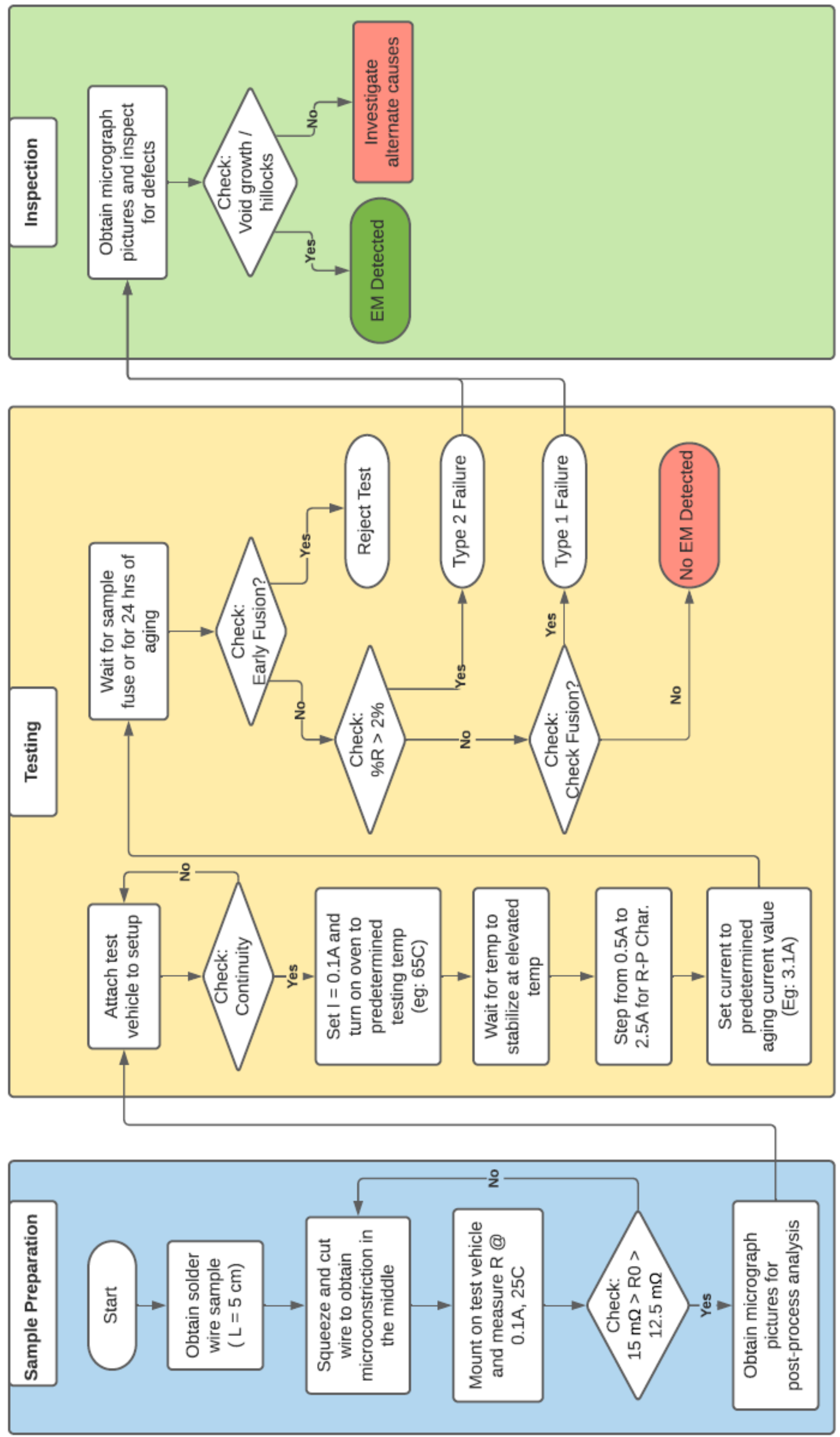

Figure 30: Flow chart of proposed EM sample preparation and testing process

Chapter 5

Results

The TR corner of the DOE is tested first with the setting listed in Table 1. The voltage vs. time data for 24 specimen tested in TR conditions is plotted in Figure 31.

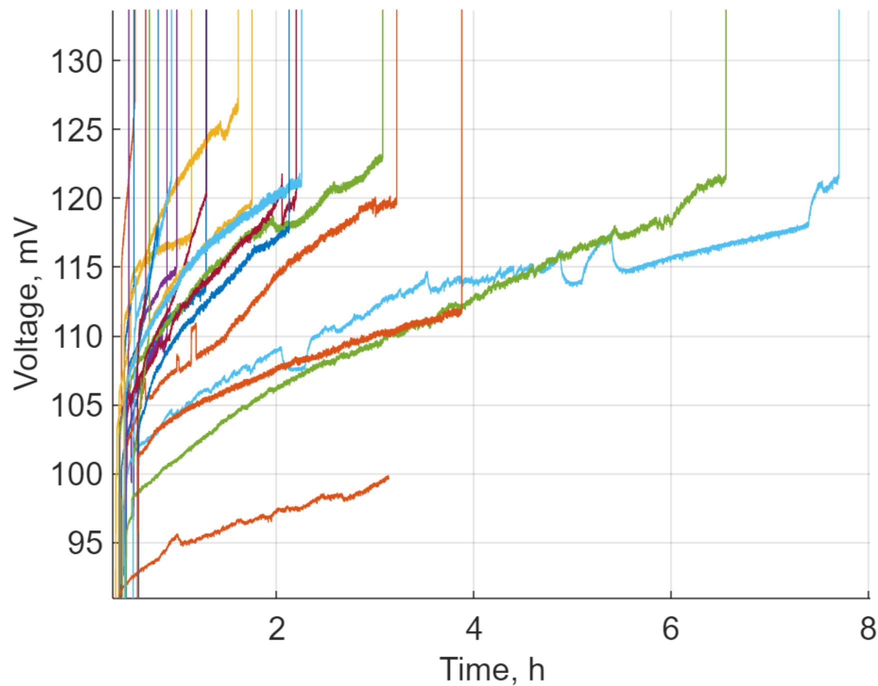

Figure 31: EM test results of voltage across Sn-0.7Cu constricted specimens tested at *FCP* = 80 % (*I* ranging from 4.4 A to 5 A) and T_A = 65 °C.

Out of 24 samples tested, 23 failed within 8 hours. It is seen that there is a gradual increase in voltage drop across the sample, before complete fusion. At this point, the voltage instantaneously rises to the set voltage of the power supply, being 8V. For the sake of this research, failure is defined as complete fusion of the sample. The penultimate point before the 8V sets, is taken as the Time-To-Failure (*TTF*).

5.1 Realtime Viewing of EM Failure

It is likely that this constant rise in resistance could be caused due to Joule heating. In order to rule this out, a room temperature aging trial is conducted under a microscope using a setup described in AbdelAziz et al. [39]. This setup, shown in Figure 32, allows the visual inspection of the sample while it is being aged. The sample is aged for 2 hours at 60% FCP and then stepping up to 80%. This data is shown in Figure 33. It is seen that at 60%, no change in voltage drop is seen, but after being stepped up to 80%, there is a gradual increase in voltage drop. The sample then fuses after approximately 2 hours. Images of the sample being aged are captured continuously and are stitched into a video. Select images are shown in Figure 34. Minimal change in geometry is seen for the first 2 hours. The sample then degrades quickly until it eventually fuses close to the 4.5-hour mark. A 12.68% resistance change is seen from the voltage data.

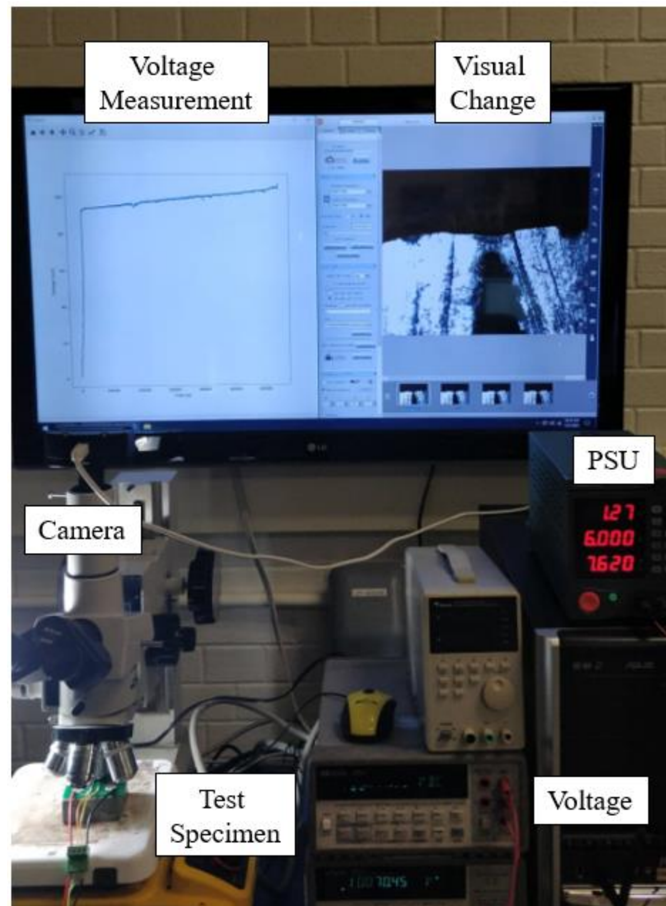

Figure 32: Realtime EM inspection setup used for visually recording EM degradation and resistance change while current stressing Sn-0.7Cu

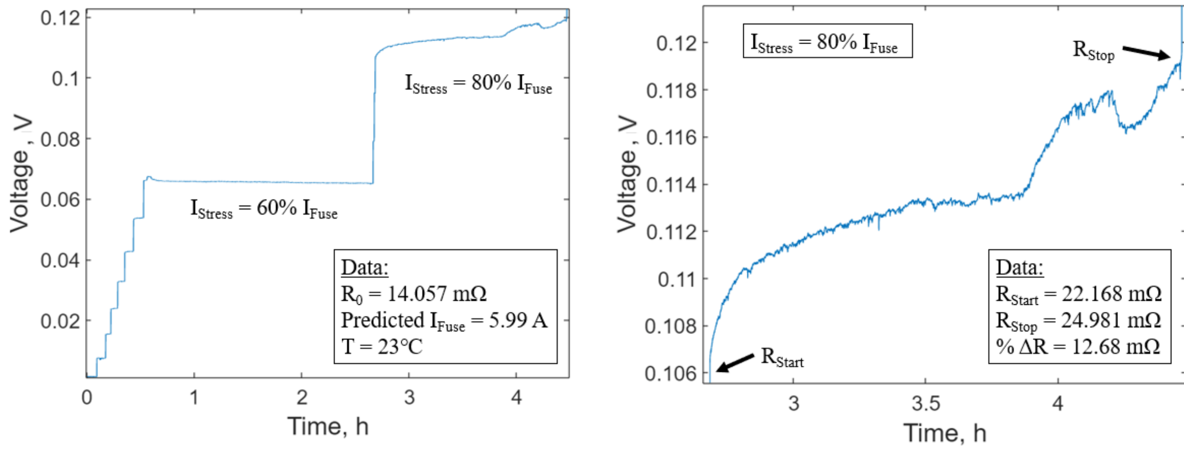

Figure 33:(a) Sn-0.7Cu specimen aged at 60% and then 80% *FCP* [I_{Fuse} = 5.99A, T_A = 23 °C]. (b) Voltage Drop of region under 80% *FCP*

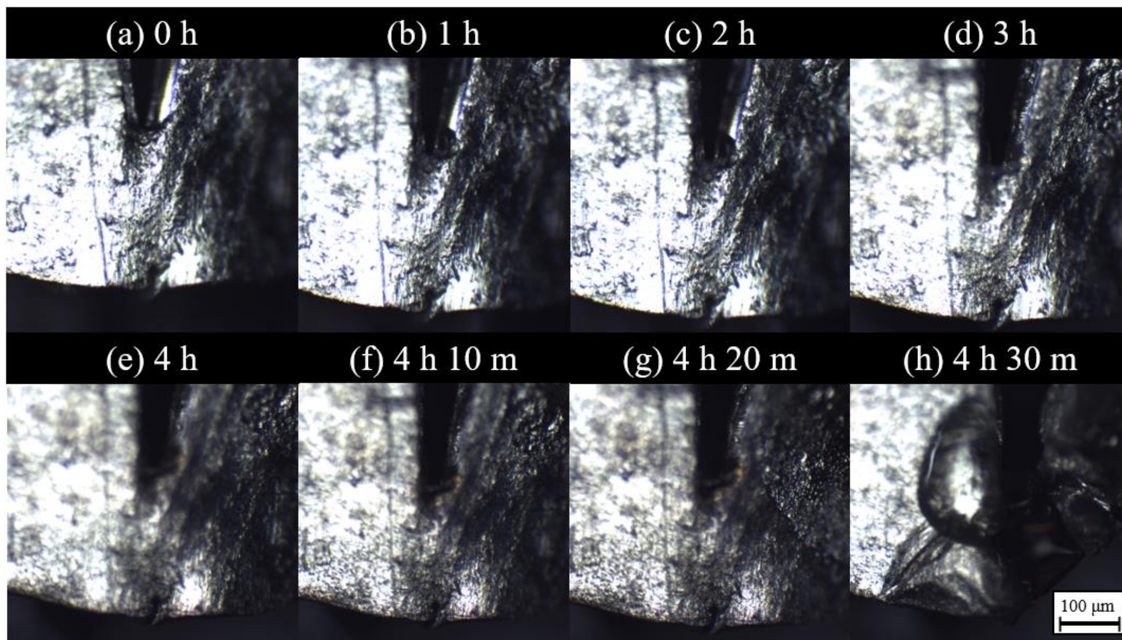

Figure 34: Real time image of Sn-0.7Cu specimen stressed at 60% and 80% *FCP* over 4.5 h

5.2 DOE Data analysis

The aging trials are repeated at all corners of the DOE and *MTTF* data is collected. The failure curves are shown in Figure 35 (a), (b), (c) and (d). As expected, the TL, BL and BR corners have less numbers of failed samples when compared to TR data. Those samples that did not fuse, reached a stable voltage after a few hours of aging and continued to show no change until the test was concluded. The *TTF* points of the failed samples are then collected from these plots for further analysis.

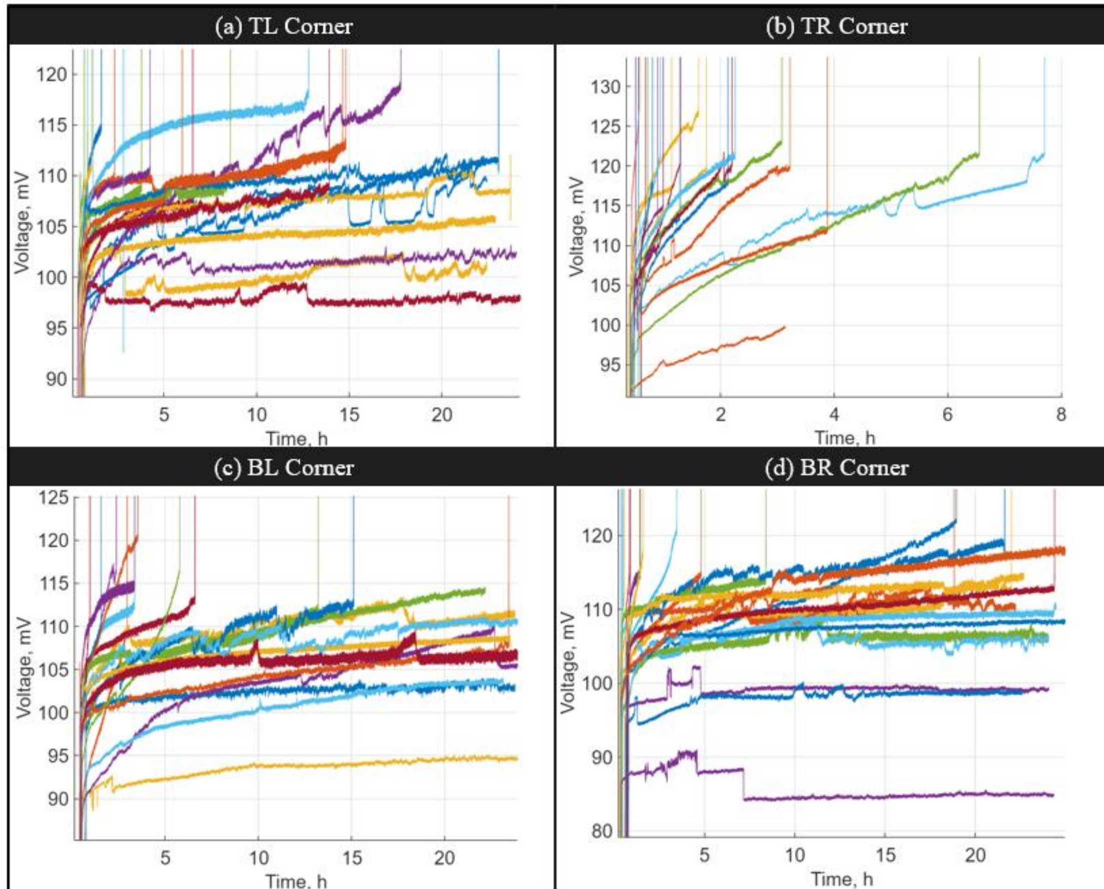

Figure 35: 24 Sn-0.7Cu specimens aged at (a) TL Corner [FCP = 75%, T_A = 78 °C] (b) TR Corner [FCP = 80%, T_A = 65 °C] (c) BL Corner [FCP = 75%, T_A = 65 °C] (d) BR Corner [FCP = 80%, T_A = 52 °C]

The data is modelled as both Weibull and Lognormal distribution to study the fit. The equations used for these fits are described in Section 2.4.1 and 2.4.2 respectively, without considering censored data. The Weibull data fit for the top right corner is shown in Figure 36, and the Lognormal fit is shown in Figure

37. Median ranking is used for developing the reliability function *R*. This allows for considering the numbers of samples failed out of the 24 tested in each corner. In first approximation, it appears that the data in both the models are not linear. However, this is due to the small N value that is tested. As N increases, the fit line will more closely follow the discrete data points. Hence, the fitting needs to be mathematically confirmed. This is done using both a χ^2 test and K-S test, as done in Kundu et al [40]. The χ^2 value and the maximum K-S CDF is found to be 20.476 and 0.115, respectively. The maximum allowable value for χ^2 and $D_{crit,KS}$ for $\alpha = 0.05$ is found to be 35.154 and 0.2700, respectively. This shows the Weibull fit is mathematically good for $\alpha = 0.05$. The η of the top-right corner is then found to be 3.036 hours.

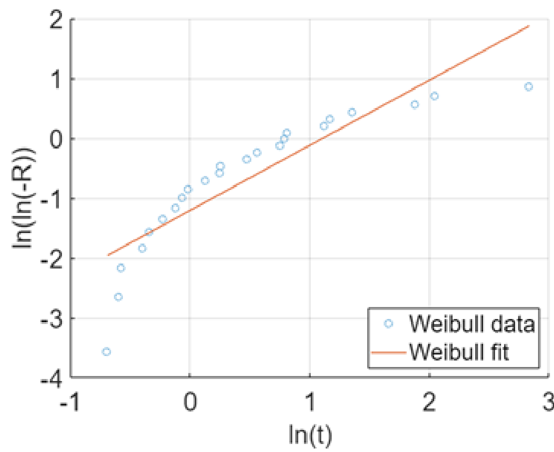

Figure 36: Weibull distribution of Sn-0.7Cu T-R data

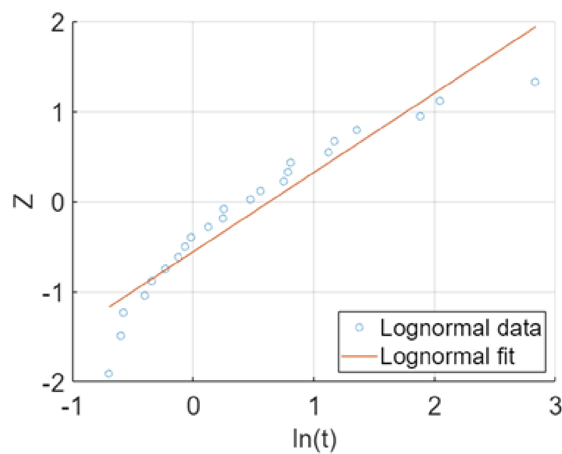

Figure 37: Lognormal distribution of Sn-0.7Cu T-R data

The fit and *MTTF* values for the other corners of the DOE are listed in Table 4. Based on the calculated χ^2 and $D_{crit,KS}$ value, Weibull and Lognormal distributions are found to be a good fit for the other corners as well. Despite Lognormal being the more popular for EM data, in this study, Weibull is found to be a better fit out of the two [26][41]. This is because of the suspiciously high *MTTF* value calculated for the BR leg using Lognormal fit, which is caused due to the predetermined end condition of the test. Since the testing is concluded after 24 h, instead of waiting until all samples fuse, the size of the corresponding data set obtained is smaller and is right-censored. Smaller data sets are better fit with Weibull distribution, which converges with Lognormal as 'K' increases [41]. The plots of the Weibull and Lognormal plots are shown in Figure 38 and Figure 39 respectively. The *TTF* data is listed in Appendix A– A.6.

Table 4: DOE test results - Lognormal and Weibull Analysis of Sn-0.7Cu data

Data		**Top-Right**	**Bottom Left**	**Top Left**	**Bottom Right**
N (Sample Tested)		24	24	24	24
K (Samples Failed)		22	12	16	14
Specimen Temp (°C)		181.25	165.25	181.25	165.25
FCP (%)		80%	75%	80%	75%
Lognormal	σ	1.135	1.795	1.797	2.489
	μ	0.634	2.909	2.42	3.1
	χ^2	10.468	7.244	2.891	12.157
	K.S.	0.106	0.089	0.0605	0.085
	MTTF (h)	3.594	91.989	56.612	492.71
Weibull	β	1.086	0.901	0.836	0.622
	χ^2	20.476	11.302	3.986	13.545
	K.S.	0.115	0.161	0.076	0.099
	η (h)	3.036	23.676	17.056	35.932

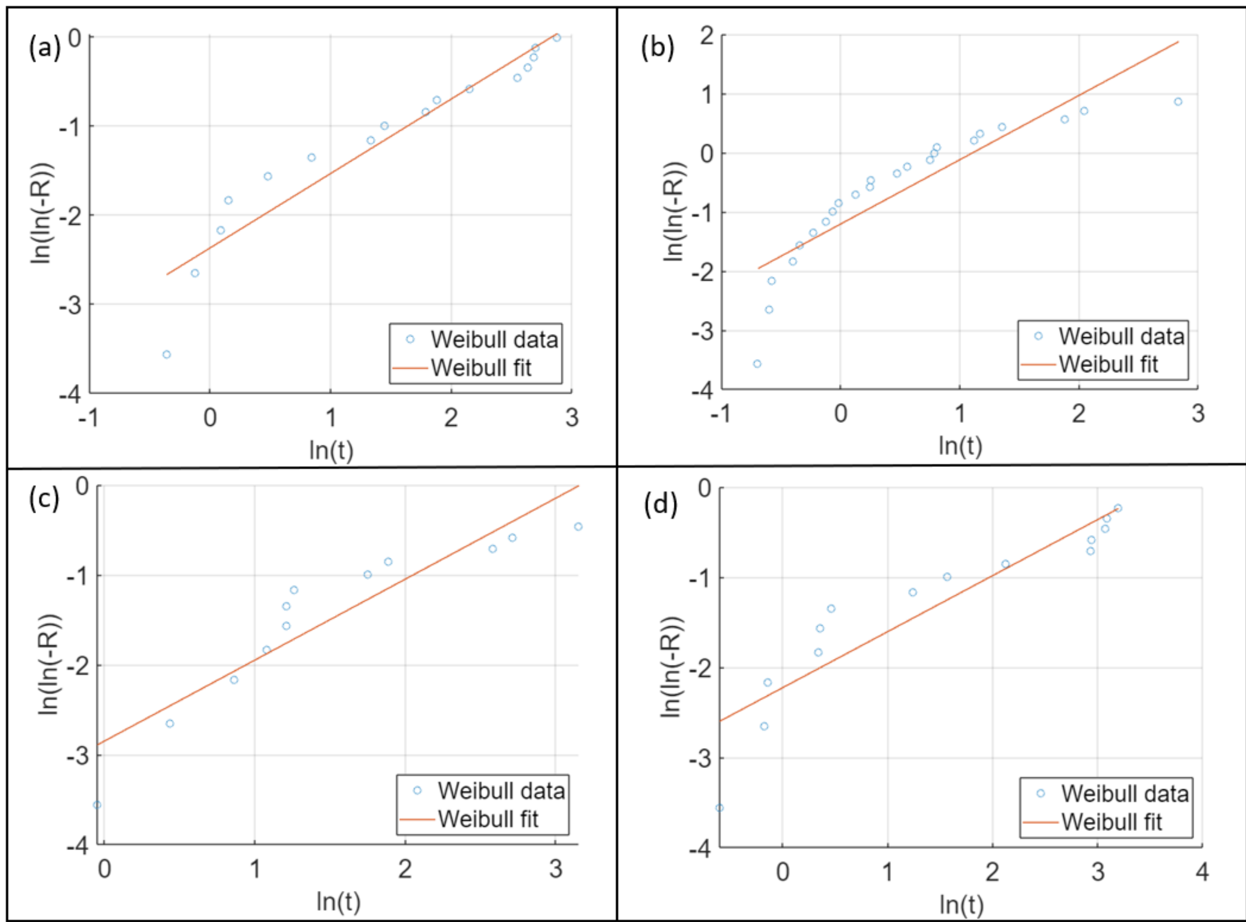

Figure 38: Weibull analysis of Sn-0.7Cu *TTF* data collected from (a) TL corner, (b) TR corner, (c) BL corner, (d) BR corner of DOE, with measured points shown in blue, and fit line shown in red

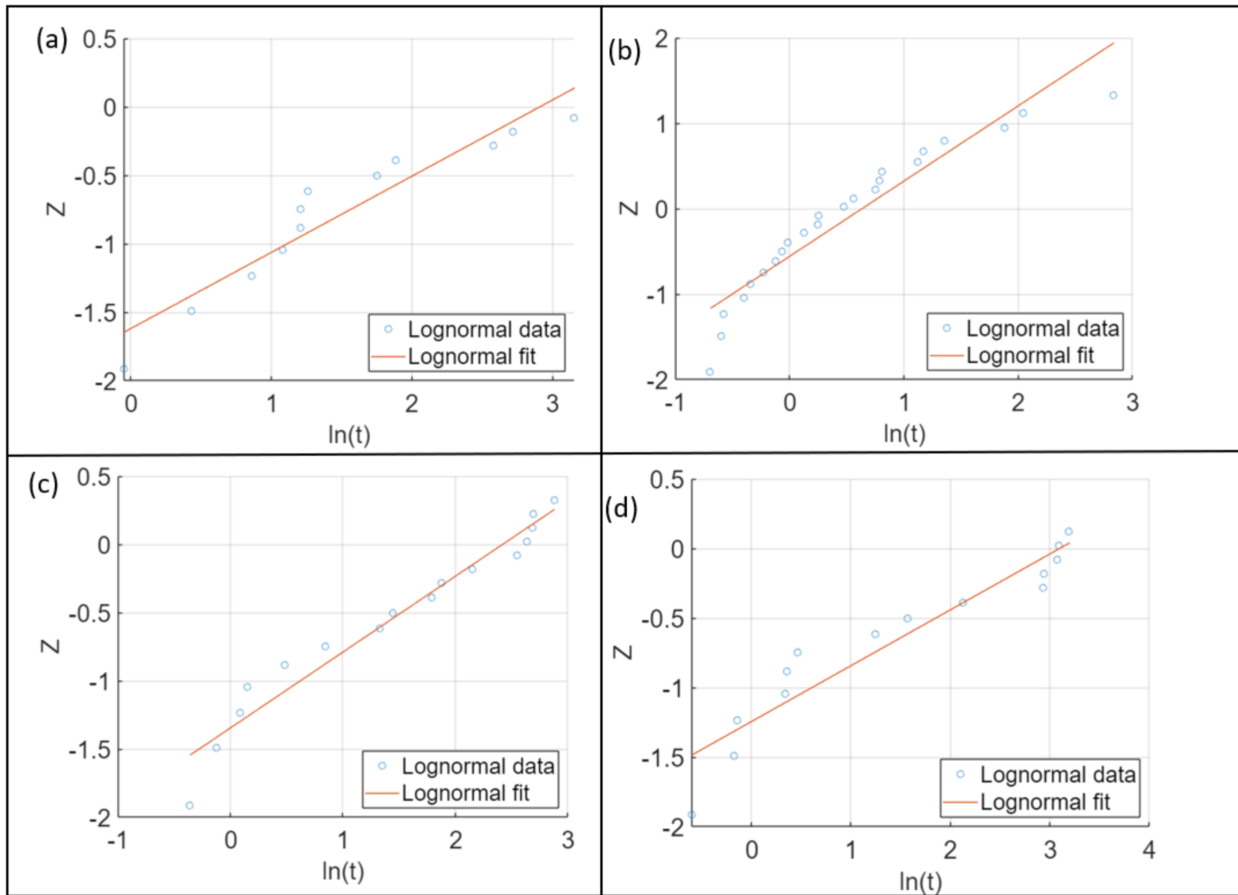

Figure 39: Lognormal analysis of Sn-0.7Cu *TTF* data collected from (a) TL corner, (b) TR corner, (c) BL corner, (d) BR corner of DOE, with measured points shown in blue, and fit line shown in red

It is expected in 2-factor DOEs that that TR leg has the highest treatment and the BL leg has the lowest treatment. Subsequently, the TR leg is expected to have the least *MTTF* while the BL has the highest. However, using conventional Weibull and Lognormal analysis, it is the BR corner which is found to have the highest *MTTF* in either case. One possible cause of this might be the improper handling of censored data in the experiments. For this reason, the data is also analysed using the techniques described in JESD37A to validate the results [28]. The equations used for this process are also described in Section 2.4.3. The censor time $T_{f\text{-}cen}$, is chosen as the last known failure time in each data set. The *N-K* unfailed samples are considered as the censored points. The plots obtained from this procedure are shown in Figure 40. The *MTTF* is calculated and is shown in Table 5. The code used is given in Appendix A– A.7.

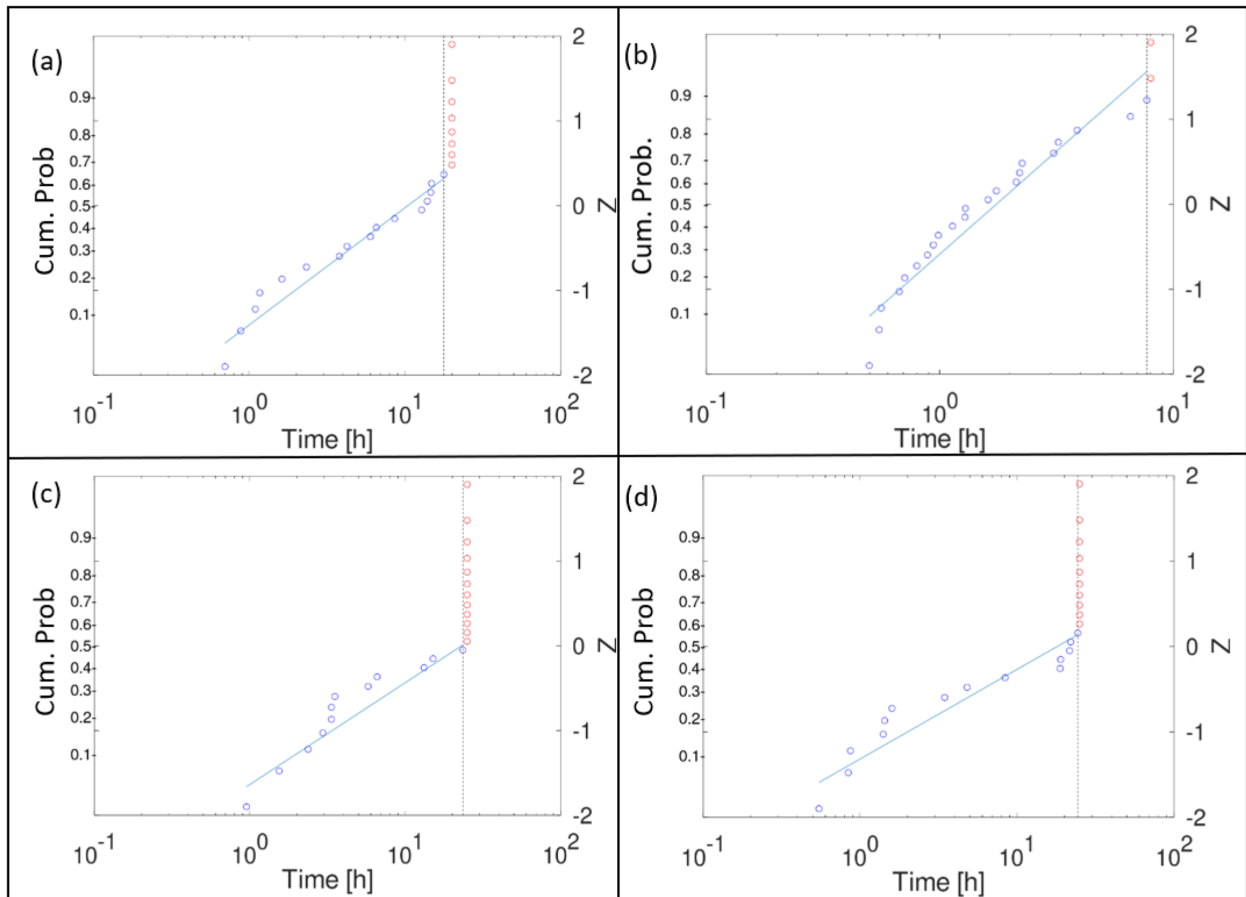

Figure 40: Censored Lognormal analysis of Sn-0.7Cu *TTF* data collected from (a) TL corner, (b) TR corner, (c) BL corner, (d) BR corner of DOE, with measured points and fit line shown in blue, censored points shown in red, and point of censoring shown in black (Left y-axis represents Cumulative Probability and right y-axis represents associated Z-score)

Table 5: DOE test results – Censored Lognormal analysis of Sn-0.7Cu data

Data	SnCu - TR	SnCu - BL	SnCu - TL	SnCu - BR
N (Tested)	24	24	24	24
K (Failed)	22	12	16	14
Specimen Temp (°C)	181.25	165.95	181.25	165.95
FCP (%)	80%	75%	75%	80%
s	0.94595	1.8912	1.6310	2.1879
$\ln(t_{50s})$	0.5563	3.1107	2.3101	2.8871
K.S.	0.10605	0.11130	0.06898	0.10939
MTTF (h)	1.7443	22.4358	10.0752	17.942

It is seen that the *MTTF* calculated using this approach appears more reasonable than estimates using conventional Weibull and Lognormal analysis. The expectation that the *MTTF* for the TR and BL legs being the shortest and longest values are also met.

5.3 SAC305 vs SnCu Comparison

The testing procedure was repeated on SAC305 (Sn-3Ag-0.5Cu) [41] as well in the TR conditions described in Section 4.3. The *TTF* data obtained is analysed using the process described in Section 2.4.3, and is compared with the TR data for SnCu. The calculated data is shown in Table 6 and the lognormal plot is shown in Figure 42. It is seen that SAC305 has a 21.6% higher *MTTF* than SnCu solder. This is supported by the study conducted by Lu *et* al., where SAC305 was predicted to have a longer lifetime under EM, due to the presence of twin structures and stable Ag_3Sn network [43].

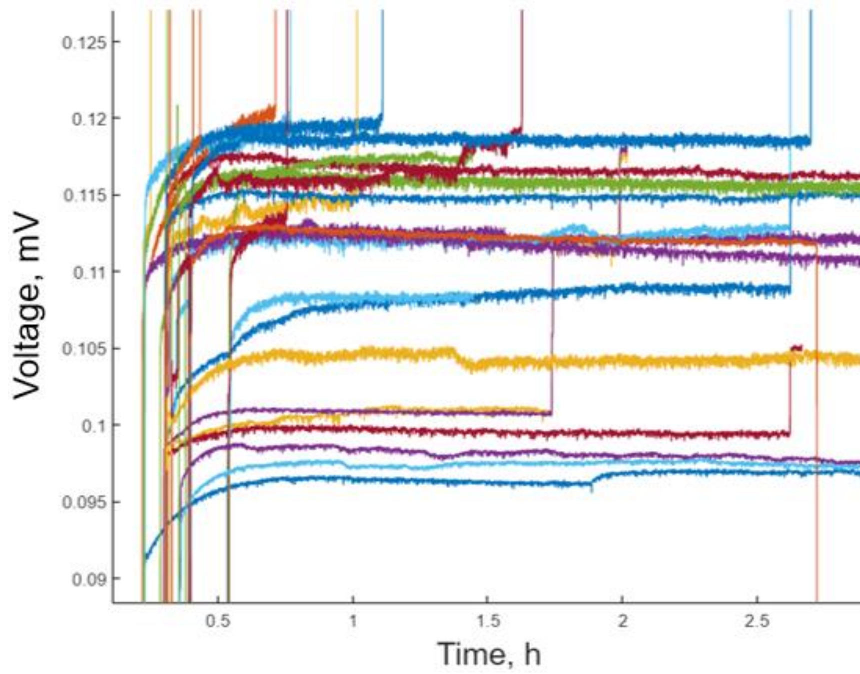

Figure 41: Voltage vs time raw data of 24 SAC305 specimen aged at *FCP* = 80%, T_A = 65 °C

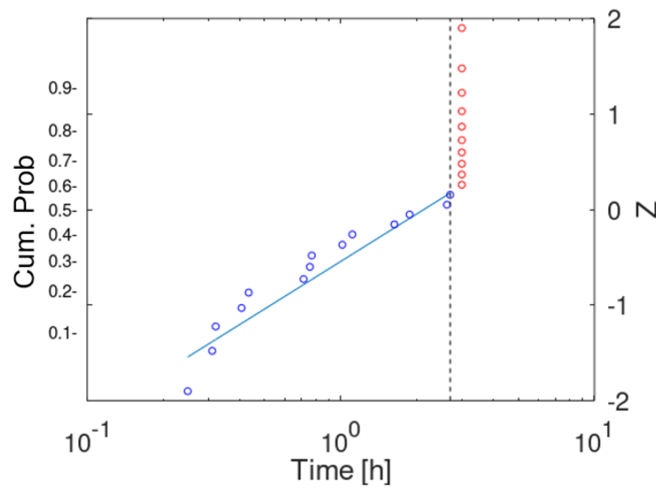

Figure 42: Censored Lognormal analysis of SAC305 *TTF* data tested at T_A = 65 °C, FCP = 80%, with measured points and fit line shown in blue, censored points shown in red, and point of censoring shown in black (Left y-axis represents Cumulative Probability and right y-axis represents associated Z-score)

Table 6: Comparison between Sn-0.7Cu and SAC305 tested at TR conditions

Data	SnCu	SAC305
N (Tested)	24	
K (Failed)	22	14
Specimen Temp (℃)	65 ℃	
FCP (%)	80%	
s	0.94595	1.3885
$\ln(t_{50s})$	0.5563	0.7519
K.S.	0.10605	0.08338
MTTF (h)	1.7443	2.1211

Chapter 6
Discussion

6.1 Raw data curves

It is obvious from Figure 31 and Figure 35 that the rate of degradation in samples is not always constant. Similar results are seen in other contemporary studies as well [20] [44-46]. This confirms the concern in Bernstein *et* al. that an exponential model like Black's equation would not be a good fit for modelling the data [8]. Hence, a Weibull fit is used to study the failure times.

The near-linear nature of the curves repeatedly seen in Figure 31, Figure 33 and Figure 35 is similar to the data presented by Minhua *et* al., where SnCu solder ball samples are tested [20]. The failure times are different to this study because of the difference in stress conditions applied. The current density exponent n reported in Minhua *et* al. has a value of 1.2. This is resemblant of void-growth limited failure as described by Lloyd [19], where n is approximately 1.

6.2 Effect of Acceleration

It is observed that the acceleration method described in this study, yields failure within a span of a few hours, while other contemporary studies take x100 – x1000 hours to reach failure [44-46]. In the study conducted by Madanipour et al. where conventional ball-solder is tested, 20-40% failure was observed in approximately 200 h [47]. Similarly, in Minhua *et* al. where SnCu solder was tested, *TTF* ranged from 150 – 250 h [20]. One reason for the faster failure time could be the achievement of higher current densities in this study (~10^5 A/cm^2), while the other studies use 10^3 – 10^4 A/cm^2. Presence of hillocks and whiskers were observed on the anode side of the wire solder specimens for all legs of the DOE, when inspected under a microscope. This indicates the dominance of EM related failure. Examples of such defects is shown in Figure 43 and Appendix C.

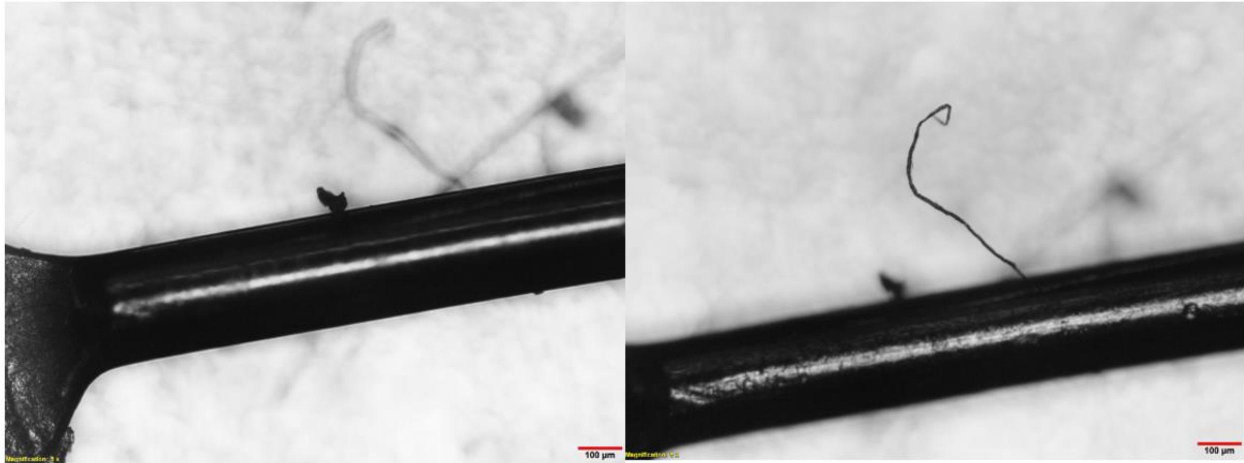

Figure 43: Example of hillock and whisker defects seen on Anode side of solder wire [*FCP* = 75%, T_A = 65°C]

6.3 DOE Effect Analysis

The censored lognormal analysis from JESD37A fits the *TTF* data gathered using the prescribed DOE, better than conventional Weibull or Lognormal data. The *MTTF* calculated in Table 5 is treated as the main effect caused by change in temperature and current. Using 2-factor effect analysis techniques, the effect of current and specimen temperature is found to be 6.412 h, and 14.279 h, respectively. The interaction effect between specimen temperature and stress current is found to be 1.918 h. This shows that a 5% increment in *FCP* reduces *MTTF* by approximately 6.4 h, while a 3% increase in *FTP* reduces the *MTTF* by approximately 14.3 h. The effect of temperature is found to be x2.22 times greater than the effect of current. This shows that temperature plays a more critical role than current for the selected DOE conditions. The interaction effect is found to be approximately 30% and 13.5% of current and temperature effect, respectively.

Chapter 7
Conclusion

7.1 Conclusions

Objectives 1, 2 and 3 listed in Section 1.1 have been met. A novel procedure for determining accelerated testing conditions using fusion current as the driving factor has been proposed. The DUT and test vehicle proposed can be used for real time EM monitoring, as demonstrated. It is also seen that under the current heuristic, meaningful EM failure is observed within 24 h of aging. The occurrences of material growth defects in the node point to EM being its dominant failure mechanism after the increase acceleration. Objective 4 has also been met. The proposed DOE was able to isolate the effects of temperature and current on *MTTF* as predicted. The proposed methodology can also be used to compare different solder material and obtain results within 24 h of testing. Factors influencing EM and TM in a material specimen may be interrelated and to determine their effects and their interaction is a complex task. To approach this task with a 2x2 DOE as reported here seems promising. Two factors should be chosen that have the strongest effect on EM and TM, respectively. For EM, a factor related to the current density in the material specimen is recommended. For TM, a factor related to the temperature gradient is recommended, in contrast to the specimen temperature used in this work. However, specimen temperature does play a role in EM, so it should be controlled, to obtain useful conclusions. More development work is required to get a truly robust method to obtain EM and TM results of solder-wire specimens within a few hours. Such an improved method would add to the in-depth understanding of EM in electronics packaging by reducing effort and cost of data collection.

7.2 Recommendations

Similar to isolating the effects of temperature and current, future experiments of this research can focus of isolating the effects of EM and TM. This can be done by controlling the R_{th} of the specimens, through active temperature regulation, such as using a fan. Alternatively, the sample preparation process could also be automated, to produce samples with a consistent R_{th}, as it is dependant of sample geometry. The effect of annealing on the specimen can also be studied. Since the specimen are formed

through mechanical processes, stresses would have likely built up, which would need annealing to normalize.

Another possible improvement would be to address the constant variance in current density or specimen temperature during the process of degradation. Under the current heuristic, current and ambient temperature are kept constant throughout the aging process and are used to calculate the initial value of the current density and specimen temperature at the start of the test. However, as the aging progresses, the AoC is bound to decrease, causing an increase in the current density and specimen temperature due to joule heating. In order to derive more accurate values from an Arrhenius fitting, the current and ambient temperature would have to be varied throughout the aging process such that the current density and specimen temperature are truly kept constant. A similar approach was considered for wafer level testing in Jones and Smith [48]. In this case the ambient temperature was kept constant, and the current was continuously varied to keep the initial resistance, and specimen temperature constant.

In this study, the conventional approach of testing samples in a daisy-chain was abandoned in favor of parallel testing. This was done because the failure of the weakest specimen in a daisy chain would cause the entire line to fail, which would lead to increased right-censoring of the resultant TTF data set. The testing topology could be altered such that multiple units of the proposed test vehicle would be used in series with a relay board designed to automatically shunt a specimen once its failure condition has been met, thereby allowing for the rest of the sample to continue aging. This eliminates the right censoring of the data. The design for such a relay board is proposed in Appendix D.

References

1. M. T. Jens Lienig, “Fundamentals of Electromigration-Aware Integrated Circuit Design”, *Springer International Publishing*, 2018.
2. P.S. Ho, T. Kwok,"Electromigration in Metals", *Rep. Prog. Phys.*, vol. 52(3), pp. 301-348, 1989
3. Merrill L. Minges (1989). “Electronics Materials Handbook: Packaging”. *ASM International*. p. 970. ISBN 978-0-87170-285-2
4. G. Georgakos, U. Schlichtmann, R. Schneider, S. Chakraborty, “Reliability challenges for electric vehicles: From devices to architecture and systems software”, *A CM/IEEE Design Automation Conference (DAC)*, 2013
5. J.R. Black, "Electromigration-A brief survey and some recent results," *IEEE Trans. on Electronic devices*, vol. 16, no. 4, pp. 338-347, Apr. 1969
6. NCES. “Consumer electronics and tech devices average lifespan 2015” *Statista - The Statistics Portal*, May 2016, Web. 19 March 2021.
7. Joseph B. Bernstein, “Chapter 3 - Failure Mechanisms, Reliability Prediction from Burn-In Data Fit to Reliability Models”, *Academic Press*, 2014, pp. 31-48, ISBN 9780128007471
8. M. White and J. B. Bernstein, “Microelectronics Reliability: Physics-of-Failure Based Modeling and Lifetime Evaluation,”, *NASA Electronics Parts and Packaging Program*, Feb-2008. [Online].
9. JEDEC Solid State Technology Association, “Guideline for Characterizing Solder Bump Electromigration under Constant Current and Temperature Stress”, JEDEC – JEP154A, 2008
10. I. A. Belch, E.S. Meieran, “Electromigration in thin aluminium films”, *J. Appl. Phys.*, vol. 40(2), pp. 485 - 491, 1968
11. H.A. Schafft, T.C. Staton, J. Mandel, “Reproducibility of electromigration measurements”, *IEEE Trans. On Elect. Dev.*, ED-34, pp. 673-681, 1987
12. W. Baerg, K. Wu, “Using metal grain size distributions to predict electromigration performance”, Solid State Technology, pp. 35-37, 1991
13. J. Cho, C.V. Thompson, “Grain size dependence of electromigration-induced failures in narrow interconnects”, Appl. Phys. Lett., vol. 54(25), pp. 2577-2579, 1989
14. R. Shaviv, G. J. Harm, S. Kumari, R. R. Keller and D. T. Read, "Electromigration of Cu interconnects under AC, pulsed-DC and DC test conditions," *2011 International Reliability Physics Symposium*, Monterey, CA, USA, 2011.

15. J. R. Lloyd, “Electromigration failure”, *J. Appl. Phys*., vol. 69(11), pp.7601-7604, 1991
16. E.C.C. Yeh, W.J. Choi, K.N. Tu, “Current crowding induced electromigration failure in flip chip solder joints”, *Applied Physics Letter*, vol. 80, no. 4, pp. 580 - 582, 2002
17. C. Basaran, S. Li, D.C. Hopkins, D. Veychard, “Electromigration time to failure of SnAgCuNi solder joints”, *J. Appl. Phys*., Vol. 106, 013707, 2009
18. W. Li, C. M. Tan, N. Raghavan, “Dynamic simulation of void nucleation during electromigration in narrow integrated circuit interconnects", *J. Appl. Phys.*, 105, 014305, 2009
19. J.R. Lloyd, “Black’s Equation Revisited - Nucleation and Growth in Electromigration Failure”, *Microelectron. Reliab.*, vol 47, no. 7, pp. 1468-1472, 2007
20. M. Lu, D.Y. Shih, “Comparison of Electromigration Behaviors of SnAg and SnCu Solders”, *47th Annual International Reliability Physics Symposium*, Montreal, 2009
21. K.N. Tu, “Solder Joint Technology - Materials, Properties and Reliability”, *Springer,* 2007
22. A. Heryanto, K.L.Pey, Y.Lim, et al., “Study of electromigration and stress migration in copper/low-k interconnects”, *IEEE International Reliability Physics Symposium (IRPS)*, pp 586 - 590, 2010
23. C. Chen, H.M. Tong, K.N. Tu, “Electromigration and Thermomigration in Pb-Free Flip-Chip Solder Joint”, *Annual Review of Materials Research*, vol. 40, pp. 531-555, 2010
24. K. N. Tu, A.M. Gusak, “A unified model of mean-time-to-failure for electromigration, thermomigration, and stress migration based on entropy production”, *J. Appl. Phys.*, vol. 12, 075109, 2019
25. K. Weide-Zaage, D.Dalleau, X.Yu, “Static and dynamic analysis of failure locations and void formation in interconnects due to various migration mechanisms”, *Material Science Semiconductor Processes*, vol. 6(1-3), pp. 85-92, 2003
26. A. Basavalingappa, J. M. Passage, M. Y. Shen and J. R. Lloyd, "Electromigration: Lognormal versus Weibull distribution," *2017 IEEE International Integrated Reliability Workshop (IIRW)*, South Lake Tahoe, CA, USA, pp. 1-4, 2017
27. D. B. Kececioglu, “Reliability Engineering Handbook, Volume 1”, *DEStech Publications*, 2002
28. JEDEC Solid State technology Association, “Lognormal analysis of uncensored data and of singly Right-Censored data utilizing the Persson and Rootzen method”, JEDEC – JESD37A, 2017
29. Lead Free No-Clean Wire Solder Sn96.5Ag3Cu0.5 (96.5/3/0.5) 24 AWG, 25 SWG Spool, 17.64 oz, Kester Solder, Illinois, USA, PN 96-7069-9520, Available: https://www.digikey.ca/en/products/detail/kester-solder/96-7069-9520/8021513 [Online]

30. COMSOL Multiphysics, “Introduction to COMSOL multiphysics”, v.5.6., COMSOL AB, Stockholm, Sweden, 2020
31. M. Zhao , L. Zhang , Z. Q. Liu , M. Y. Xiong & L. Sun, “Structure and properties of Sn-Cu lead-free solders in electronics packaging”, *Science and Technology of Advanced Materials*, 20:1, pp. 421-444, 2019
32. D. R. Smith, T. Seiwert, L. Stephen, J. C. Madeni, “Database for Solder Properties with Emphasis on New Lead-free Solders”, 2002
33. Python Core Team (2021). Python: A dynamic, open-source programming language. Python Software Foundation
34. P. Raybaut, (2009). Spyder-documentation. Available online at: pythonhosted.org
35. A.V. Sudharsan, (2021) Electromigration Data Analysis, GitHub repository, https://github.com/SudhaVenky/Electromigration-Data-Analysis
36. MATLAB. version 9.10.0.1629609 (R2021a). Natick, Massachusetts: The MathWorks Inc.; 2021
37. John W. Eaton, David Bateman, Søren Hauberg, Rik Wehbring (2019). GNU Octave version 5.2.0 manual: a high-level interactive language for numerical computations.
38. Mark Mikofski (2021). polyVal2D and polyFit2D (https://www.mathworks.com/matlabcentral/fileexchange/41097-polyval2d-and-polyfit2d), MATLAB Central File Exchange. Retrieved February 20, 2021.
39. M. AbdelAziz, D. E. Xu, G. Wang, M. Mayer, “Electromigration in Solder Joint: A cross-sectioned model system for real time observation”, *Microelectronics Reliability*, vol. 119, 2021
40. D. Kundu, A. Manglick, “Discriminating between the Weibull and Lognormal Distributions”, *Naval Research Logistics*, vol. 51, No. 6, pp. 893-905, 2004
41. Lead Free 2.7% REM1 Flux Wire Solder Sn99.3Cu0.7, 24 AWG, 50 mg, Lidl - Parkside, Germany, IAN 322640
42. S.R. Cain, “Distinguishing between lognormal and weibull distributions [time-to-failure data]”, *IEEE Transactions on Reliability*, Vol. 51, No. 1, pp. 32-38, 2002
43. M. Lu, D.Y. Shih, P. Lauro, C. Goldsmith, D.W. Henderson, “Effect of Sn grain orientation on electromigration degradation mechanism in high Sn-based Pb-free solder”, *Appl. Phys. Lett.,* vol. 92, 211909, 2008

44. S. Bae, J. Judy, I.F. Tsu, E. Murdock, “Electromigration-induced failure of single layered NiFe Permalloy thin films for a giant magnetoresistive read head”, *Journal of Applied Physics*, vol. 90. pp. 2427-2432, 2001
45. K. Lee, K.S. Kim, Y. Tsukada, K. Suganuma, K. Yamanaka, K. Suichi, M. Ueshima, “Effects of the crystallographic orientation of Sn on the electromigration of Cu/Sn-Ag-Cu/Cu ball joints”, *Journal of Materials Research*, vol. 26, pp. 467-474, 2011
46. Q. Sun, Y. Lu, C. Tang, H. Song, C. Li, C. Zou, “Current Induced Changes of Surface Morphology in Printer Ag Thin Wires”, *Materials*, vol. 12, 3288, 2019
47. H. Madanipour, Y.R. Kim, C.U. Kim, D. Mishra, P. Thompson, “Study of electromigration in Sn-Ag-Cu micro solder joint with Ni Interfacial layer”, *J. Alloy. Comp.*, vol. 862, 2021
48. R.E. Jones, L.D. Smith, “A new wafer level isothermal Joule-heated electromigration test for rapid testing of integrated circuit interconnect”, J. Appl. Phys., vol. 61(9), pp. 4670 - 4678, 1987

Appendix A
Matlab and Python Code

The code in this section is used for generating the plots presented in this thesis. They can be obtained online from [35].

A.1 Fusion Current Testing (Python)

This code is used for measuring the fusion current of a specimen, as shown in Section 4.1.

File name: SW-001-FusionCurrentTesting

```
# -*- coding: utf-8 -*-
"""
Created on Thu Sep 26 13:23:50 2019
1. This program measures fusing current of a given sample
   by stepping the current from 0.1A to 5A with a step of 0.1A
2. Time and voltage of the sample are recorded
Insturments:
    Keysight N6700C 5A Power Supply
    Keysight 34461A 10A DMM

@author: sazisurv
"""

#%% Reset All
from IPython import get_ipython
get_ipython().magic('reset -sf')


#%% Import packages required for this code
import visa
import time
import matplotlib.pyplot as plt
import subprocess
import scipy.io

#%% Close all plotting windows
plt.close('all')

#%% Saving File Name Initialization, Change before Run!
sampleName = ' FusionTest - Microconstriction - 4W - T1'
fname=time.strftime("%y%m%d%H%M%S",time.localtime()) + sampleName
```

```
SetCurrent = 0.1
cycleDone = 0
t_step = 10
#%% initialize variable
V = []
t = []
T = []
a = []

#%% Call PyVisa's Resource Manager
rm = visa.ResourceManager()

#%% Open GPIB Addresses, Change before Run!
#ammeter = rm.open_resource('USB0::0x2A8D::0x1301::MY59005979::0::INSTR')

#A34411 = rm.open_resource('USB0::0x2A8D::0x1301::MY59005979::0::INSTR')  #
measure voltage
DCsource = rm.open_resource('USB0::0x2A8D::0x0002::MY56008842::0::INSTR') #
DC Power Supply
multiplexer = rm.open_resource('GPIB0::25::INSTR') # Multiplexer for Voltage
measurement


#A34411.write('SYSTem:REMote')
#A34411.write('*RST') #factory reset
#A34411.write('*CLS') #clear memory
#A34411.write('CONFigure:VOLTage:DC') #Setup to measure V

multiplexer.write('*RST')
multiplexer.write('*CLS')
multiplexer.write('CONFigure:VOLTage')

DCsource.write('*RST')
DCsource.write('*CLS')
DCsource.write('VOLT 8,(@1)')
DCsource.write('CURR %s,(@1)' % (str(SetCurrent)))
DCsource.write('OUTPUT ON,(@1)')

#%% Start the Timer
tic = time.perf_counter()
multiplexer.write(':ROUTe:OPEN:all') # Open all channels
multiplexer.write(':ROUTe:CLOSe (%s)' % ('@102')) #close a channel for
reading
rawstr = multiplexer.query('read?')
index=rawstr.find('VDC')
volStr = rawstr[0:index]
```

```
Vvalue = float(volStr)


while cycleDone == 0:

    for i in range (1, 31):   #Stepping from 0-3A

        StepStart = time.perf_counter()

        while time.perf_counter() - StepStart <t_step:
            DCsource.write('CURR %s,(@1)' % (str(i * SetCurrent)))
            multiplexer.write(':ROUTe:OPEN:all') # Open all channels
            multiplexer.write(':ROUTe:CLOSe (%s)' % ('@102')) #close a
channel for reading
            rawstr = multiplexer.query('read?')
            index=rawstr.find('VDC')
            volStr = rawstr[0:index]
            Vvalue = float(volStr)
            toc=time.perf_counter()
            V.append(Vvalue)
            t.append(toc-tic)

        # End of While loop

    #End of For loop

    for i in range (1, 41):   #Stepping from 3A - 5A

        StepStart = time.perf_counter()

        while time.perf_counter() - StepStart <t_step:
            DCsource.write('CURR %s,(@1)' % (str(3 + i*0.05 )))
            multiplexer.write(':ROUTe:OPEN:all') # Open all channels
            multiplexer.write(':ROUTe:CLOSe (%s)' % ('@102')) #close a
channel for reading
            rawstr = multiplexer.query('read?')
            index=rawstr.find('VDC')
            volStr = rawstr[0:index]
            Vvalue = float(volStr)
            toc=time.perf_counter()
            V.append(Vvalue)
            t.append(toc-tic)

        # End of While loop

    #End of For loop
```

```
    DCsource.write('CURR 0.1,(@1)')
    DCsource.write('OUTPUT OFF,(@1)')

    data = {}
    data['t'] = t
    data['V'] = V
    cycleDone = 1

    scipy.io.savemat('%s.mat' % fname, data)
#End of While Loop
#%% close instruments
multiplexer.close()
DCsource.close()
```

A.2 Fusion Current Plotting (Matlab)

The code in this section is used for generating the fusion current characterization plot shown in Section 4.1.

File name: SW-002-FusionCurrentPlotting

```
% In this document the initial resistance and fusion current data points are
% manually entered into the arrays
%% ----------Fusion Current Char.----------------%
R0 = [17.12 14.21 14.78 16.59 18.16 20.38 15.89 12.95 12.61 10.79 11.16 12.93
13.95];
Ifuse = [5 6.1 5.8 5.1 4.8 4 5.5 6.25 6.4 7.2 6.9 6.25 6.1];
fusefit = polyfit(R0,Ifuse,1);
slope = fusefit(1);
int = fusefit(2);
figure (3);
set(gca, 'Fontsize', 22)
grid on
hold on
scatter (R0,Ifuse);
plot(R0, slope*R0 + int);
xlabel('R_0 @ 22C, 0.1A, [mΩ]','FontSize',22);
ylabel('Fusion Current [A]','FontSize',22);
legend({'Fuse Point','Fusion Fit'}, 'Location', 'NorthEast');
hold off
```

A.3 Constant Current Aging Code (Python)

This code is used for aging the specimen under constant current and temperature conditions, used to generate the data in Section 4.2 and Section 5.0.

File name: SW-003-Swet-ConstantCurrentAging

```
# -*- coding: utf-8 -*-
"""
Created on Thu Sep 26 13:23:50 2019
1. This program measures the voltage using a Multiplexer
2. Specimen are tested at constant current and temperature
3. Time is also recorded
Instruments:
    Circuit Specialist PS
    Hammatek PS
    KeySight NC6700
    2700 Multiplexer
    10A DMM

@author: Sudharsan Azisur Venkatesan
"""

#%% Reset All
from IPython import get_ipython
get_ipython().magic('reset -sf')


#%% Import packages required for this code
import visa
import time
import matplotlib.pyplot as plt
import subprocess
import scipy.io
from math import sqrt

#%% Close all plotting windows
plt.close('all')

#%% Saving File Name Initialization, Change before Run!
sampleName = ' Microconstriction - 4W - SnCu - Fusion Example'
fname=time.strftime("%y%m%d%H%M%S",time.localtime()) + sampleName

PRchange=0
#%% Define Functions
def roots(a,b,c):
```

```
    # Don't Make Changes
    """
    This function uses quadratic formula to get the real root (positive and
less than 300)
    of an expression ax^2+bx+c=0 by entering (a,b,c).
    Note that this function will return an error if trying to obtain an
imaginary root
    """
    disc = b**2 - 4*a*c #discriminant
    if disc >= 0:
        if ((-b + sqrt(disc))/(2*a))<300 and ((-b + sqrt(disc))/(2*a))>00:
            return (-b + sqrt(disc))/(2*a)
        elif ((-b - sqrt(disc))/(2*a))<300 and ((-b - sqrt(disc))/(2*a))>0:
            return (-b - sqrt(disc))/(2*a)
    else:
        return -10000000
#%% initialize variable
n = 1
V = [[] for z in range(n)]
#V_check = [[] for z in range(n)]
I = [[] for z in range(n)]
I1 = []
I2 = []
t = []
T = []
A = 3.9083E-3               #Constants for tp1000 temperature sensor
B = -5.775E-7               #Constants for tp1000 temperature sensor
RealTimeReadings = 100      #Real time plotting that only show a window of
this number of values

#%% List of Channel number and corresponding color while plotting
channel=['@103']
#channel=['@101','@102','@103']
color=['b']
#color=['b','g','r']

#%% Call PyVisa's Resource Manager
rm = visa.ResourceManager()

#%% Open GPIB Addresses, Change before Run!

Ammeter =
rm.open_resource('USB0::0x2A8D::0x1301::MY59005695::0::INSTR')  #measure
current across Circuit Specialist
N6700C = rm.open_resource('USB0::0x2A8D::0x0002::MY56008842::0::INSTR') # DC
Power Supply
```

```
multiplexer = rm.open_resource('GPIB0::25::INSTR') # Multiplexer for Voltage
measurement
tempsensor =
rm.open_resource('USB0::0x2A8D::0x1301::MY59005979::0::INSTR')  # measure
voltage

Ammeter.write("SYSTem:REMote")
Ammeter.write("*RST")  # factory reset
Ammeter.write("*CLS")  # clear memory
Ammeter.write("CONFigure:CURRent:DC 10")  # sets the ammeter to measure at
the 10A range

N6700C.write('*RST')
N6700C.write('*CLS')
N6700C.write('VOLT 8,(@1)')
N6700C.write('CURR 0.1,(@1)')
N6700C.write('OUTPUT ON,(@1)')

multiplexer.write('*RST')
multiplexer.write('*CLS')
multiplexer.write('CONFigure:VOLTage')

tempsensor.write("SYSTem:REMote")
tempsensor.write("*RST")  # factory reset
tempsensor.write("*CLS")  # clear memory
tempsensor.write("CONFigure:SCALar:FRESistance")  # 4-wire config. to measure
temperature

#%% Start the Timer
tic = time.perf_counter()
testDone = 0

while testDone == 0:

    #Find the temperature value from the resistance reading from tp1000
according to the formula
    TRstr = tempsensor.query("READ?")  # The format of reading from temp.
sensor is '### OHM'
    index = TRstr.find("OHM")  # Find the index of 'OHM' to only obtain the
numbers before it
    TRvalue = float(TRstr[0:index])
    Tvalue = roots(B * 1000, A * 1000, 1000 - TRvalue)

#    Avalue1 = float(Ammeter.query("READ?"))
#    Avalue2 = float(N6700C.query('MEAS:CURR? (@1)'))
#
```

```
    for i in range(n):

        Vvalue = -10000
#        while Vvalue == -10000:
#            try:
#                multiplexer.write(':ROUTe:OPEN (%s)' % ('@101:103')) # Open
3 channels
#                multiplexer.write(':ROUTe:CLOSe (%s)' % (channel[i])) #close
channel for reading
#                rawstr = multiplexer.query('read?')
#                index = rawstr.find('VDC')
#                volstr = rawstr[0:index]
#            except:
#                    Vvalue = -10000;

        multiplexer.write(':ROUTe:OPEN:all') # Open all channels
        multiplexer.write(':ROUTe:CLOSe (%s)' % (channel[i])) #close a
channel for reading
        rawstr = multiplexer.query('read?')
        index=rawstr.find('VDC')
        volStr = rawstr[0:index]
        Vvalue = float(volStr)

        # Append voltage value of each channel to list
        V[i].append(Vvalue)

        #Append current value of each channel to list
        #Avalue3 = 1.96
        #I.append(Avalue2)

    # End of For loop

    #saving found values
    #I[0].append(Avalue1)
    toc=time.perf_counter()
    T.append(Tvalue)
    t.append(toc-tic)

 #%% Plot Tvst, Rvst in real-time

#    plt.ion()
#    f = plt.figure(1)
##            plt.cla() #clear the plots for real time readings
#    #Real time plotting
#    plt.plot(t[max(0, len(t)-RealTimeReadings):],T[max(0, len(t)-
RealTimeReadings):],'b')
#    plt.xlabel('Time [s]', fontsize=30)
```

```
#    plt.ylabel('Temperature [℃]', fontsize=30)
#    plt.rcParams['xtick.labelsize']=32
#    plt.rcParams['ytick.labelsize']=32
#    plt.show()
#    #Flush the data for the real time plotting window
#    f.canvas.draw()
#    f.canvas.flush_events()

    data = {}
    data['t'] = t
    data['V'] = V
    data['T'] = T

    scipy.io.savemat('%s.mat' % fname, data)
#End of While loop

#%% close instruments
#A34411.close()
#tempsensor.close()
N6700C.write('OUTPUT OFF,(@1)')
N6700C.close()
```

A.4 DOE Determination (Matlab)

This code is used for generating the thermo-electric characterization plots described in Section 4.2.

File name: SW-004-DOEDetermination

```
format long g
load '210118152717 Microconstriction - 4W - SnCu - Temp+Pow Char.mat'
figure (7)
plot(t/3600,V)
set(gca, "fontsize", 25)
xlabel('Time, h','FontSize',20); ylabel('Voltage, V','FontSize',20);
r00 = V(1,10)*1000/0.1
%--------------------------------SnCu----------------------------------------
%------Sample 1------
V_25 = [
0.0014549   0.0073137   0.0148054   0.0228348   0.0312786   0.0404899   0.051
2365   0.0638992 ];
V_45 = [
0.0015775   0.0079450   0.0161241   0.0247558   0.0339114   0.0439870   0.055
6152   0.0701271 ];
V_65 = [
0.0017160   0.0086143   0.0174690   0.0269392   0.0369307   0.0480336   0.060
5540   0.0752175 ];
V_85 = [
0.0018075   0.0090981   0.0185511   0.0285228   0.0394006   0.0517772   0.065
1807   0.0815565 ];
V_100 =
[0.0019195   0.0096469   0.0195912   0.0302165   0.0414842   0.0538457   0.06
81387   0.0866470 ];
%------Sample 2------
% V_25 = [
0.0012857   0.0064819   0.0130837   0.0198504   0.0269895   0.0345459   0.042
9820   0.0521857 ];
% V_45 = [
0.0013889   0.0070515   0.0142791   0.0216720   0.0294940   0.0377418   0.047
1627   0.0569798 ];
% V_65 = [
0.0014942   0.0075385   0.0152390   0.0232364   0.0316683   0.0407058   0.050
4903   0.0606230 ];
% V_85 = [
0.0015298   0.0077351   0.0158341   0.0242772   0.0331206   0.0425225   0.052
3821   0.0635134 ];
% V_100 =
[0.0016160   0.0081585   0.0165091   0.0250710   0.0341105   0.0437175   0.05
43966   0.0663214 ];
%-----Sample 3-------
```

```
% V_25 = [
0.0014168   0.0074601   0.0151398   0.0231025   0.0315058   0.0404922   0.050
5369   0.0617709 ];
% V_45 = [
0.0015361   0.0081000   0.0165074   0.0251798   0.0343698   0.0442038   0.054
9286   0.0666349 ];
% V_65 = [
0.0016487   0.0086427   0.0175534   0.0268578   0.0366305   0.0471742   0.058
2461   0.0699127 ];
% V_85 = [
0.0016689   0.0087389   0.0179237   0.0275897   0.0375842   0.0482247   0.059
1580   0.0710596 ];
% V_100 =
[0.0017194   0.0090257   0.0183309   0.0280101   0.0381846   0.0490655   0.06
08794   0.0742893 ];
%---------------SnCu--------------------
I = [0.1 0.5 1.0 1.5 2.0 2.5 3.0 3.5 ];
T = [25 45 65 85 100];
V = [V_25;V_45;V_65;V_85;V_100;];
I_vec = [I;I;I;I;I;];
R = V ./I *1000;
R_25 = V_25./I*1000;
R_45 = V_45./I*1000;
R_65 = V_65./I*1000;
R_85 = V_85./I*1000;
R_100 = V_100./I*1000;
%TCR calc.:
[p1, s1, u1] = polyfit(I,R_25,2);
[R_25_0 , R_25Del] = polyval(p1,0,s1,u1);
[p2, s2, u2] = polyfit(I,R_45,2);
[R_45_0 , R_45Del] = polyval(p2,0,s2,u2);
[p3, s3, u3] = polyfit(I,R_65,2);
[R_65_0 , R_65Del] = polyval(p3,0,s3,u3);
[p4, s4, u4] = polyfit(I,R_85,2);
[R_85_0 , R_85Del] = polyval(p4,0,s4,u4);
[p5, s5, u5] = polyfit(I,R_100,2);
[R_100_0 , R_100Del] = polyval(p5,0,s5,u5);
R = [R_25_0 R_45_0 R_65_0 R_85_0 R_100_0];
TR_fit = polyfit(T,R,1);
TCR_0 = TR_fit(1)/TR_fit(2);
TCR = 1/(25+(1/TCR_0))
figure (1)
plot(T,R, 'o-')
hold on
plot(T, TR_fit(1)*T + TR_fit(2),'--');
hold off
% title('Temperature vs Resistance R0','FontSize',22)
```

```
set(gca, "fontsize", 22)
xlabel('Temperature, [℃]','FontSize',22);ylabel('Resistance,
[mΩ]','FontSize',22);
% Power Calc:
P_25 = V_25.*I*1000;
P_45 = V_45.*I*1000;
P_65 = V_65.*I*1000;
P_85 = V_85.*I*1000;
P_100 = V_100.*I*1000;
coeff1 = polyfit(P_25,R_25,1);
Rth1 = 1000*coeff1(1)/TCR/R_25(1,1)
Rth1_err = slopeErr(P_25,R_25)
coeff2 = polyfit(P_45,R_45,1);
Rth2 = 1000*coeff2(1)/TCR/R_45(1,1)
Rth2_err = slopeErr(P_45,R_45)
coeff3 = polyfit(P_65,R_65,1);
Rth3 = 1000*coeff3(1)/TCR/R_65(1,1)
Rth3_err = slopeErr(P_65,R_65)
coeff4 = polyfit(P_85,R_85,1);
Rth4 = 1000*coeff4(1)/TCR/R_85(1,1)
Rth4_err = slopeErr(P_85,R_85)
coeff5 = polyfit(P_100,R_100,1);
Rth5 = 1000*coeff5(1)/TCR/R_100(1,1)
Rth5_err = slopeErr(P_100,R_100)
Rth = [Rth1 Rth2 Rth3 Rth4 Rth5]
Rth_err = [Rth1_err Rth2_err Rth3_err Rth4_err Rth5_err]
T_25 = P_25*Rth1/1000 + 25;
T_45 = P_45*Rth2/1000 + 45;
T_65 = P_65*Rth3/1000 + 65;
T_85 = P_85*Rth4/1000 + 85;
T_100 = P_100*Rth5/1000 + 100;
T_spec = [T_25;T_45;T_65;T_85;T_100;]
figure (2)
hold on
plot(I,T_25, 'o-')
plot(I,T_45, 'o-')
plot(I,T_65, 'o-')
plot(I,T_85, 'o-')
plot(I,T_100, 'o-')
% title('Specimen Temperature profile with reused sample','FontSize',22)
set(gca, "fontsize", 22)
xlabel('Current, [A]','FontSize',22);ylabel('Temperature,
[℃]','FontSize',22);
figure (3)
hold on
plot(P_25,R_25, 'o-')
plot(P_45,R_45, 'o-')
```

```
plot(P_65,R_65, 'o-')
plot(P_85,R_85, 'o-')
plot(P_100,R_100, 'o-')
set(gca, "fontsize", 25)
% title('R-P Char. profile stressed to 3.5A','FontSize',22)
xlabel('Power, [W]','FontSize',25);ylabel('Resistance, [mΩ]','FontSize',25);
hold off
figure (4)
hold on
plot(I,R_25, 'o-')
plot(I,R_45, 'o-')
plot(I,R_65, 'o-')
plot(I,R_85, 'o-')
plot(I,R_100, 'o-')
% title('R vs I profile with reused sample','FontSize',22)
set(gca, "fontsize", 25)
xlabel('Current, A','FontSize',25);ylabel('Resistance, mΩ','FontSize',25);
figure (5)
errorbar(T,Rth,Rth_err)
% title('Rth vs Temp with Error','FontSize',22)
set(gca, "fontsize", 25)
xlabel('Temperature, [℃]','FontSize',25);ylabel('Rth,
[mΩ/℃]','FontSize',25);
figure (6)
surf(I,T,T_spec)
ylabel('T_A, [℃]','FontSize',18);
xlabel('I, [A]','FontSize',18);
zlabel('T_S, [℃]','FontSize',18);
T_oven = [ 25  25  25  25  25  25  25  25 ...
          45  45  45  45  45  45  45  45 ...
          65  65  65  65  65  65  65  65 ...
          85  85  85  85  85  85  85  85 ...
          100 100 100 100 100 100 100 100];
I_samp = [I I I I I];
T_samp = [T_25 T_45 T_65 T_85 T_100];
PFit = polyFit2D(T_samp,I_samp,T_oven,2,2);
Fval = polyVal2D(PFit,2,85,2,2)
%-----Error Calc------------%
[row,col] = size(T_spec);
T_calc = zeros(row,col);
I_mat =  [I;I;I;I;I];
T_mat =  [ 25  25  25  25  25  25  25  25; ...
          45  45  45  45  45  45  45  45; ...
          65  65  65  65  65  65  65  65; ...
          85  85  85  85  85  85  85  85; ...
          100 100 100 100 100 100 100 100 ];
for n = 1:row
```

```
   for m = 1:col
       T_calc (n,m) = polyVal2D(PFit,I_mat(n,m),T_mat(n,m),2,2);
   end
end
T_err = T_calc - T_spec;
func_err = mean(mean(abs(T_err)))

function t_oven = OvenTempCalc(p,T,I)
 A = p(1,1)*I^2 + p(2,1)*I + p(3,1);
 B = p(4,1)*I^2 + p(5,1)*I + p(6,1);
 C = p(7,1)*I^2 + p(8,1)*I + p(9,1) - T;
 t_oven = roots([A,B,C]);
end

function [sm] = slopeErr(x,y)
 n=length(x);
 mu_x=mean(x);
 mu_y=mean(y);
 qx=sum((x-mu_x).^2);
 qy=sum((y-mu_y).^2);
 qxy=sum(x.*y)-sum(x)*sum(y)/n;
 m=qxy/qx;
 sm=sqrt((qy/qx-m^2)/(n-2));
 b=mu_y-m*mu_x;
 sb=sqrt( (qy-qxy^2/qx)*(1/n+mu_x^2/qx)/(n-2) );
end
```

A.5 T_A vs I_{Stress} Contour Plot generation (Matlab)

The code in this section is used for generation the contour plots and DOE box used in Section 4.

File name: SW-005-TSContourPlot

```
% filename: chara.m
% runs in GNU Octave 6.1.0
close all
x = [0.01 0.1:.2:5.2]'; % Current
y = [1 5:5:100];  % Temperature
P1 = 1.476E-4; P2 = -2.543E-4; P3 = 9.161E-5;  P4 = -6.871E-3; P5 = 1.989E-2;
P6 = 0.992;
P7 = 5.913; P8 = -4.103; P9 = 1.261;

AmbientTemp=y;
for j=2:length(x);AmbientTemp=[AmbientTemp;y];end
SpecTemp= P1*x.^2*y.^2+ P2*x.^1*y.^2+ P3*x.^0*y.^2+ P4*x.^2*y.^1+
P5*x.^1*y.^1+ P6*x.^0*y.^1+ P7*x.^2*y.^0+ P8*x.^1*y.^0+P9*x.^0*y.^0 ;

% DOE box

% determine current level based on %-fusion current, normalized to R0=15mOhm
R0=14.57; %must be in mOhm
i_high=(-.317*R0+10.47)*80/100;
i_low=(-.317*R0+10.47)*75/100;
trx=i_high; tlx=i_low; brx=i_high; blx=i_low; % top-left/right, bottom-
left/right, of x
tr_y=65; tly=78; bry=52; bly=65; % ..., of y
xx=[trx tlx blx brx trx]; yy=[tr_y tly bly bry tr_y];

% plot everything

fs=25; % fontsize for graphs
lw=2; % linewidth for graphs

figure(1); %subplot(1,2,1)
pause(1);set(gcf,'Position',[ 55   55   1601   701])
z=SpecTemp'; maz=max(max(z)) ;
levels_=[0 1:floor(maz/10)]*10;levels=levels_(1:round(end/10):end);
[c,h]=contourf(x,y,z,levels,"linewidth", lw);
clabel (c, h,"LabelSpacing",444, "fontsize", round(.9*fs));
hold on; plot(xx,yy,'r',"linewidth", lw,xx,yy,'ro',"markersize",13)
ylabel('T_A [°C]');xlabel('I [A]')
title('T_S [°C]')
STint=interp2(y,x,SpecTemp,yy,xx);
```

```
for j=2:5;text(xx(j),yy(j),['  '
num2str(round(10*STint(j))/10)],"fontsize",fs*.9);end
set(gca, "linewidth", 1.5, "fontsize", fs)

figure (2)
%subplot(1,2,2)
z=(SpecTemp-AmbientTemp)'; maz=max(max(z)) ;
levels_=[0 1:floor(maz/10)]*10;levels=levels_(1:round(end/10):end);
[c,h]=contourf(x,y,z,levels,"linewidth", lw);
clabel (c, h,"LabelSpacing",444, "fontsize", round(.9*fs));
%colorbar(gca,"linewidth",lw,"fontsize",fs,"EastOutside")
hold on; plot(xx,yy,'r',"linewidth", lw,xx,yy,'ro',"markersize",13)
ylabel('T_A [°C]');xlabel('I [A]')
title('T_d_i_f_f (T_S - T_A) [K]')
STint=interp2(y,x,SpecTemp-AmbientTemp,yy,xx);
for j=2:5;text(xx(j),yy(j),['  '
num2str(round(10*STint(j))/10)],"fontsize",fs*.9);end
set(gca, "linewidth", 1.5, "fontsize", fs)

pause(1)
print -djpeg datfig.jpg
print -dpdfcrop datfig.pdf
```

A.6 Weibull and Lognormal Distribution Analysis (Matlab)

This code is used for generating the Weibull and Lognormal plots, the mttf and the eta values shown in Section 5.

File name: SW-006-WeibullLognormalDist

```
% In this document the time-to-failure data points are manually entered
% into the arrays. Weibull and Lognormal analysis is conducted on the
% arrays
%--------------------Failure Times------------------------
% t = [ 0.499,0.55,0.561,0.6702,0.708,0.797,0.885,0.938,0.985,1.134,1.281,...
%       1.287,1.609,1.747,2.124,2.197,2.251,3.073,3.215,3.874,6.55,7.698,
17.035]; % T-R Corner
% t = [
0.951,1.545,2.371,2.949,3.347,3.349,3.523,5.765,6.592,13.196,15.108,...
%       23.433 ]; % B-L Corner
% t = [2.327,12.799,3.786,14.63,6.549,4.239,0.698,1.62,0.883,17.772,5.997,...
%       1.167,8.574,13.914,1.093,14.808 ]; % T-L Corner
t = [ 18.948,4.803,18.819,0.842,0.547,8.393,3.462,0.868,21.617,21.984,...
      1.434,1.405,24.38,1.596]; % B-R Corner
% t = [ 0.249, 0.713, 0.311, 0.768, 1.11, 0.406, 0.321, 2.622, 1.014,
0.755,...
%       0.433, 2.698, 1.626, 1.867]; % SAC-305 T-R
n = 24;
i = 1:length(t);
t = sort(t);
% Median Ranking - [Used to take into account the probability density of the
% failure times]
F = (i - 0.3)/(n + 1);
R = 1 - F;
%% ------------------ Weibull Fit ---------------------
X = log(t);
Y = log(-log(R));
% Weibull Distribution
wblfit = polyfit(X,Y,1);
beta = wblfit(1);
eta = exp(-wblfit(2)/beta); % Time by which 63.2% of samples have failed
% Plotting
figure (1);
set(gca, 'Fontsize', 22)
grid on
hold on
scatter (X,Y);
plot(X, wblfit(1)*X + wblfit(2));
xlabel('ln(t)','FontSize',22);
ylabel('ln(ln(-R))','FontSize',22);
```

```
legend({'Weibull data','Weibull fit'}, 'Location', 'SouthEast');
hold off
% ----------Goodness of fit test-----------
% K-S Test
F_predicted = 1 - exp(- ((t./eta).^beta)) ;
CDF_diff = abs(F - F_predicted);
CDF_diff_max = max(CDF_diff);
% Chi-square
X_predicted = Y / beta + log(eta);
t_predicted = exp(X_predicted);
chi_sq_all = ((t_predicted - t).^2)./t_predicted;
chi_sq = sum(chi_sq_all);
fprintf('Weibull Fit Data')
fprintf('No. of Failures: %d\n', i(end))
fprintf('Eta: %d\n', eta)
fprintf('Beta: %d\n', beta)
fprintf('KS Fit: %d\n', CDF_diff_max)
fprintf('Chi_sq: %d\n', chi_sq)
fprintf('')
% ---------------------Lognormal Distribution----------------------------
X = log(t);
yln = norminv(F);
lnfit = polyfit(X,yln,1);
sigma = 1/lnfit(1);
mu = -lnfit(2)*sigma;
mttf = exp(mu + (sigma^2)/2); % Time by which 50% of samples have failed
figure (2);
set(gca, 'Fontsize', 22)
grid on
hold on
scatter (X,yln);
plot(X, lnfit(1)*X + lnfit(2));
xlabel('ln(t)','FontSize',22);
ylabel('Z','FontSize',22);
legend({'Lognormal data','Lognormal fit'}, 'Location', 'SouthEast');
hold off
% ----------Goodness of fit test-----------
% K-S Test
F_predicted = normcdf(X,mu,sigma);
CDF_diff = abs(F - F_predicted);
CDF_diff_max = max(CDF_diff);
% Chi-square
X_predicted = yln * sigma + mu;
t_predicted = exp(X_predicted);
chi_sq_all = ((t_predicted - t).^2)./t_predicted;
chi_sq = sum(chi_sq_all);
fprintf('Lognormal Fit Data')
```

```
fprintf('No. of Failures: %d\n', i(end))
fprintf('Mttf: %d\n', mttf)
fprintf('Mu: %d\n', mu)
fprintf('Sigma: %d\n', sigma)
fprintf('KS Fit: %d\n', CDF_diff_max)
fprintf('Chi_sq: %d\n', chi_sq)
fprintf('')
```

A.7 Right censored Lognormal Distribution Analysis (Matlab)

File name: SW-007-JESD37ADataFittingRev4.0

```
% how to determine average and stdev values corrected for right censored data
%
% formulas and procedure taken from J.A. Lechner, 1991, "Estimators for Type-
II Censored (Log)Normal Samples"
% available from
https://ieeexplore.ieee.org/stamp/stamp.jsp?arnumber=106773&casa_token=Poz-
A3d7t3IAAAAA:kKbf7mRVgaq9PTE_LPs3d8xw28DxIU5kXxOsDlDbuYUAPub2KlCDK9utpvK4TGWH
9ZELSP5Utz4&tag=1

close all
pkg load statistics  % script works with octave only and not matlab

% data which was not interrupted: x ln(times) [[ example data taken from
table C.5 in Jedec Std. JESD37A
##x=log([0.499,0.55,0.561,0.6702,0.708,0.797,0.885,0.938,0.985,1.134,1.281,..
.
##       1.287,1.609,1.747,2.124,2.197,2.251,3.073,3.215,3.874,6.55,7.698 ]);
##% data which was interrupted: y ln(times)
##y=log([8 8]);

##% BL CORNER
##x=log([0.951,1.545,2.371,2.949,3.347,3.349,3.523,5.765,6.592,13.196,15.108,
...
##       23.433 ]);
##% data which was interrupted: y ln(times)
##y=log([25,25,25,25,25,25,25,25,25,25,25,25]);
##
##%TL CORNER
##x=log([0.698,0.883,1.093,1.167,1.62,2.327,3.786,4.239,5.997,6.549,8.574,...
##       12.799,13.914,14.63,14.808,17.772]);
##% data which was interrupted: y ln(times)
##y=log([20,20,20,20,20,20,20,20]);
##
##%BR CORNER
##x=log([0.547,0.842,0.868,1.405,1.434,1.596,3.462,4.803,8.393,18.819,18.948,
21.617,21.984,24.38]);
##% data which was interrupted: y ln(times)
##y=log([25,25,25,25,25,25,25,25,25,25]);

##%SAC305 TR Corner
x=log([0.249,0.311,0.321,0.406,0.433,0.713,0.755,0.768,1.014,1.11,1.626,1.867
,2.622,2.698]);
```

```
% data which was interrupted: y ln(times)
y=log([3,3,3,3,3,3,3,3,3,3]);


N=length(x)+length(y);K=length(x);
% normal cumulative distribution function in octave is normcdf
% normcdf(z0) = 1/2*erfc(-z0/sqrt(2))  [[ see
https://en.wikipedia.org/wiki/Error_function#Cumulative_distribution_function
]]
% inverse of normcdf is probit funzction
z0=-norminv(K/N);%-.7128;  % norminv; I had to put a - in front of the probit
fct to avoid complex result
% define z0 by gauf(z0)=K/N; % gauf is the cumulative distribution function
% (wikipedia) use the inverse of normcdf  is known as the normal quantile
function, or probit function and may be expressed in terms of the inverse
error function as

F=K/N;
function retval=gaud(x); % see p. 87pdf, 5-1 section, in
https://apps.dtic.mil/dtic/tr/fulltext/u2/a027372.pdf
  retval=exp(-x^2/2)/sqrt(2*pi);
endfunction
M=mean(x);
Cr=y(1);%sqrt([x(end)*y(1)]); % censoring point
S=std(x);% stdev of observed x's
SRML=1/2*(z0*(Cr-M)+(z0^2*(Cr-M)^2+4*((Cr-M)^2+(1-1/K)*S^2))^0.5);
alpha=(N/K)*gaud(z0);
SPR_biased=((K-1)*S^2/K+alpha*(alpha-z0)*SRML^2)^0.5
MPR=M+alpha*SRML
SPR_unbiased=K/(K-1)*(1.8*N+5)/(1.8*N+6)*SPR_biased
CMPR=MPR+(.98/K+.068/K/F-1.15/N)*SPR_unbiased
expSPR=exp(SPR_biased)
expMPR=exp(MPR)
expCSPR=exp(SPR_unbiased)
expCMPR=exp(CMPR)
disp(['biased estimate of  t50 : ' num2str(expMPR) ' units; +-1-sigma range:
' num2str(exp(MPR-SPR_biased)) '-' num2str(exp(MPR+SPR_biased)) ' units'])
disp(['unbiased estimate of t50: ' num2str(expCMPR) ' units; +-1-sigma range:
' num2str(exp(CMPR-SPR_unbiased)) '-' num2str(exp(CMPR+SPR_unbiased)) '
units'])

% KS Test
P=([1:N]-.3)/(N+.4);
P_x = P(1:length(x));
Z = (x - CMPR)/SPR_unbiased;
P_predicted = normcdf(Z);
CDF_diff = abs(P_x - P_predicted);
```

```
CDF_diff_max = max(CDF_diff)

% Plotting
figure;
plot([x y],P,'o',[CMPR CMPR],[0 1.1],[CMPR CMPR]-SPR_unbiased,[0 1.1],'--
',[CMPR CMPR]+SPR_unbiased,[0 1.1],'--',y,[0 1.1],'k')
set(gca, 'Fontsize', 18)
xlabel('ln(Time)','FontSize',22);
ylabel('Cumulative Probability','FontSize',22);
title('mean +- stdev corrected for censoring according to Persson-
Rootzen','FontSize',22);

%norminv converts cum prob to Z
%normcdf converts Z to cum prob

figure;
semilogx(exp([x y]),P,'o',exp([ y]),P(end-length(y)+1:end),'r',exp([
y]),P(end-length(y)+1:end),'r*',exp([CMPR CMPR]),[0 1],exp([CMPR CMPR] -
SPR_unbiased),[0 1],'--',exp([CMPR CMPR] + SPR_unbiased),[0 1],'--')
set(gca, 'Fontsize', 18)
xlabel('Time [h]','FontSize',22);
ylabel('Cumulative Probability','FontSize',22);
title('mean +- stdev corrected for censoring as per Persson-
Rootzen','FontSize',22);

semilogx(exp(x),Z)
hold on
scatter(exp(x), norminv(P_x), 'b');
scatter(exp([ y]),norminv(P(end-length(y)+1:end)),'r')% plot censored data
line([exp(x(end)) exp(x(end))],[-2 2],"linestyle", "--","color",'k')
##line(exp(x), Z+norminv(CDF_diff_max), "linestyle", "--", "color", "b");%
fitting error
##line(exp(x), Z-norminv(CDF_diff_max), "linestyle", "--", "color", "b");%
fitting error
Pi=[0:.1:1]
for j=1:length(Pi);
  text(0.07,norminv(Pi(j)),strcat(num2str(Pi(j)),'-'),"Fontsize",15)
endfor
set(gca, 'Fontsize', 22)
ylabel('Z','FontSize',25);
set(gca,'YAxisLocation','right');
xlabel('Time [h]','FontSize',25);
```

Appendix B
COMSOL Simulation Results

B.1 Unmodified Wire Current Density

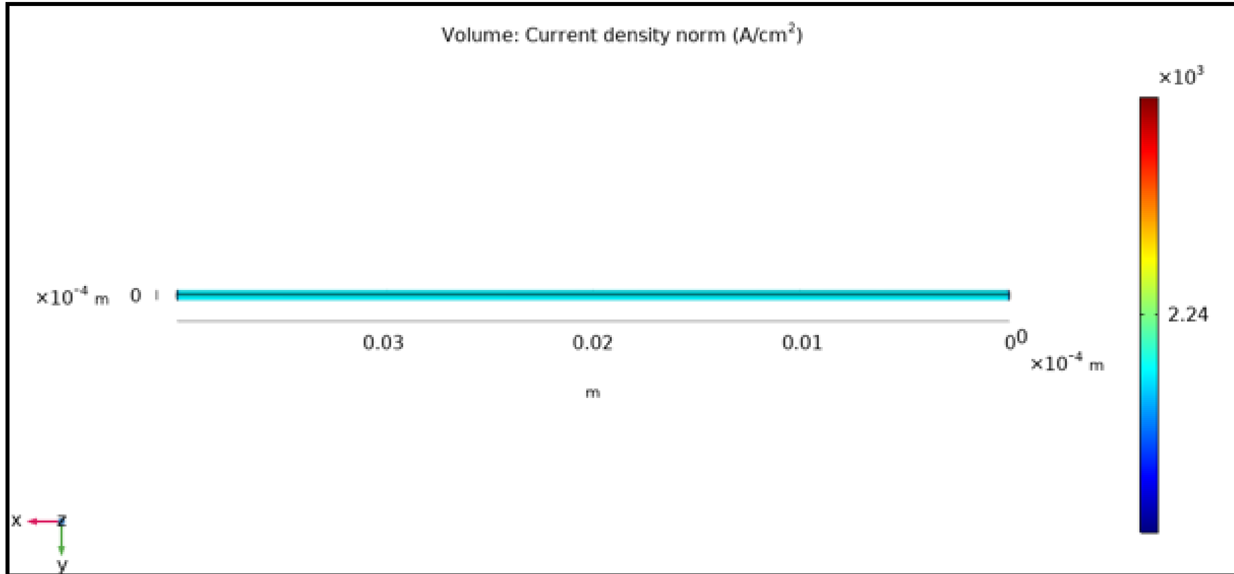

B.2 Stamped Wire Current Density

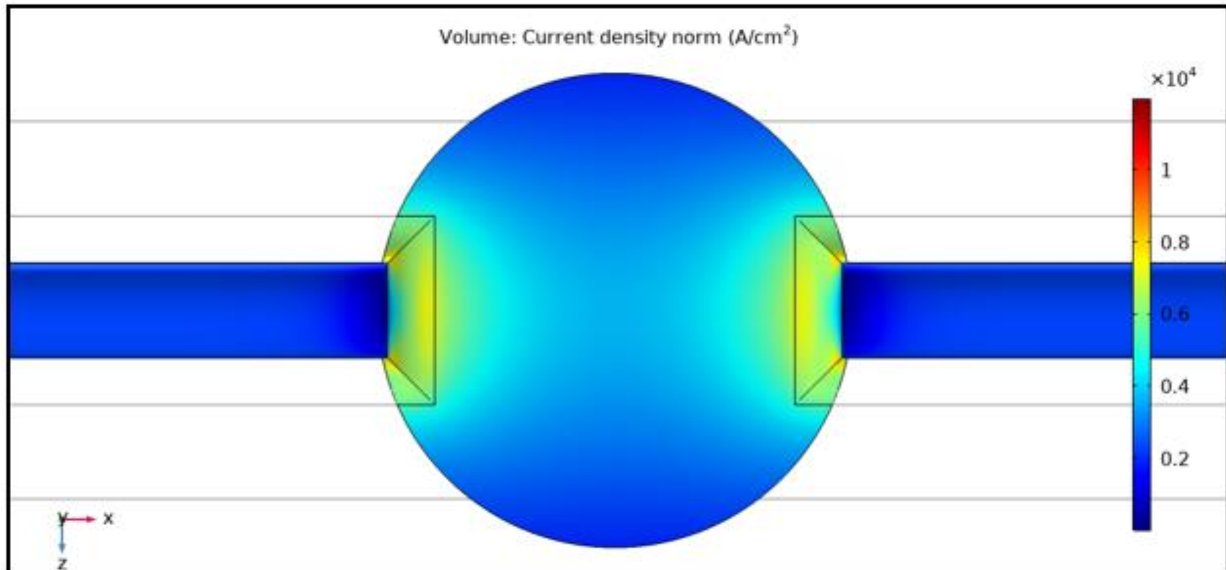

B.3 Micro Constricted Wire Current Density Slices

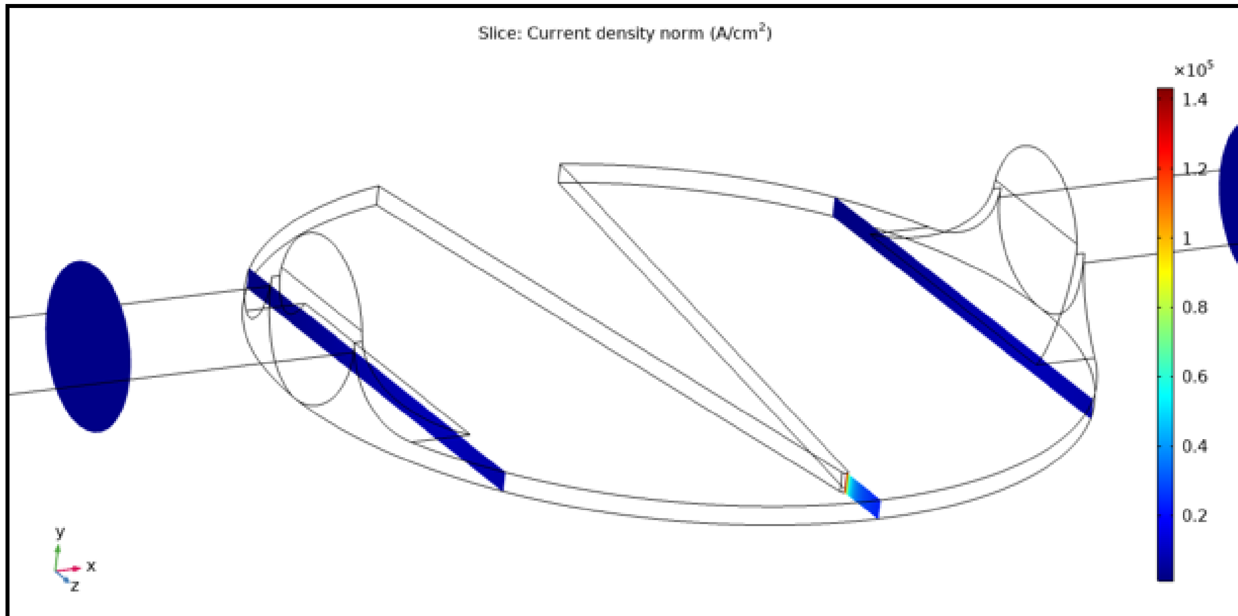

B.4 Micro Constricted Wire Current Flow

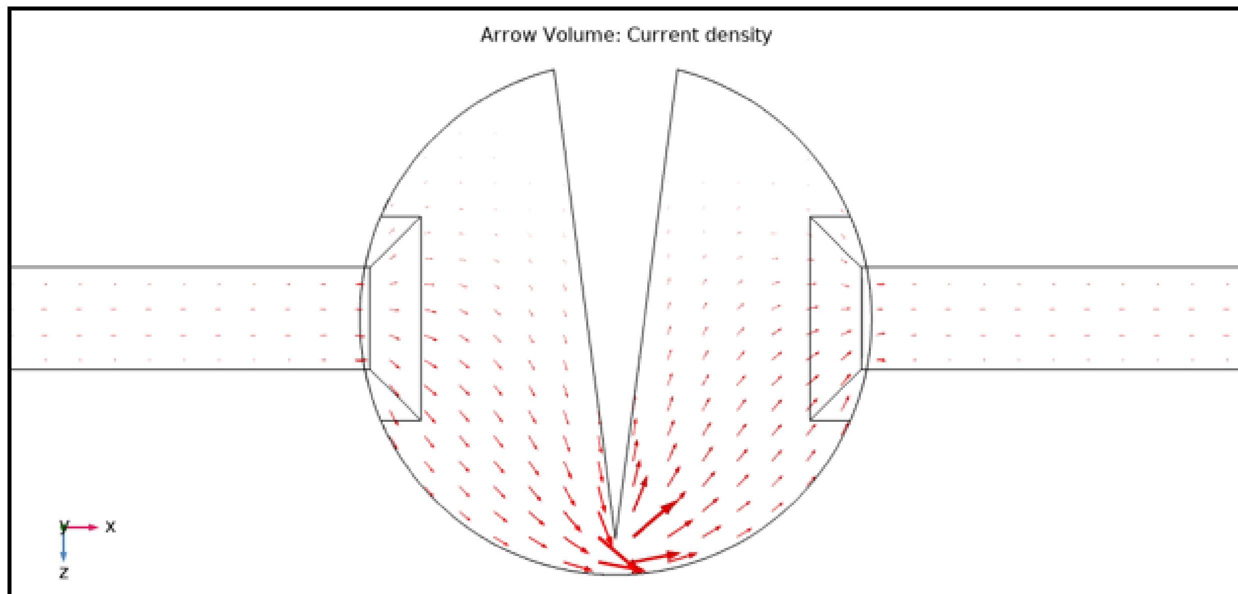

B.5 Unmodified Wire Temperature Gradient

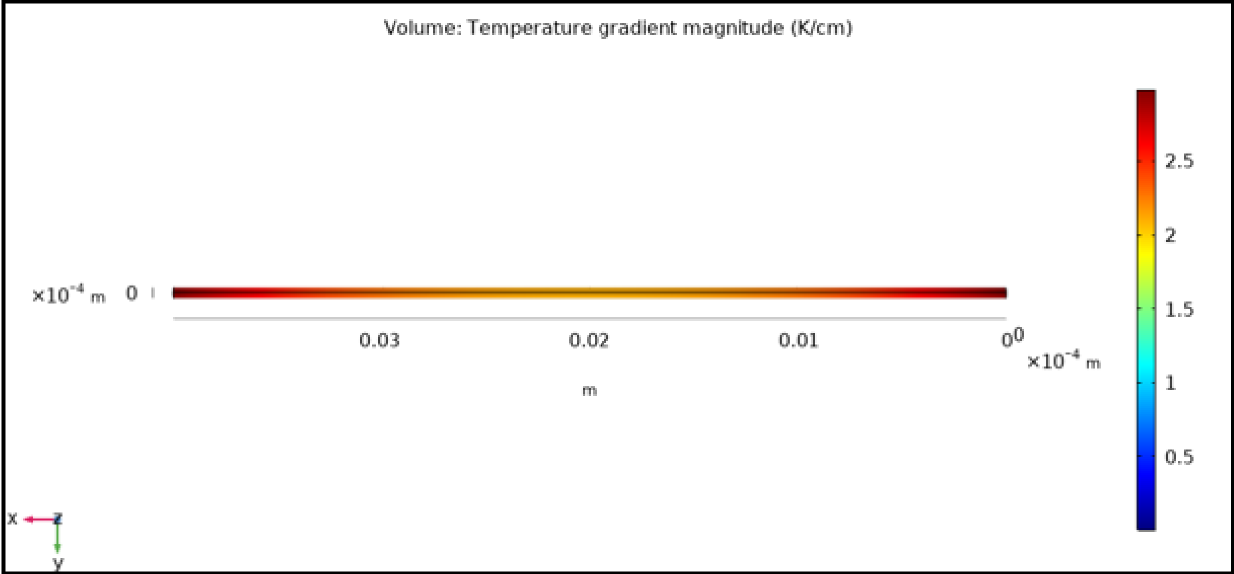

B.6 Stamped Wire Temperature Gradient

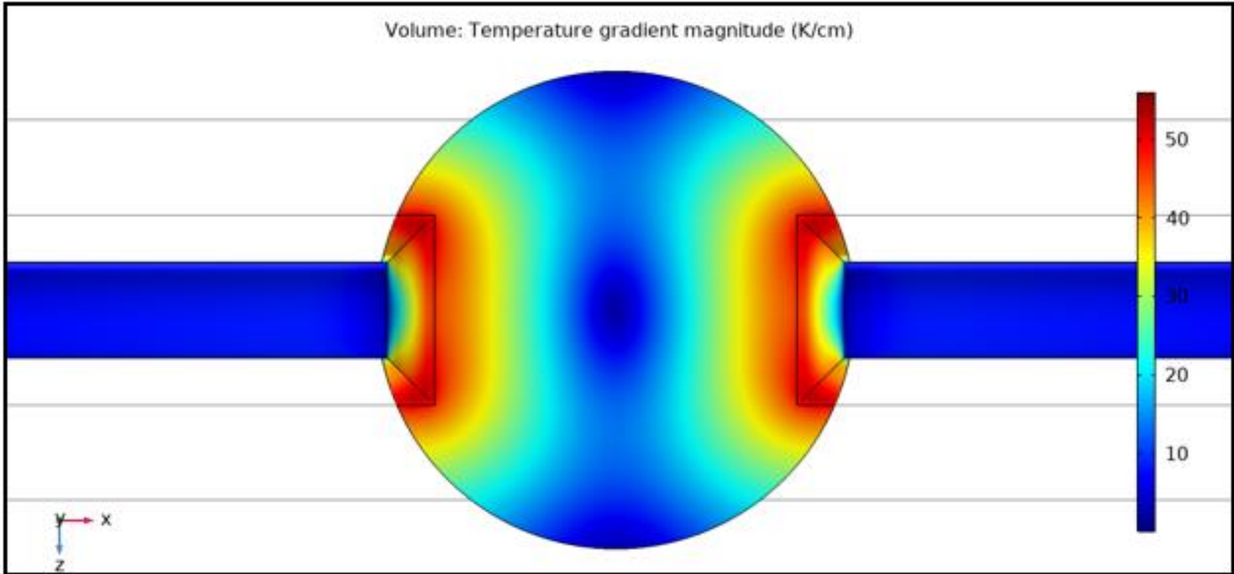

Appendix C

Anode Side Defect Images

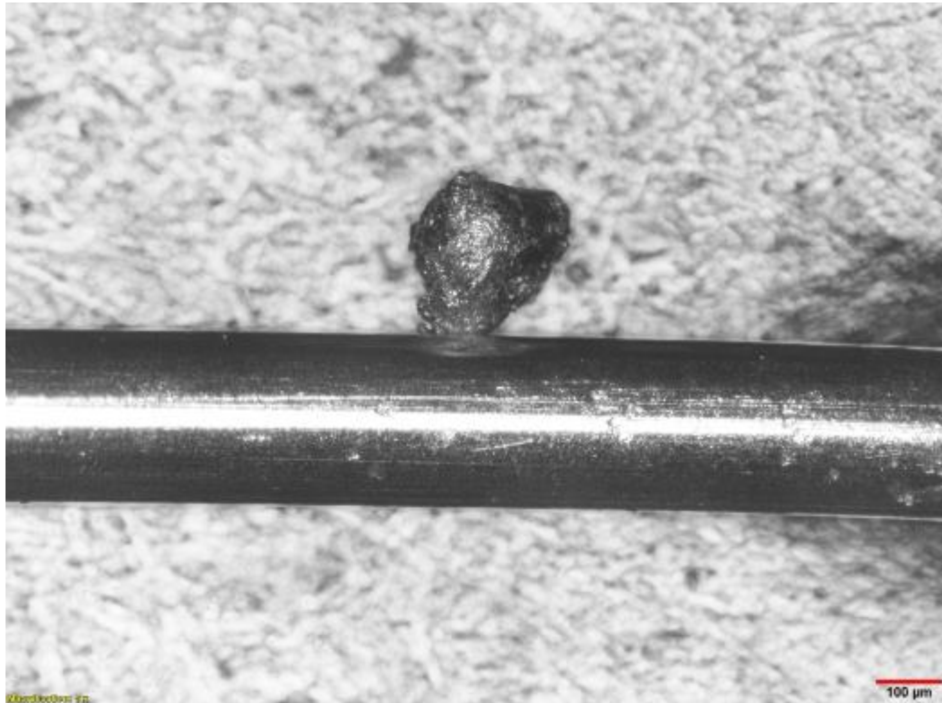

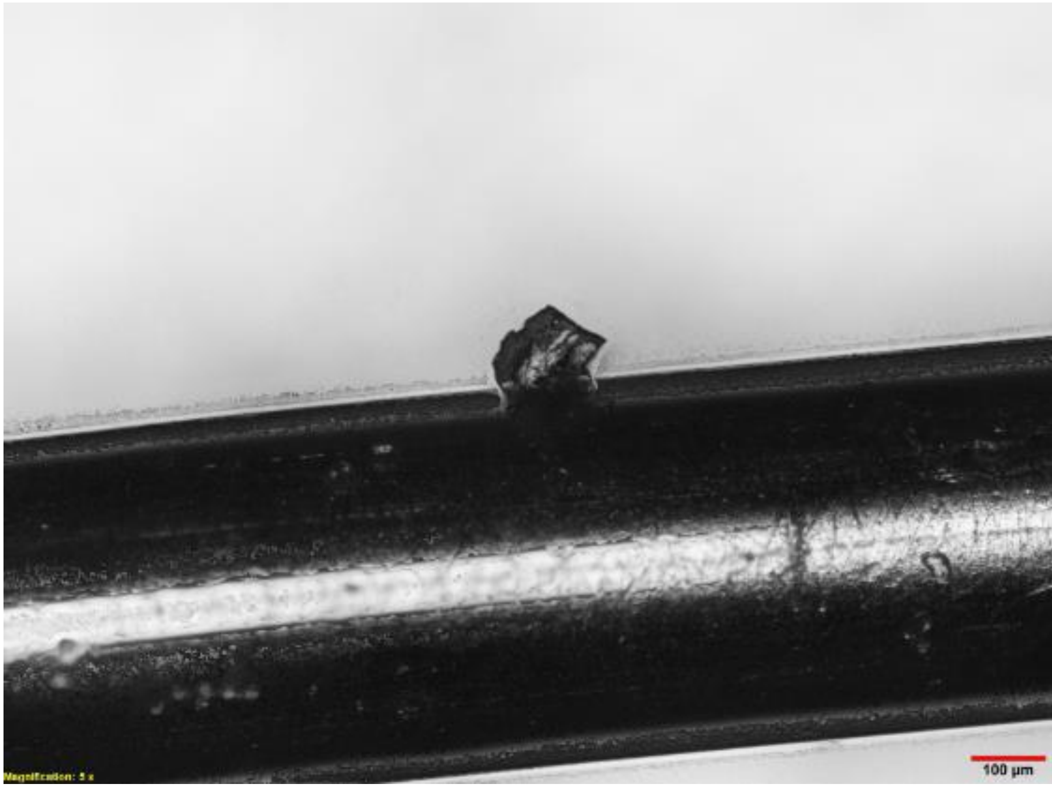
Magnification: 5 x
100 µm

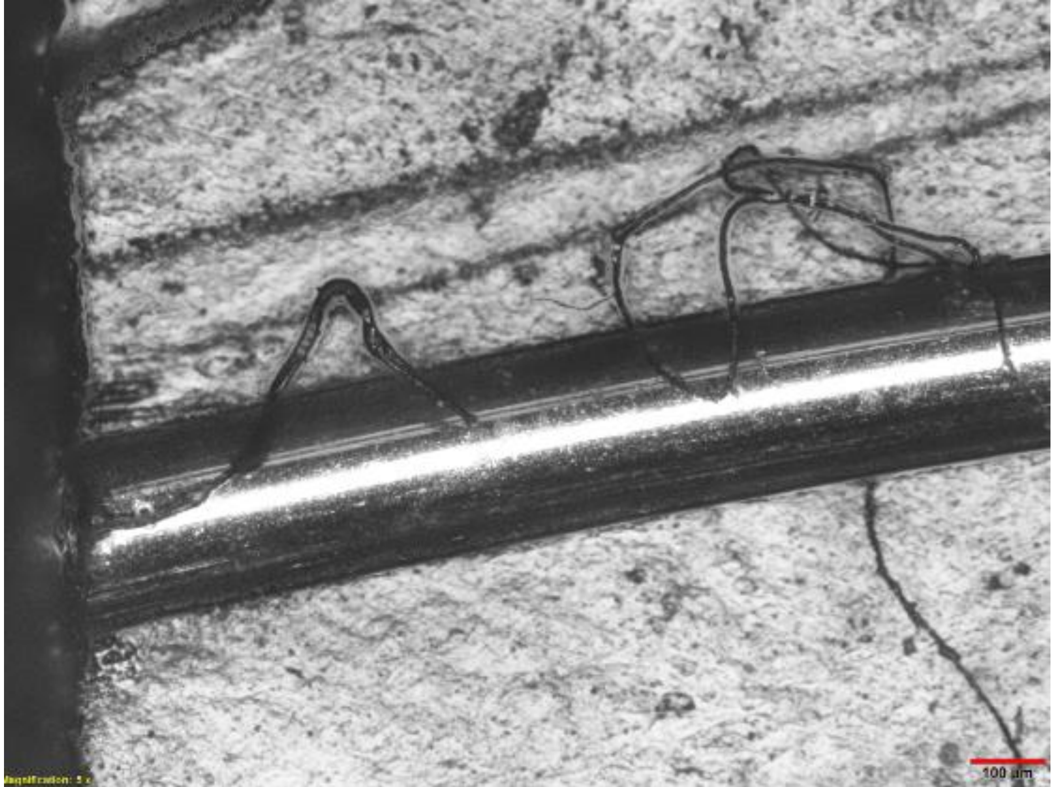
Magnification: 5 x
100 µm

Appendix D

Recommendation for future improvements

C.1 Switch Array PCB used for daisy-chaining Test Vehicles described in Section 3.2

Gerber file name: EMDaisyBrd (found in [35])